AN EXPERIMENTAL STUDY ON THE TEMPERATURE STEP RESPONSE OF MMA POLYMERIZATION IN A BATCH REACTOR

A Thesis Submitted
in Partial Fulfilment of the Requirements
for the Degree of
MASTER OF TECHNOLOGY

by

T. SRINIVAS

to the

DEPARTMENT OF CHEMICAL ENGINEERING
INDIAN INSTITUTE OF TECHNOLOGY, KANPUR

March, 1994

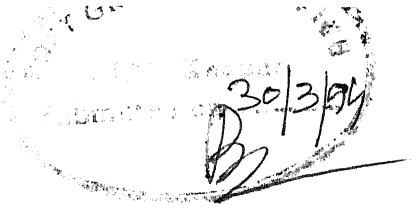

CERTIFICATE

This is to certify that the present work entitled " **AN EXPERIMENTAL STUDY ON THE TEMPERATURE STEP RESPONSE OF MMA POLYMERIZATION IN A BATCH REACTOR** " has been carried out by **Mr.T.Srinivas** under our supervision and has not been submitted elsewhere for a degree.

Dr.S. K. Gupta
Professor
Department of Chemical Engineering
Indian Institute of Technology
Kanpur-208 016

March, **1994.**

Dr. D. N. Saraf
Professor
Department of Chemical Engineering
Indian Institute of Technology
Kanpur-208 016

March, **1994.**

DEDICATED TO
MY PARENTS

ACKNOWLEDGEMENTS

I am vastly indebted to many people who have helped and inspired me, in various ways, to start, continue and complete this work. First and foremost, my gratitude goes to both my thesis supervisers, Dr.S.K.Gupta and Dr.D.N.Saraf for supporting me and strengthening my resolve in so many direct and indirect ways. Their thoughtful and valuable reviews and suggestions have helped me enormously to improve the presentation of this work.

The weekly meetings with Dr.Saraf were very constructive, the suggestions evolved in these meetings proved fruitful in the end.

It is a pleasure to acknowledge Dr.Gupta's unflinching support obtained in such abundant measures but for which this would neigh been possible. Working under his umbrella and sharing his research thoughts have been a memorable experience which I would cherish for years to come. Truely, to both I owe a timeless debt.

Thanks are due to Mr.Chauhan, Mr.Virdi, Mr.S.D.Singh, Mr.N.P.Singh and Mr Kannaujia, for their timely help during the experiments.

I cannot find words to describe the debt I owe to all my colleagues Mukund, Sanjay, Dua, Seth, Sareen, Shailesh and Geetu for having created a stimulating research atmosphere, the basic element of such an endeavor.

Shyam, Prem, Venu, Sarma, Ramki, JayKrishna, Reddy, Subba, Sudhakar, Manish and Chandra may not have realized what an influence their presence and friendship have had in my stay at IIT K. I am without words to thank them. I also thank all the members of the Hall-4 cricket team and ChESS members for making my stay a pleasant one.

Finally, to my parents and brothers goes my eternal gratitude for their love and support.

T. Srinivas

Table of Contents

List of Figures

ABSTRACT

Several free radical addition polymerizations exhibit the diffusion limited gel or Trommsdorff effect. The models available till recently predict the behaviour of batch reactors reasonably well but are inapplicable to semibatch operations or to reactions under non-isothermal conditions, operations which are of industrial importance. The recent model of Ray et al. (23) focuses on such reactors, but needs to be confirmed experimentally. An experimental set-up to study polymerization in such reactors has been assembled. Methyl methacrylate (MMA) is polymerized in a computer controlled, 1-liter Parr reactor. A series of experiments on bulk polymerization of MMA under different temperature histories [near-isothermal, step decrease and step increase] at a fixed initiator (AIBN) concentration of 25.8 mol/m^3, have been conducted. Two important process output variables, namely, monomer conversion and average molecular weight, as determined from intrinsic viscosity, have been measured at different sampling times during the course of polymerization. The conversion and molecular weight data are compared with the model predictions obtained using the experimental (non-isothermal) temperature histories. Reasonable agreement is observed between theory and experiment. It may be added that the parameters of the model of Ray et al. were evaluated using *isothermal batch* reactor data from the literature, and no additional curve fitting has been performed in the present study.

NOMENCLATURE

D_n	dead polymer molecule
e	error
f_o^s	initial volume fraction of solvent in reaction
h	heating
i	sampling instant
I	moles of initiator at any time t ,mol
k_d, k_f, k_i,	rate constants for the reactions in Table 1 at
k_s, k_{td}, k_{tc}	any time t,s^{-1} or m^3 mol^{-1} s^{-1}
K	process gain
M	moles of monomer in liquid phase ,mol
P_n	growing polymer radical having n repeat units
R	primary radical
S	moles of solvent in liquid phase,mol
$S^{\cdot}$	solvent radical
t_d	process dead time
τ_I	integral time constant
T	reaction temparature
T_{sp}	set point
τ_p	time constant of the process
X(s)	process input
Y(s)	process output

CHAPTER 1

INTRODUCTION

Ever since Norrish and Smith (1) and Trommsdorff et al. (2) reported the presence of the gel or auto acceleration effect in free radical polymerizations, scientists have been trying to obtain a fundamental understanding of this phenomenon. The gel effect is characterized by a sudden increase in the rate of reaction as the conversion increases beyond a certain point. This effect is associated with an increase in the viscosity of the reaction mixture, which causes a decrease in the termination rate constant k_t ($= k_{tc} + k_{td}$) (see Table 1) due to diffusional limitations. This leads to higher monomer conversions than predicted by conventional models. As the reaction proceeds, the glass effect is also exhibited at higher conversions, when the glass transition temperature, T_g, of the reaction mass becomes higher than the reaction temperature, T. This decreases the propagation rate constant, k_p, causing the reaction to stop short of complete conversion.

Mathematical modeling of the gel and glass effects has been attempted by several workers (3-5) in the past few years. They modeled these effects using time-varying rate constants for the termination and propagation reactions. The bulk polymerization data on methyl methacrylate (MMA) published by Balke and Hamielec (6) allowed the tuning of the parameters in these models. Friis and Hamielec (3) and Ross and Laurence (4) used simple empirical correlations to describe the polymerization kinetics in terms of monomer conversion, temperature and free volume, and curve-fitted their parameters. Cardenas and O'Driscoll (5), on the other hand, considered the polymer species as a set of two populations, one having a degree of polymerization (DP) below some critical value and the other, having higher values of DP. Two different values of the termination rate constant, k_t, were taken. These were curve-fit parameters based on previous experimental data (6).

TABLE 1

KINETIC SCHEME FOR POLYMERIZATION OF MMA

1. Initiation

$$I \xrightarrow{k_d} 2R$$

$$R + M \xrightarrow{k_i} P_1$$

2. Propagation

$$P_n + M \xrightarrow{k_p} P_{n+1}$$

3. Termination

by combination $\quad P_n + P_m \xrightarrow{k_{tc}} D_{n+m}$

by disproportionation $\quad P_n + P_m \xrightarrow{k_{td}} D_n + D_m$

4. Chain transfer to monomer

$$P_n + M \xrightarrow{k_f} P_1 + D_n$$

5. Chain transfer to monomer via solvent

$$P_n + S \xrightarrow{k_s} S^{\cdot} + D_n$$

$$S^{\cdot} + M \xrightarrow{\text{fast}} S^{\cdot} + D_n$$

or

$$P_n + M \xrightarrow{k_s} D_n + P_1$$

---

where

I = Azobisisobutyronitrile (initiator)

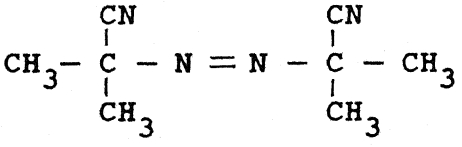

M = Methylmethacrylate (monomer)

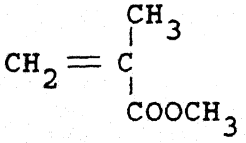

All these models introduce an artificial break-point in either the monomer conversion or the chain length, or both, at which the diffusional restrictions become dominant. These and several other of the earlier theories have been reviewed by O'Driscoll (7) and Hamielec (8).

Diffusional limitation was introduced as an integral part of the termination and propagation reactions by Chiu et al. (9). The effects of composition, temperature and molecular weight were accounted for continuously. The phenomenological nature of this model led to several interesting studies (10-18), with reference to engineering applications, focusing on aspects such as parametric sensitivity (15), optimization (13,16), optimal parameter estimation (17,18), etc. More recently, Achilias and Kiparissides (19,20), extended the model of Chiu et al. using the diffusion theory of Vrentas and Duda (21), and the theory of excess chain-end mobility (22), to give a molecular basis for the theory.

The model developed by Soong and coworkers for *batch* polymerizations, though applied to the simulation and optimization of *semibatch* reactors (13,14), is questionable in its extension to such operations. This doubt arises from the use of the initial value of the initiator concentration, $[I]_o$, in the model to account for the molecular weight dependence of the diffusivity of polymer radicals. Thus, it is unclear as to what should be used in place of $[I]_o$ in the model after the sudden addition of initiator, monomer or solvent to the reaction mass. This is an important question, in view of the fact that in industrial reactors such additions are made routinely to obtain optimal operation. A similar doubt is present in the theory of Achilias and Kiparissides (19,20), in which an empirical curve-fit parameter, j_{co}, related, in turn, to the *initial* number average chain length, $\mu_{n,o}$, is introduced to give proper curve-fit of isothermal experimental data. Some work has been reported (18,23) recently which attempts to resolve this controversy. A new model has been developed (23) for the gel and glass effects which is applicable to both batch and semibatch reactors under a variety of operating conditions. The validity of this theoretical

model, however, needs to be established using experimental data under nonisothermal and semibatch reactor conditions. The present study focuses on the nonisothermal operation of batch reactors.

Work on *isothermal* bulk polymerization of MMA has been reported earlier (6). These results are based on experimental studies on ampoule reactors in which mixing effects as well as heat and mass transfer limitations do not play an important role. In the present work, however, a 1 liter stainless steel Parr reactor (Parr Instrument Company, Moline, IL, USA) has been interfaced with a PC-XT and methyl methacrylate is polymerized in it under controlled temperature histories. Several physico-chemical phenomena which are present in industrial reactors (e.g. vaporization, heat transfer through the viscous reaction mixture, etc.) are also present in our experimental reactor, and so our experimental results can be used more meaningfully to develop techniques, models and design-methodologies for larger prototypes. Experimental data on the monomer conversions and average molecular weights have been obtained for a variety of (nonisothermal) temperature histories, such as step increase and step decrease, and the results compared against model (23) predictions.

The implementation of a desired temperature history in polymer reactors is not a trivial task. Achieving good temperature control is not easy due to the unfavorable combination of high heats of reaction and very high viscosities of the polymerizing mixture. Added to this is the complication introduced by the unsteady nature of the batch reactor. Very little work has been reported on this aspect. Elicabe and Meira (24) reviewed the literature in this area, but a detailed discussion is not being presented here for the sake of brevity. Amrehn (25) discussed a simple model-predictive controller qualitatively, which manipulates the jacket liquid temperature to control the temperature of a polymerization reactor. More recently, the performance of several kinds of controllers on polymerization reactors has been simulated by Congalidis et al. (26), and by Hidalgo and Brosilow (27). Soroush and Kravaris (28) have recently tested a globally linearizing control (GLC) algo-

rithm experimentally on a 5 liter stirred glass batch reactor in which MMA is polymerized under an *optimal* temperature history. They used the model of Chiu et al. (9) to compute this optimal history. Their control algorithm was found to track this temperature history very well. In our study, however, we decided to employ a simple proportional-integral (PI) algorithm with set-point changes, to control the reactor temperature in the desired manner. Actually, facility for both heating and cooling the reaction mass was provided, the rates of which could be manipulated using two different PI controllers. An empirical gain scheduling was also included in the control algorithm. This scheme was found to give a fairly rapid heating-up of the reaction mass when required, as for example, during the initial period, or in experiments involving a step increase in the temperature at some point of time. The controller could also implement reasonably fast decreases in temperature, when so required. In addition, this controller could maintain the temperature constant whenever this was desired. However, the simple PI controller does not work too well when the rate of release of the (exothermic) heat of reaction becomes very rapid, some time after the onset of the gel effect, and simultaneously mixing becomes difficult due to the high viscosity of the reaction mixture. In spite of this defeciency, we were able to obtain experimental data uptil sufficiently high conversions and were able to validate the theoretical model of Ray et al.(23).

In this thesis, Chapter 2 describes the experimental set up used along with details of computer interfacing to record and control the reactor temperature. Chapter 3 elucidates the dynamics of the control variables, the temperature controller design and the software to implement the controller. Chapter 4 gives the procedure followed to carry out the polymerization and the analytical methods adopted to estimate conversion and molecular weights. Results and discussions are presented in Chapter 5. Conclusions drawn from the present study and recommendations for future work are included in Chapter 6.

CHAPTER 2

EXPERIMENTAL SET-UP

In this chapter the experimental set-up, which includes the Parr reactor assembly, the computer and its peripherals, sensors and their calibration, transducers and actuators, is described.

2.1 REACTOR

The polymerization was carried out in a one liter stainless steel Parr reactor (Fig.1a) (Parr Instrument Company, Moline, IL, USA). This reactor is designed to operate at pressures upto 1.4×10^4kPa and tempertures upto 350°C. It has split ring closures for easy access to the interior of the bomb without using heavy screw caps or cumbersome cover clamps. In this design the closing force between the head and the bomb is developed by six cap screws which are held in a hardened steel clamping ring that has been split into two halves. These rings slide into place from the sides of the bomb so as not to disturb any fittings attached to the bomb head. A steel retaining ring raised into place from the bottom of the bomb completes the assembly.

The reactor assembly can be lowered into a furnace (Fig. 1b) which is provided with electric heating coils (1.5 kW), surrounded by a thick layer of insulating material. A helical cooling coil is placed inside the bomb (Fig. 1c). The contents of the reactor are mixed with two turbine impellers each with six blades, placed one above the other on a stirrer shaft. The reactor is fitted with three valves for different purposes (Fig. 1a). Valve V_1 is a gas release valve which can also be used to apply vacuum to the reactor. Valve V_2 is the gas charging valve. Valve V_3, connected in the same line as V_2, is meant for

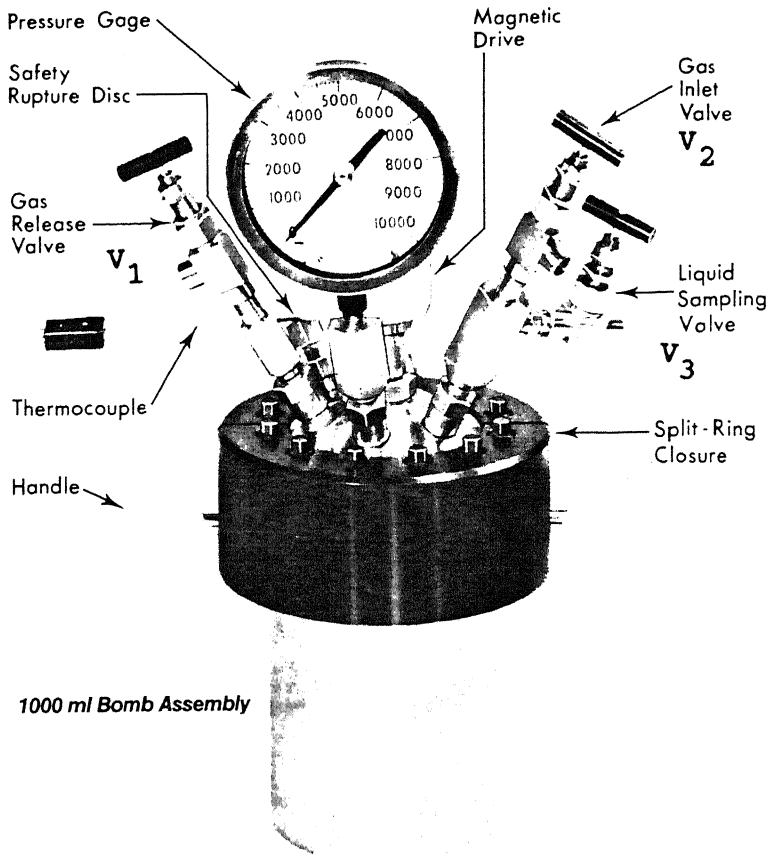
Pressure Gage
Safety
Rupture Disc
Gas
Release
Valve
V_1
Thermocouple
Handle
Magnetic
Drive
Gas
Inlet
Valve
V_2
Liquid
Sampling
Valve
V_3
Split-Ring
Closure
1000 ml Bomb Assembly

(a)

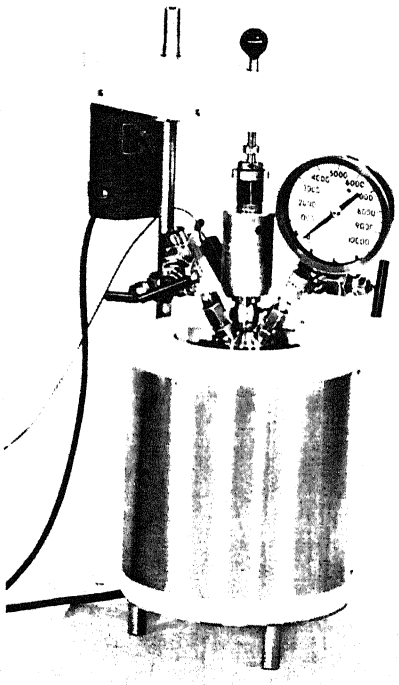

(b)

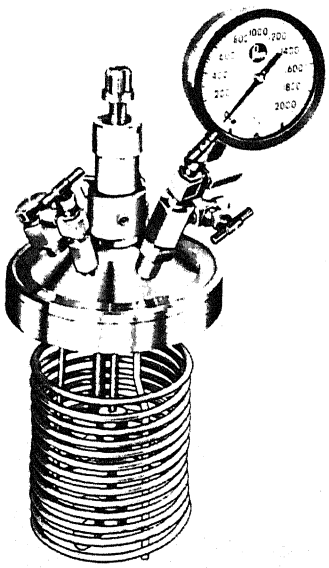

(c)

collecting liquid samples from the reactor when the latter is pressurized. Valves V_2 and V_3 are installed on a dip tube which extends to the bottom of the reactor. There is a pressure gauge ($0 - 1.4 \times 10^4$ kPa) connected to the reactor through a needle valve. This valve helps in isolating the pressure gauge while the reactor is being evacuated. There is a thermowell fitted to the reactor head which extends into the liquid section of the reactor. A non-conducting and thermally stable liquid, silicone oil, is used as the thermowell liquid. An Argon gas (IOL-AR2, Indian Oxygen Limited, New Delhi, India) cylinder is used to pressurize the reactor and to carry out the reactions in an inert atmosphere.

A 1.25cm SS needle valve operated with a stepper motor (Unique Systems and Control Private Ltd., New Delhi, India) is fitted to a cooling water line (1.25cm steel pipe) connected, in turn, to an overhead water tank, to enable control of cooling water flow rate. The flow rate of the cooling water is measured with an orificemeter (orifice diameter 0.3176 cm).

2.2 COMPUTER SYSTEM

The system consists of an IBM compatible (WIPRO) PC-XT with a 640 kB RAM, 20 MB hard disk, one floppy disk drive, a DT-2805 I/O interface card (Data Translation Inc., Marlborough, MA, U.S.A) with its companion DT-707T screw terminal, and a printer.

2.2.1 I/O INTERFACE CARD

A DT-2805 low level analog and digital I/O interface card has been used for interfacing the process with the computer (Fig.2). The card provides 8 differential ADC (Analog to Digital Converter) channels with programmable gains of 1, 10, 100 and 500 and two DAC

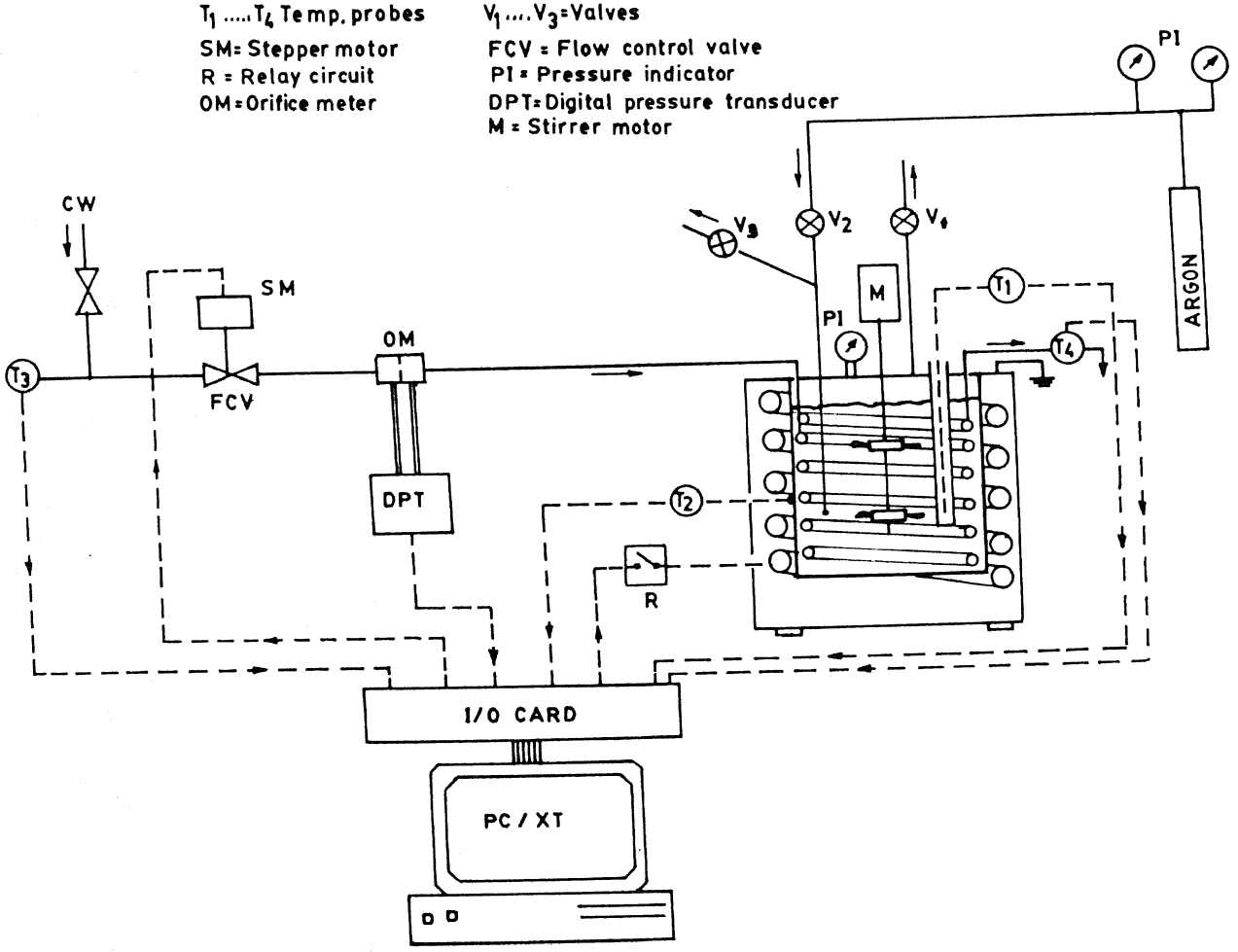

Fig.2 Schematic diagram of experimental set-up

(Digital to Analog Converter) ports. The two ports (ports 0 and 1) of the digital I/O section have 8 bits each for data transfer. These ports can be addressed separately or in combination as a single port by choosing a proper binary value (mask value). The analog channels are used to measure analog inputs like thermocouple signal, pressure transducer signal, etc. The digital ports are used to run a stepper motor and to switch a solid state relay.

The I/O card can be programmed to perform 12-bit [resolution $1/(2^{12}-1)$] analog to digital (A/D) conversion at 40 kHz and digital to analog (D/A) conversion at 33 kHz. As this is a low level card capable of accepting signals as low as 20 mV (full scale), differential inputs become necessary to eliminate noise.

All the outputs, analog or digital, are held constant until changed or the board is reset by the in-built zero order hold circuit. It has its own on-board clock and processor for fast operation. An external clock can also be used. The jumper settings have to be chosen carefully for different configurations.

The interface card is mounted in one of the slots of the mother board of the PC. It draws 1.2 A at 5 V from the mother board. The DT-707T screw terminal is connected to the board with a ribbon cable. The sensor and actuator connections are conveniently made to the screw terminal which resides outside the computer. This screw terminal also supports the measurements for a set of standard thermocouples. Room temperature is measured with a built-in solid state sensor connected to channel 0 of the screw terminal and this temperature is used for making cold junction compensation.

2.3 SENSORS AND TRANSDUCERS

2.3.1 TEMPERATURE MEASUREMENT

There are four temperature sensors used in this experiment (Fig.2), which measure the reactor inside temperature, the cooling water outlet temperature, the reactor outside wall temperature and the cooling water inlet temperature. The first three of them are copper-constantan thermocouples, and the fourth is a solid state sensor connected with a temperature transmitter (Analog Devices Inc., Norwood, MA, USA, model 2B57A) and energized with a 28 V power supply. This solid state sensor has a span of 100°C in the range of 0 -140° C and was used to measure the inlet temperature of the cooling water. The 4-20 mA output of the sensor is converted into a voltage signal by connecting a resistor (500 ohm) in series in the circuit. The circuit diagram is given in Fig.3.

The procedure for calibrating the solid state sensor is as follows. First, the range of the sensor is adjusted to be 0-100°C by trimming the zero and span of the analog device over the full range of voltage measurement (for example, 0- 10V) by dipping it in melting ice and in boiling water. Then, the voltage drop is measured as a function of temperature by immersing the sensor in a constant temperature bath (Julabo Labortechnik, Seelbach, Switzerland, model F10MH) maintained at different temperatures, and measuring the voltage after it stabilizes. The calibration information is shown in Fig.4. The data points were correlated using the following linear relationship:

$$T(^{\circ}C) = 13.9313V - 27.8533 \quad (1)$$

where V is in volts.

The temperature measurement by thermocouples is done by the subroutine ' MeasureThermocouple '. The details of the measurement procedure can be found in the PCLAB

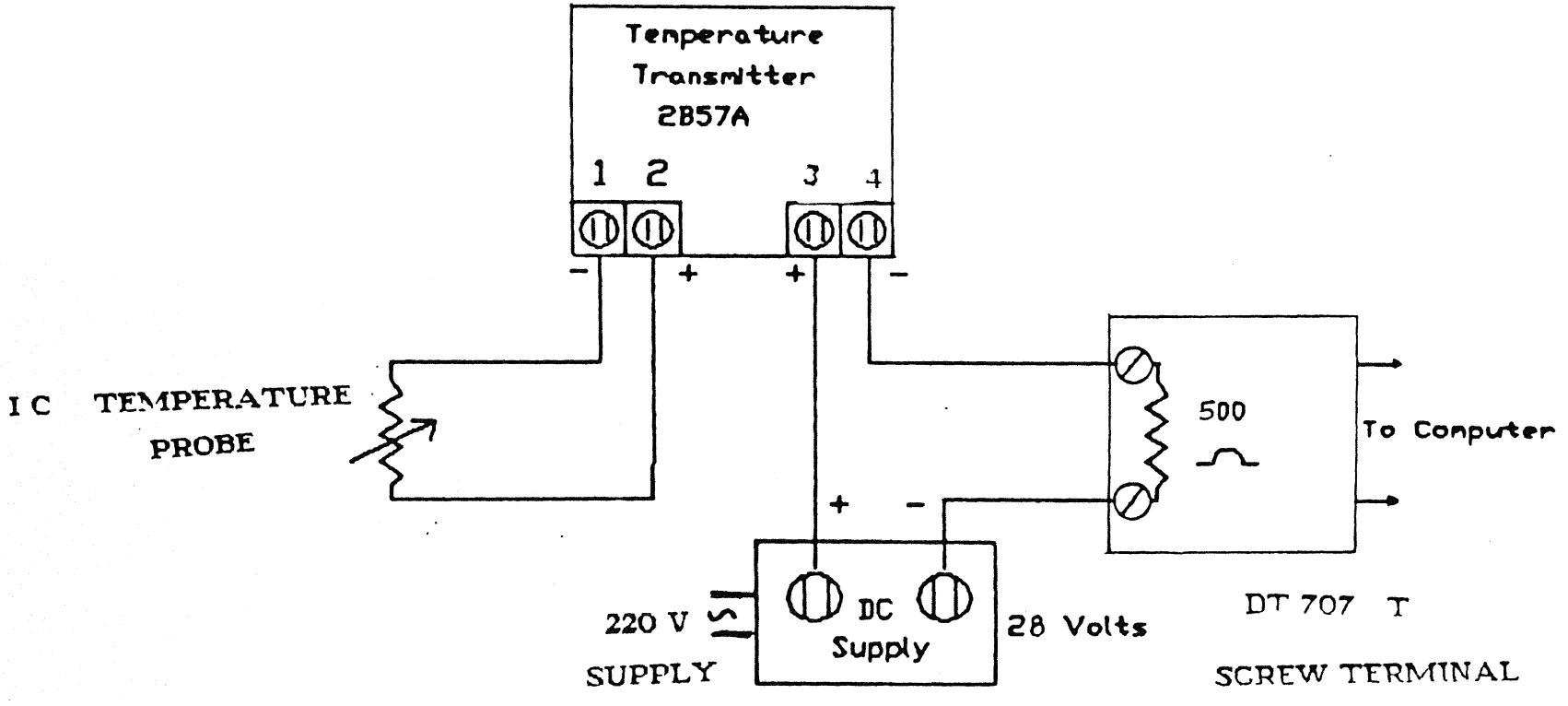

Fig.3 Circuit diagram for the solid state temperature sensor

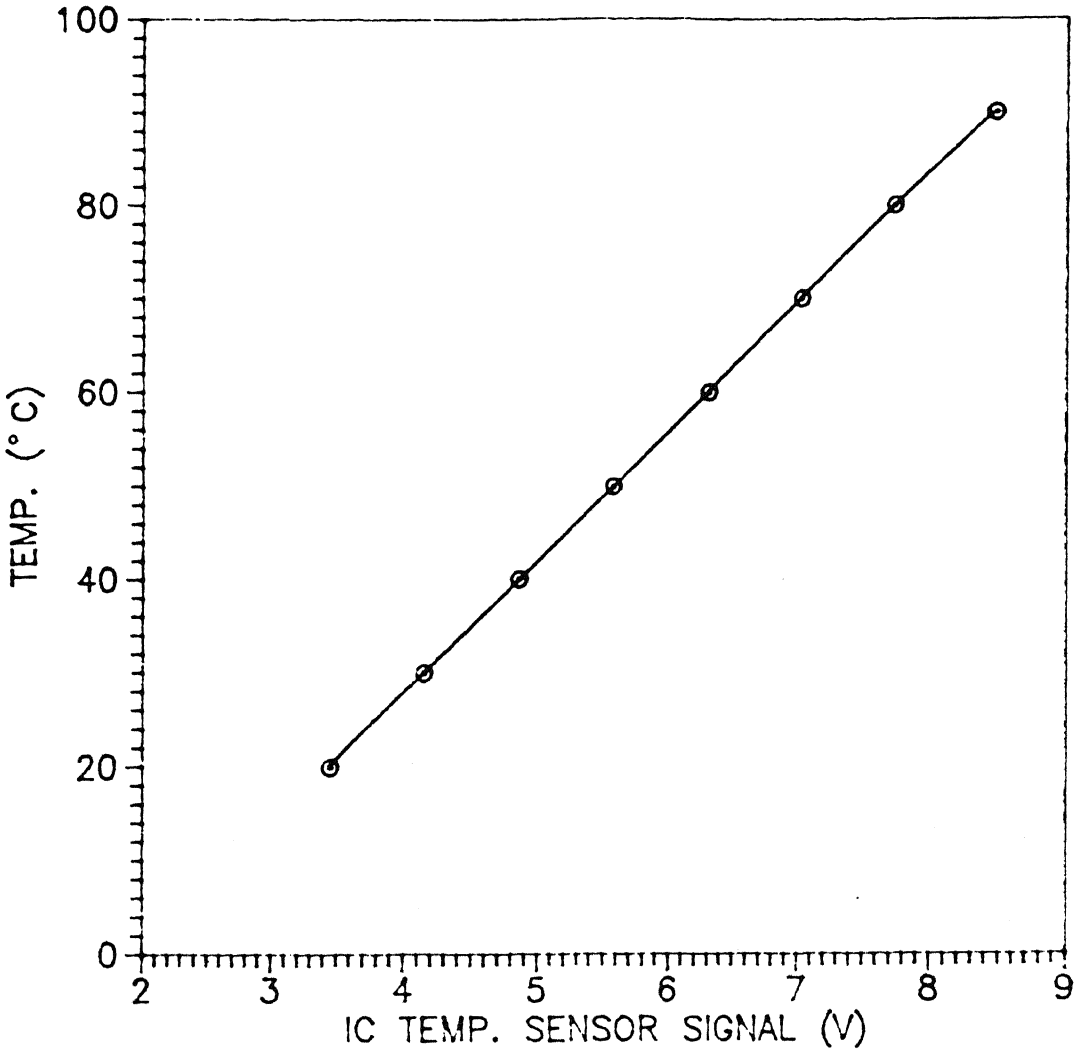

Fig.4 Calibration of the solid state temperature sensor used for cooling water inlet temperature measurement (T_3 in Fig.2)

manual (Data Translation Inc., Marlborough, MA, U.S.A) (29). Although the interface card supports the copper-constantan thermocouples, it was found necessary to recalibrate the individual thermocouples from time to time. This was achieved using the Julabo F10MH constant temperature bath. The temperature read by the computer was calibrated against the actual (bath) temperature and these data were fitted with a straight line and used for more accurate measurement. The least squares fit equations are:

For the reactor temperature,

$$T_{actual} = 0.996114\ T_{measured} + 1.08907 \tag{2}$$

For the cooling water outlet temperature,

$$T_{actual} = 1.05097\ T_{measured} + 2.96102 \tag{3}$$

For the reactor outside wall temperature

$$T_{actual} = 0.99976\ T_{measured} + 1.19875 \tag{4}$$

These calibrations were checked from time to time. The above equations represent the temperature corrections made for the near isothermal 50°C run (NI50). This pseudo calibration information for the two thermocouples is shown in Figs.5 and 6. The thermocouple which measures the reactor temperature was calibrated along with the thermowell. This procedure allowed taking into account the static lag of the thermowell. The noise problem experienced with the thermocouples was greatly reduced after grounding the reactor with the 'ground' of the I/O card.

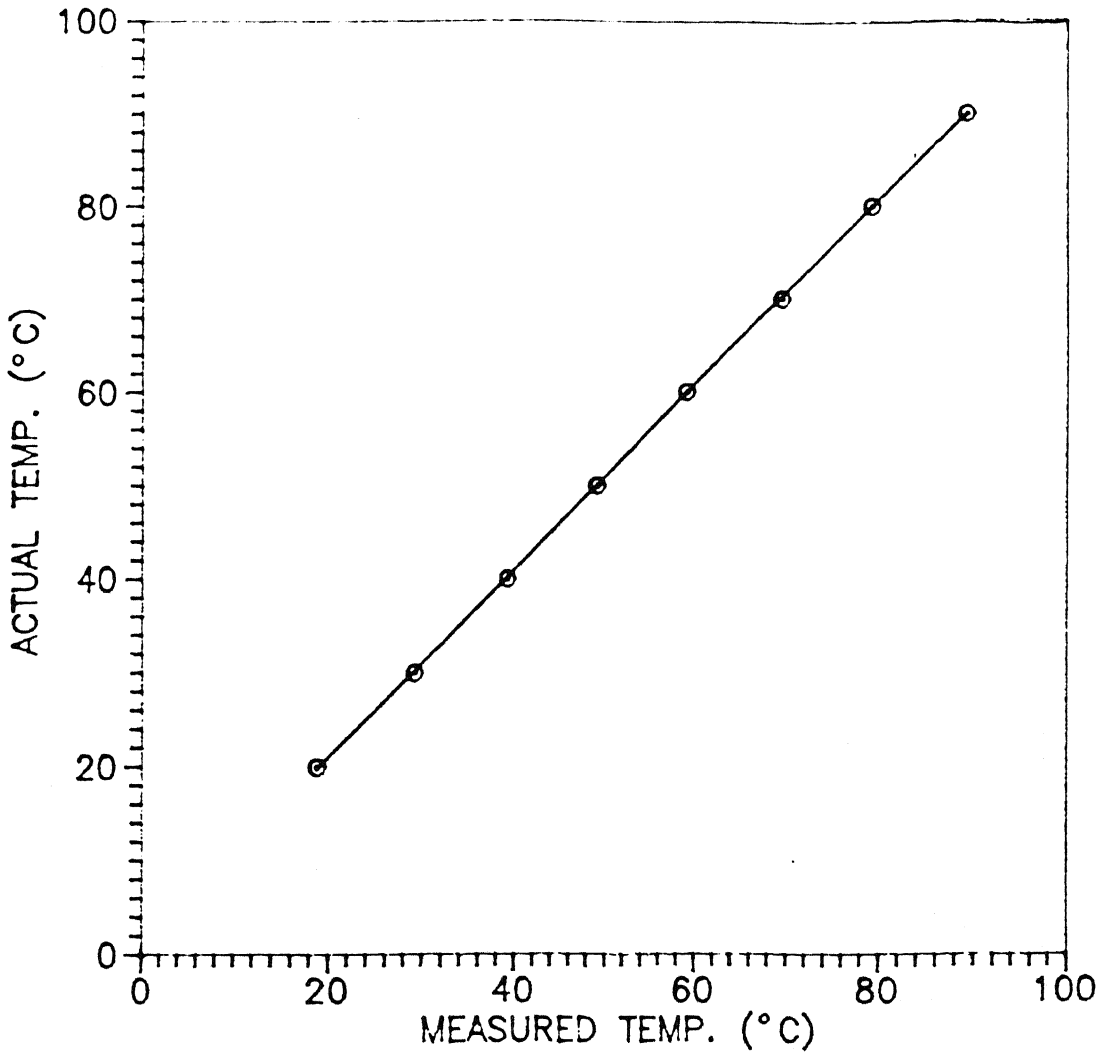

Fig.5 Calibration of the copper-constantan thermocouple used for measuring the reactor temperature (T_1 in Fig.2)

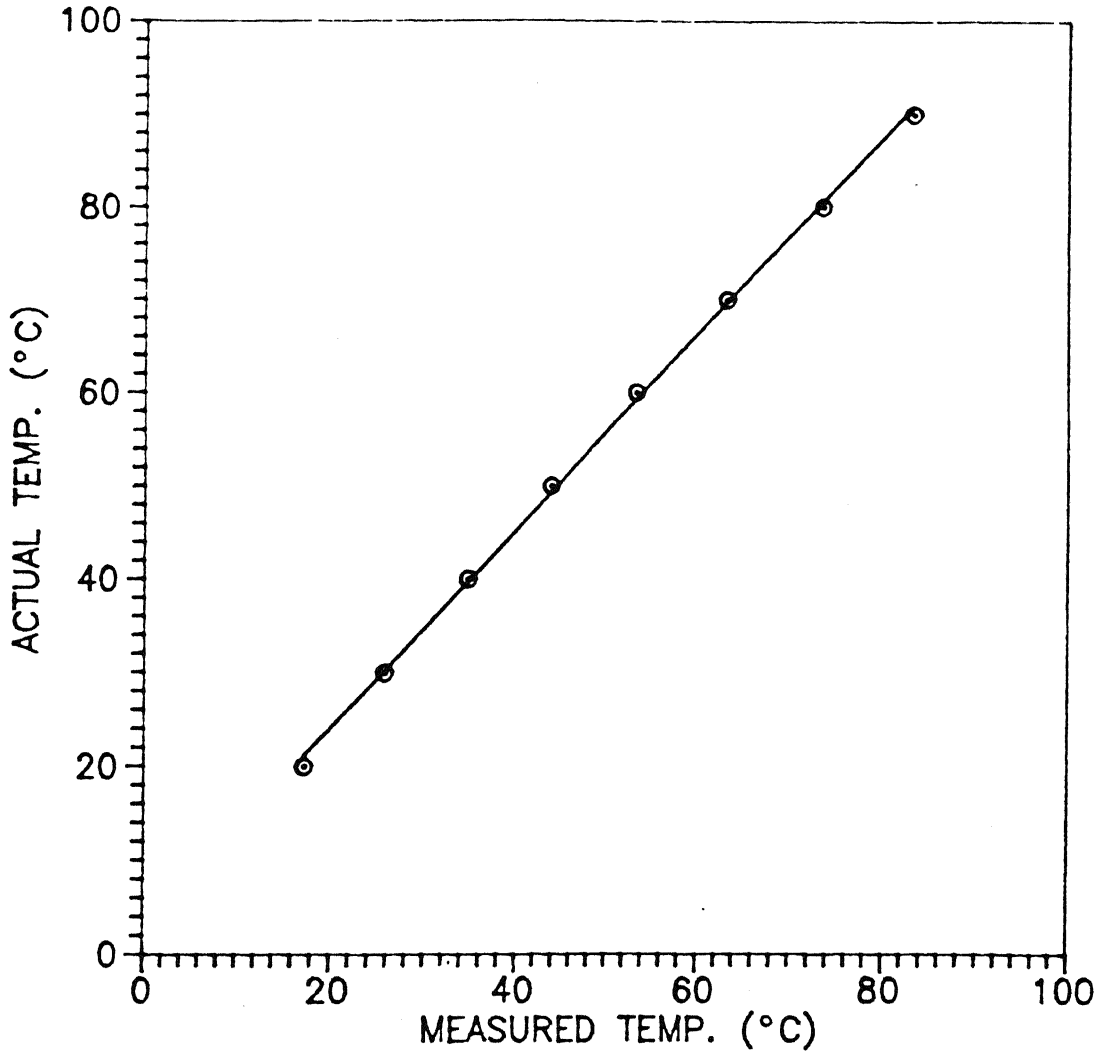

Fig.6 Calibration of the copper-constantan thermocouple used for measuring the cooling water outlet temperature (T_4 in Fig.2)

The solid state temperature sensor had an excellent stability and reproducibility, but its response was sluggish when compared to that of the thermocouples. It was therefore used to measure the inlet temperature of the cooling water whose variation was expected to be the least. A thermocouple was used to measure the outlet temperature of the cooling water. Even though the inlet and outlet temperatures of the cooling water were not used for control at present, these are available for future use in advanced control applications.

2.3.2 FLOW MEASUREMENT

The cooling water flow rate is one of the two manipulated variables for the control of the reactor temperature. An orifice meter was designed and fabricated in-house (Fig. 7) to measure the cooling water flow rate. The pressure drop across the meter was measured with a differential pressure transmitter (DPT, Taylor Instruments, Faridabad, India) having a range of 0 - 10 cm. of water. The 4-20 mA current output of the DPT was converted into a voltage drop by passing it through a 500 ohm resistor. The DPT was energized with a 24 V DC power supply. The circuit diagram of the DP cell is shown in Fig.8.

For calibration, the range of the sensor was first adjusted to be between the minimum flow rate (4 mA) and the maximum flow rate (20 mA) by trimming the zero and span adjustments repeatedly until further adjustments were not required. Then the voltage drop was measured and recorded as a function of water flow rate in the system by changing the valve opening. The flow rate was found by measuring the water collected for a known interval of time. The flow rate (fr) *vs.* voltage drop (V in volts) information is given in Fig.9. The experimental data were fitted with two best-fitting polynomials in two zones.

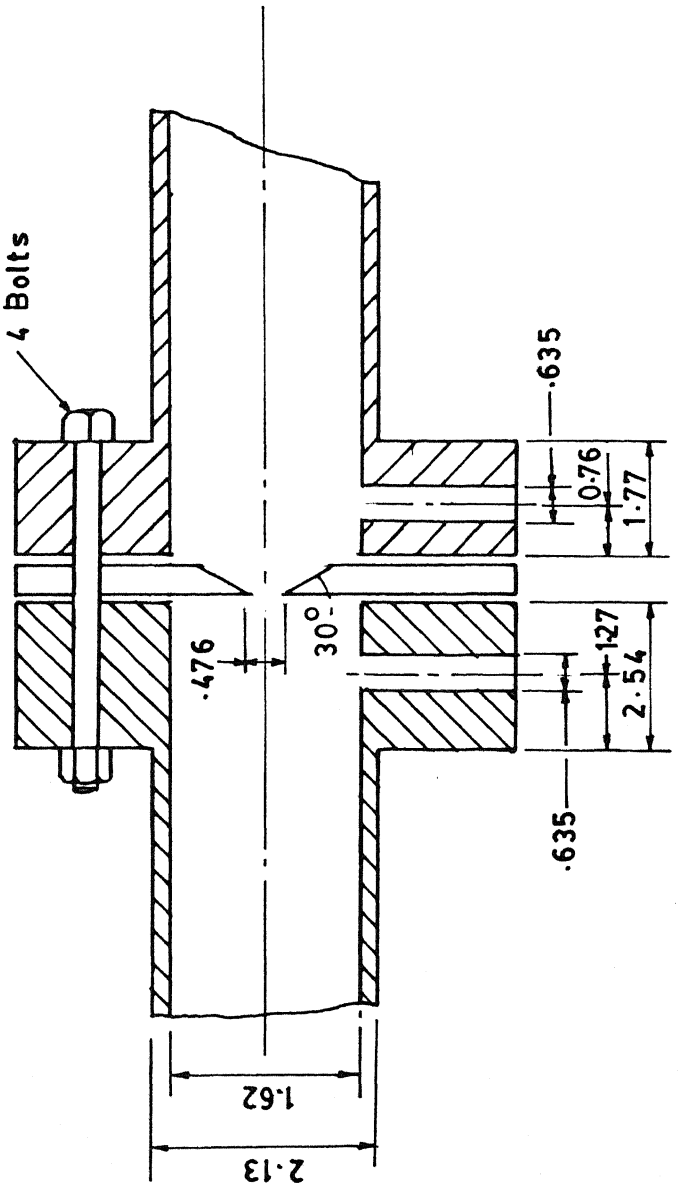

Fig.7 Details of the orifice plate flow meter used for cooling water flow rate measurement

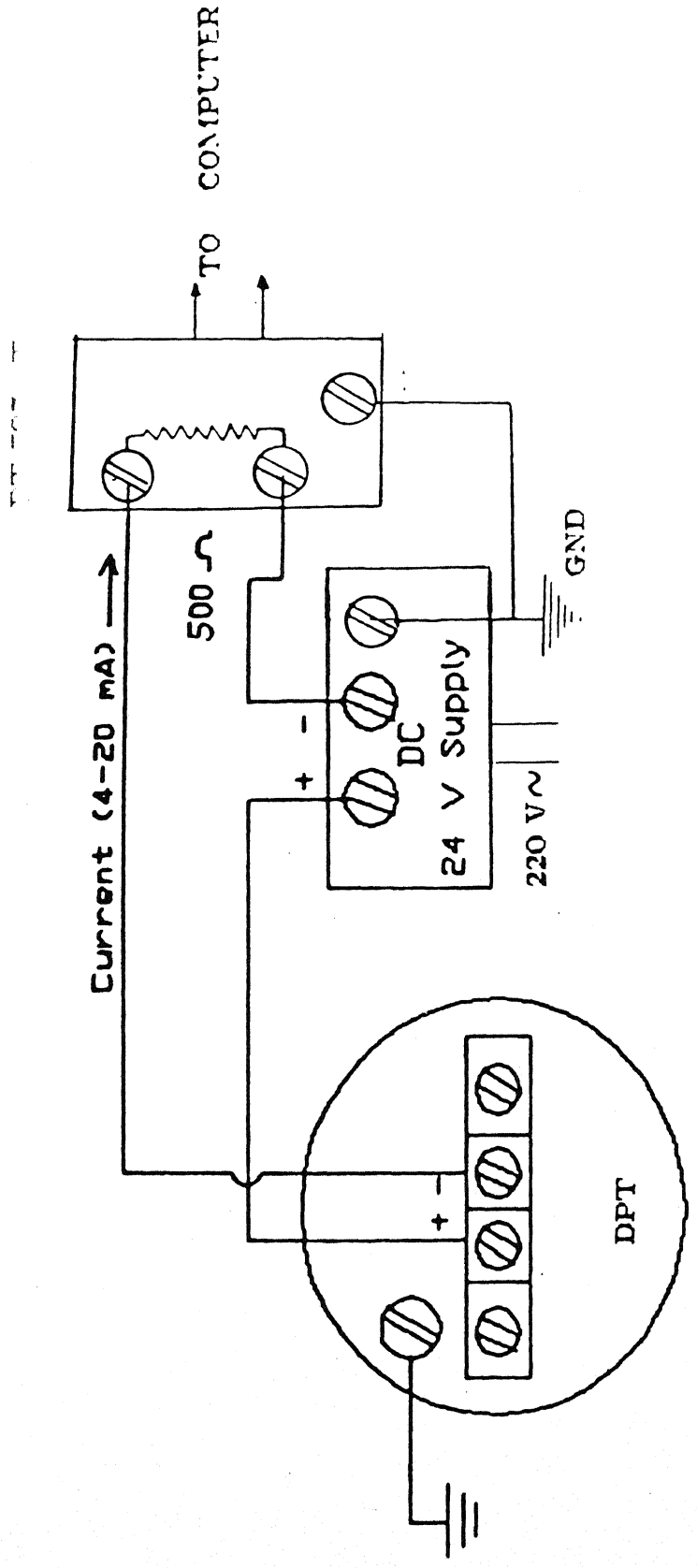

Fig.8 Circuit diagram for the DPT

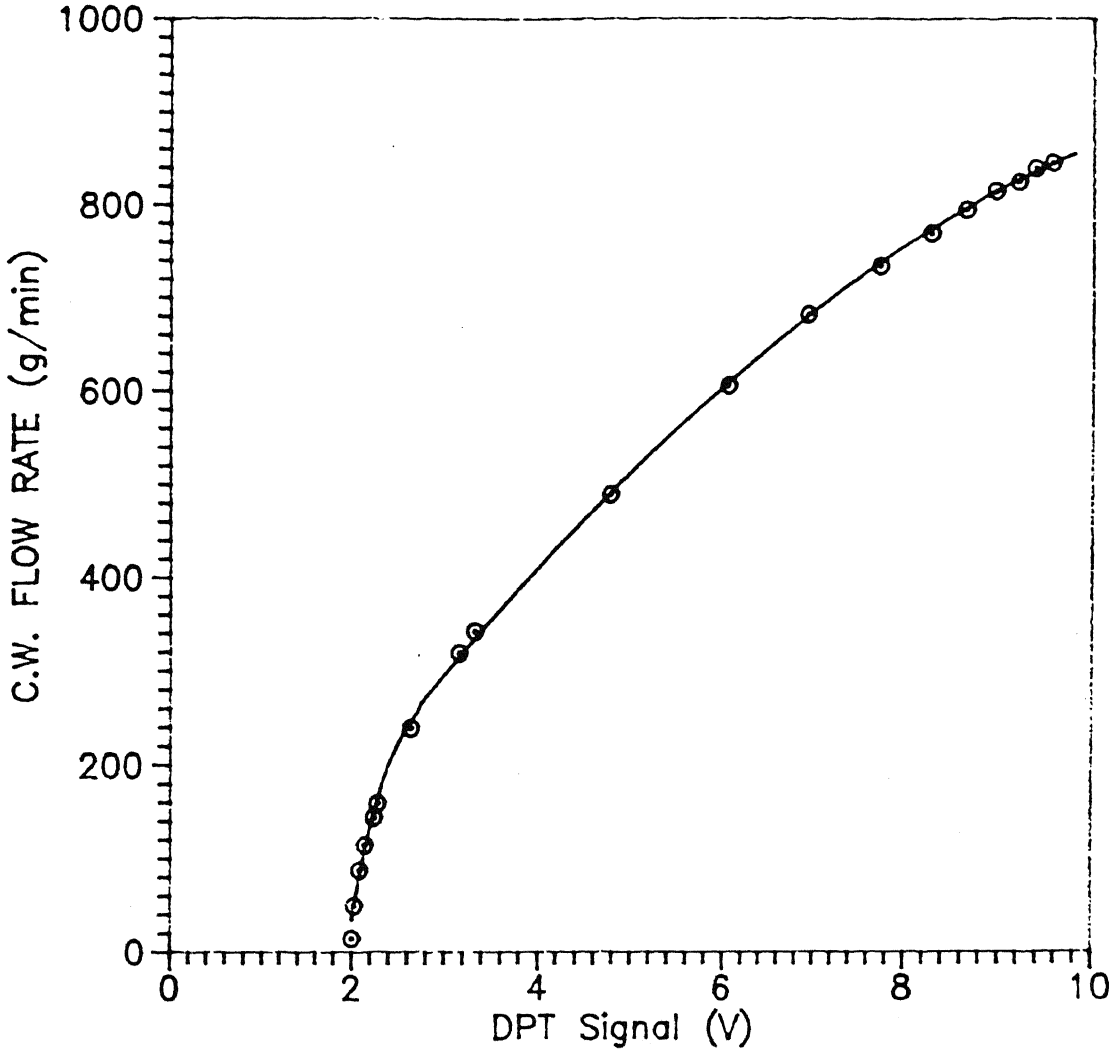

Fig.9 Calibration for the orificemeter

They are given by:

For 2 < V < 2.7

$$fr(g/min) = 227.062V^3 - 1946.25V^2 + 5672.84V - 5342.18 \quad (a)$$

For 2.7 ≤ V < 10.0

$$fr(g/min) = -5.4522V^2 + 152.036V - 110.311 \quad (b) \quad (5)$$

Where V is in Volts.

2.4 ACTUATORS

2.4.1 STEPPER MOTOR

The cooling water flow rate was controlled with a needle valve (1.25 cm) actuated by a stepper motor (Unique Systems and Control Private Ltd., New Delhi, India). The shaft of the motor is rigidly fastened to the stem of the needle valve through a coupling. Since one revolution of the motor shaft is divided into 200 steps, each step rotates the stem through 1.8° angle. One sequence of pulses will rotate it in the clockwise direction (closing the valve) while the reverse sequence will rotate it in the anticlockwise direction (opening the valve). These sequences, along with the binary values if connected to the first four bits of a port are shown in Tables 2 and 3.

The TTL (Transistor Transistor Logic) output from the computer cannot run the stepper motor directly. The pulses from the computer are sent to a board having diodes and solid state relays connected as shown in Fig.10 which converts the pulses into a synchronized

Table - 2

Sequence of pulses to stepper motor for clockwise motion of the shaft

Step No.	I	II	III	IV	Binary
1	1	1	0	0	12
2	0	1	1	0	6
3	0	0	1	1	3
4	1	0	0	1	9
5	1	1	0	0	12

Table - 3

Sequence of pulses to stepper motor for anticlockwise motion of the shaft

Step No.	I	II	III	IV	Binary
1	1	0	0	1	9
2	0	0	1	1	3
3	0	1	1	0	6
4	1	1	0	0	12
5	1	0	0	1	9

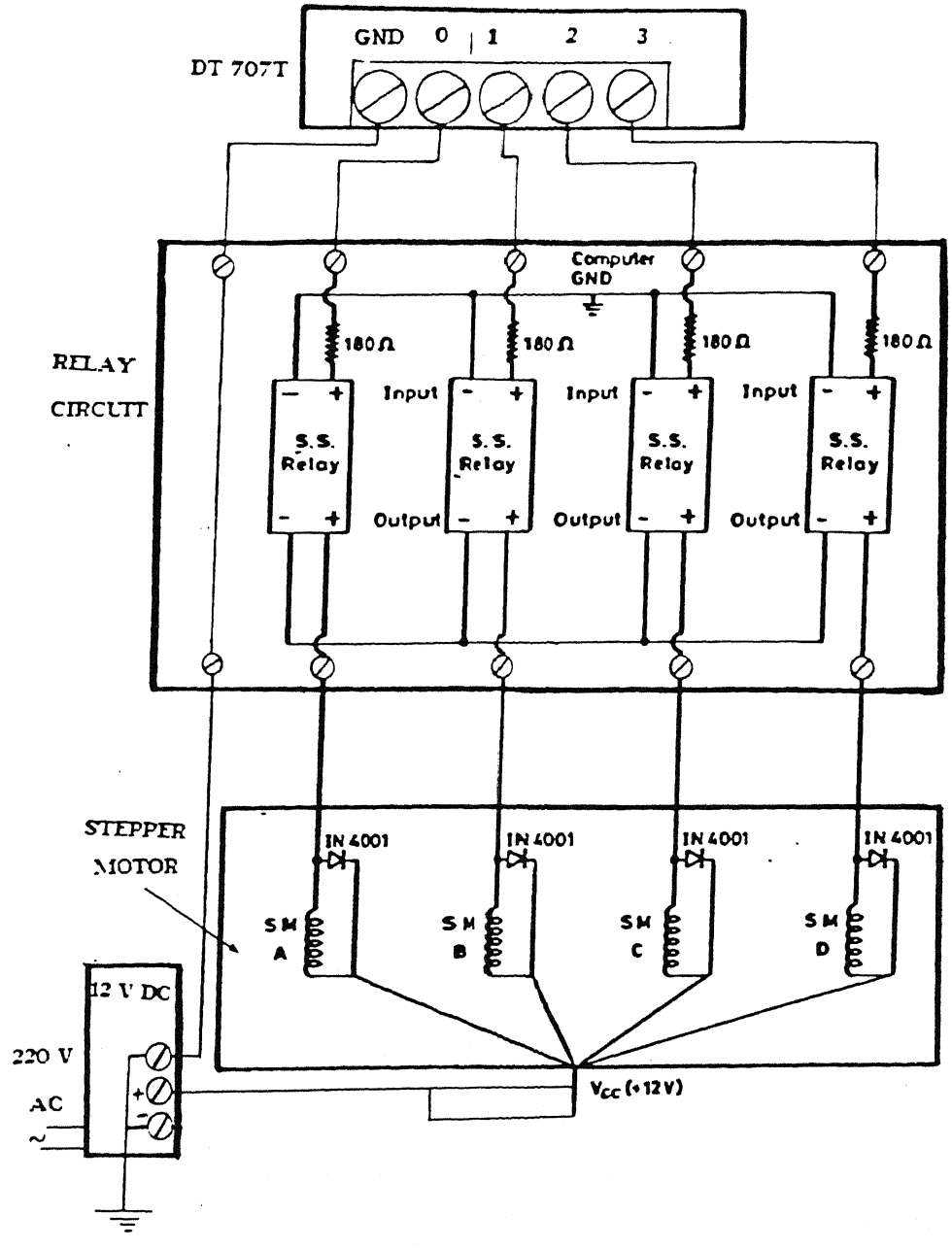

Fig.10 Driving circuit for the stepper motor

pulse train. The stepper motor requires a 12 V DC power supply. The stepper motor driver program is given in Appendix-2.

2.5 FINAL CONTROL ELEMENTS

2.5.1 NEEDLE VALVE

A mult-turn 1.25 cm needle valve was used as the final control element to control the flow of the cooling water. The stem of the valve is connected to the stepper motor by a rigid coupling which eliminates any backlash. The motor was mounted on a flexible cushion seat to allow up-and-down motion, while at the same time it was restricted from rotation around its axis by fixing it rigidly at its corners with long bolts. It takes nearly 8 turns for the needle valve to open completely. As mentioned earlier, 200 steps of the stepper motor lead to one rotation of the stem. Therefore, 1600 steps are required to open the valve completely. Such a large number of discrete positions of the valve make the control action almost continuous.

The stem position (in steps of the stepper motor, S) of the needle valve was also calibrated against the cooling water flow rate [fr(g/min)]. The experimental data were fitted with the following two polynomials:

For $15 < \text{fr} < 500$

$$S = 8.49779 \times 10^{-7} fr^3 - 6.76177 \times 10^{-4} fr^2 + 0.42872 fr + 0.843042 \quad (a)$$

For $500 \leq \text{fr} < 900$

$$S = 6.74481 \times 10^{-11} fr^5 - 1.59919 \times 10^{-7} fr^4 + 1.45021 \times 20^{-4} fr^3$$
$$-0.0615486 fr^2 + 12.1968 fr - 800.288 \quad (b) \qquad (6)$$

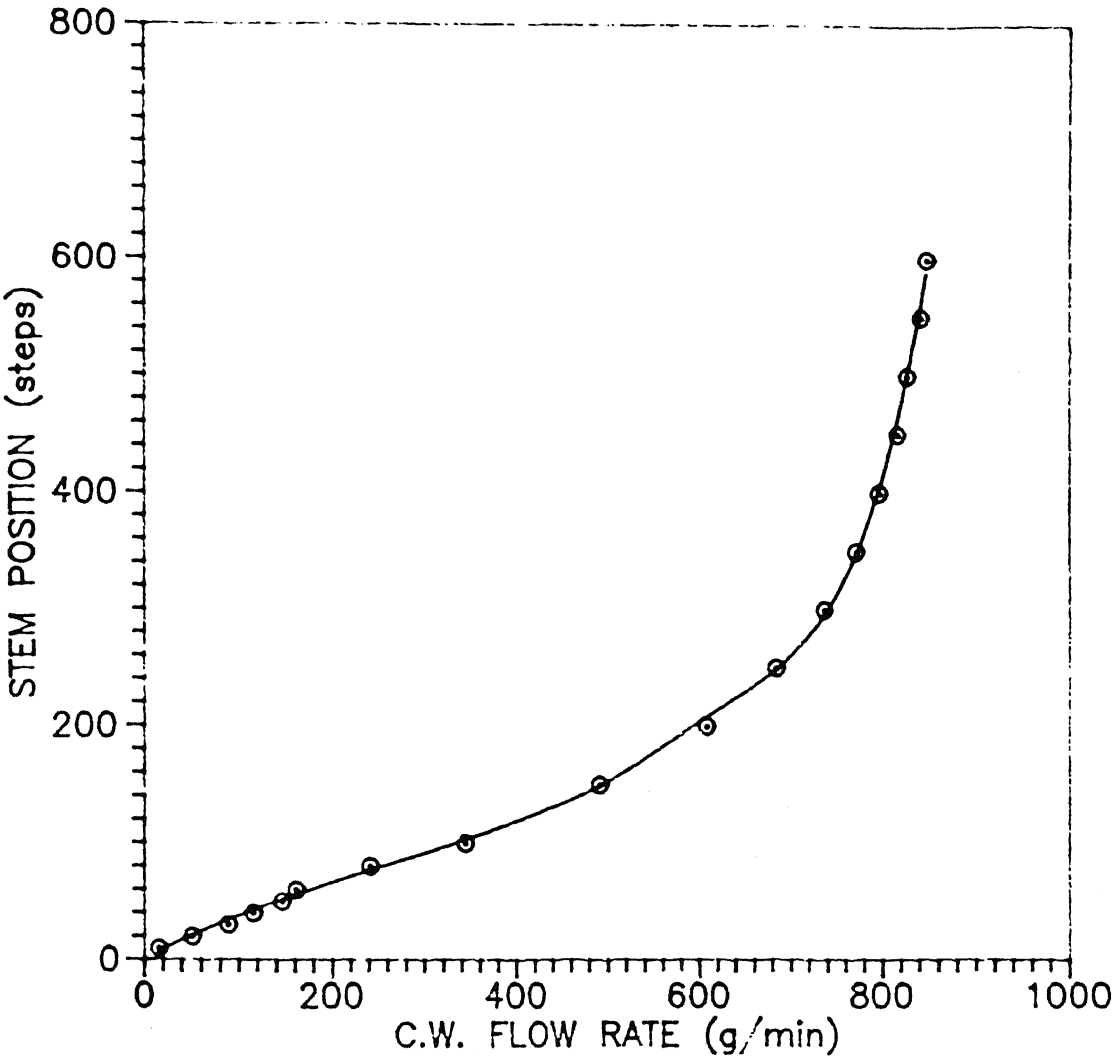

Fig.11 Calibration for the stepper motor

These equations were used for controlling the flow rate. Fig.11 gives the information on calibration.

2.5.2 FURNACE CONTROL

The heater power input is time-proportioned and implemented using a solid state relay (JDA 331000, Electronic Relays, Bangalore, India). The DC terminals of the relay are directly connected to a digital bit of the DT-707T. This relay can be set ON (high) or OFF (low) by the interface board. In the AC terminals of the relay, the furnace coil is connected in series with the 230 V AC power mains regulated with a variac (see Fig.12). A neon lamp was connected in parallel with the furnace which glowed to indicate the ON position of the heater.

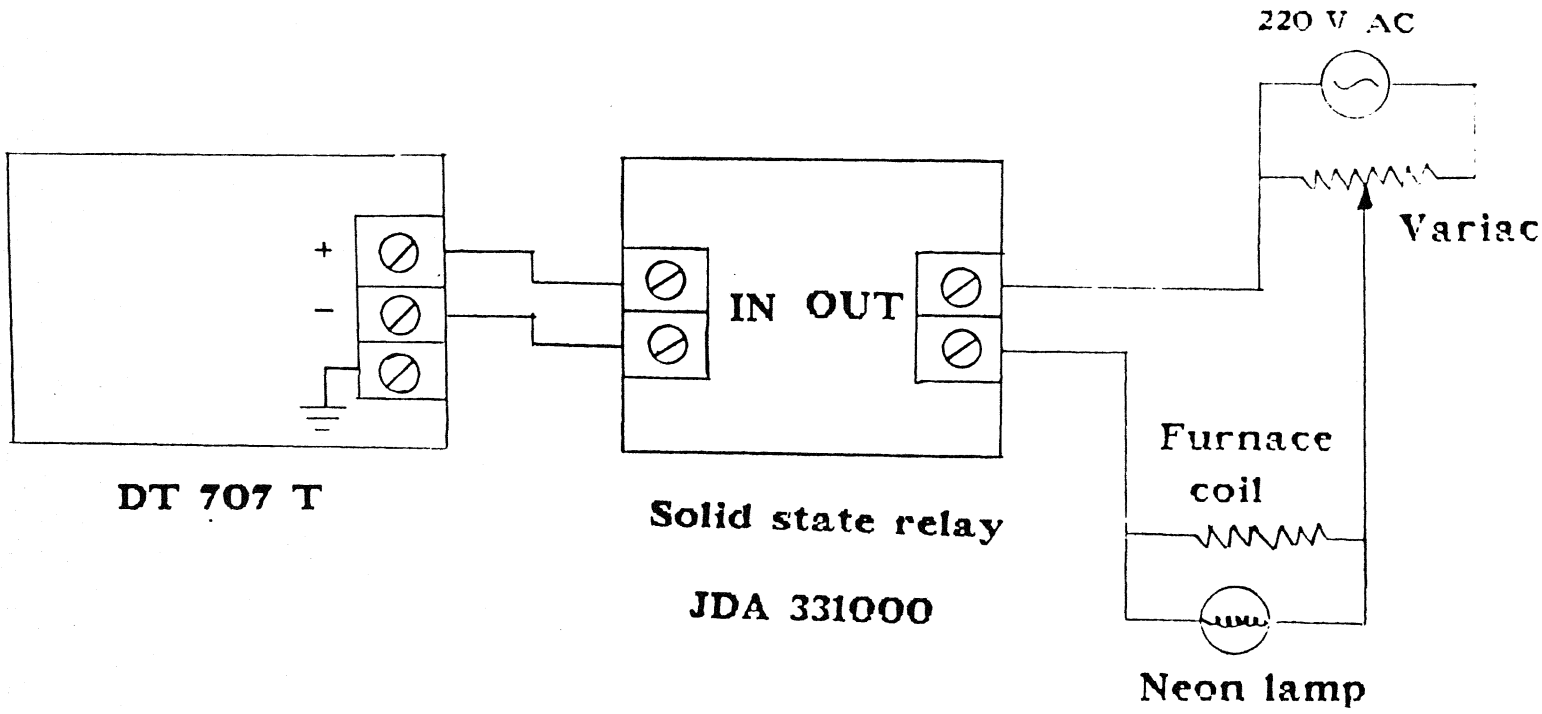

Fig.12 Furnace control circuit

CHAPTER 3

REACTOR TEMPERATURE CONTROL

The problems often encountered in industrial liquid phase bulk polymerization reactors are associated with heat released by exothermic reactions and increase in viscosity. The heat of reaction ranges from 40 to 85 kJ/mol causing an adiabatic temperature rise of about 200-400°C. Large generation of heat, coupled with low thermal diffusivities of the system often cause thermal runaway as well as significant spatial gradients. Since higher temperatures give products of low DP (degree of polymerization), this can lead to disastrous consequences in terms of product quality. Because of these additional features, polymerization reactors pose a challenging control problem.

Efficient control of temperature during exothermic heat release calls for a powerful cooling system. An equally effective strategy is necessary for rapid heating of the system from room temperature to the required temperatures (50-90°C), and to compensate for heat losses. Therefore, a single control variable, namely, reactor temperature, can be controlled best in such cases by suitably manipulating two variables, viz., cooling water flow rate and heater power input. In the present set-up it was decided to control one of the two variables at any time, depending on the sign of the error, T_{sp}-T, instead of lumping the two variables into one (28).

3.1 OPEN LOOP PROCESS DYNAMICS

The process response curves (30) were obtained for the two manipulated variables by conducting step tests to study the heating and cooling dynamics of the present system individually. These open loop dynamic tests were conducted using water in the reactor.

The process output of the step response test, reactor temperature, was fitted in the least squares sense to a first order-with-dead time model represented by:

$$G(s) = \frac{Y(s)}{X(s)} = \frac{K_p \exp(-t_d s)}{\tau_p s + 1} \qquad (a)$$

where

K_p = process gain = $\frac{change\ in\ output\ temperature}{change\ in\ heater\ power/\ coolant\ flow\ input}$ (b)

$Y(s), X(s)$ = process output and input in transformed coordinates (c)

t_d = process dead time or transportation lag (d)

τ_p = time constant of the process (e) (7)

The model parameters were obtained by using the Gauss-Newton technique with the Levenberg-Marquardt modification [code in Cuthbert (31) as modified by Maiti (32)].

3.1.1 HEATING CYCLE DYNAMICS

The heater power input was controlled by the computer using time proportioning. The manipulated variable is the fraction of time for which the heater (150 V AC from the variac) is ON during a cycle time (20 s in this case). In the long run, this is effectively equal to the control on the average power to the heater. Thus, for example, to give 50% average power to the heater, full power is supplied for 50% of the cycle time (for 10 s in a 20 s cycle).

To obtain the heating dynamics, the reactor was first brought to a steady state temperature by continued heating for 2 s in a 20 s sampling time. During this test no cooling water was circulated through the cooling coil. Steady state was achieved in about 4 hr. Then, a step of 2 s /20 s was applied by changing the heating time to 4 s/20 s. The

response of the system was followed by recording the reactor temperature at every sampling instant. This was continued for about 3 hr. The system parameters were obtained as (33),

$$\begin{aligned} K_p^h &= 361.082^oC\ /full\ power\ (i.e.\ 20\ s\ heating\ /\ 20\ s\ cycle) \\ \tau_p^h &= 213.87\,\text{min} \\ t_d^h &= 7.556\,\text{min} \end{aligned} \tag{8}$$

where the superscript, h, indicates heating.

3.1.2 COOLING CYCLE DYNAMICS

. The reactor was first brought to a steady state temperature of about 70°C. Both heating and cooling loops were then turned off. The cooling water flow was then suddenly turned on at a rate of 200 g/min. The falling temperature of the reactor was noted at every 10s. This gives the required dynamics of the cooling process alone. Here again the response was modeled using a first order-with-dead time transfer function. The calculated parameters of the cooling dynamics are (33),

$$\begin{aligned} K_p^c &= -0.2009^oC\ /(g/min) \\ \tau_p^c &= 6.8251\,\text{min} \\ t_d^c &= 0.6756\,\text{min} \end{aligned} \tag{9}$$

where the superscript, c, indicates cooling.

3.2 CONTROL ALGORITHM

. The main thrust in the present work was to study the reaction kinetics of MMA polymerization under near-isothermal conditions and with step changes in temperature. For this reason, relatively simple but efficient control algorithms were used in this work.

The control law studied was a simple coordination law between heating and cooling. This gave fairly satisfactory results. The decision to heat or cool is taken depending on whether the reactor temperature is below the set point or above it, i.e., if e(i) [$=T_{sp}$-T(i)], the error signal at time t_i is greater than a number ϵ, then the reactor is heated using the heating PI controller. On the other hand, if e(i) is less than $-\epsilon$, then the cooling water loop is actuated using the cooling PI controller. Here, ϵ is a small tolerance (=0.25°C) to account for the noise in the temperature signal. If the|error| is within ϵ, then neither heating nor cooling is done and the controller waits for the next sampling time.

The simple control strategy discussed above gave satisfactory performance in terms of rapid set-point tracking. The performance curves for two experimental runs with water alone and with polyvinyl alcohol solution in the reactor are shown in Fig.13, using the value of the controller parameters as given in Table 4. As seen in the figures, the control scheme performed satisfactorily. A combined control variable like the net heat added to the system could have been used (28) instead, but was not attempted.

It was observed during trial runs with water in the reactor that once the temperature in the reactor dropped, it took a considerable amount of time for it to reach the set point again. This problem is to be expected in view of the delay time for the heater being an order of magnitude larger than that for the cooling system. To overcome this, power was supplied to the heater for 0.5 s / 20 s during both the cooling and the waiting periods. The exact amount of heating was tuned in such a way that it compensated for most of the heat loss to the surroundings.

A sampling time of 20 s for heating and 10 s for cooling was used in this study since the cooling dynamics was relatively faster. The derivative action was not included for digital control as the temperature measurements were relatively noisy and derivative action without an effective filter would have been useless.

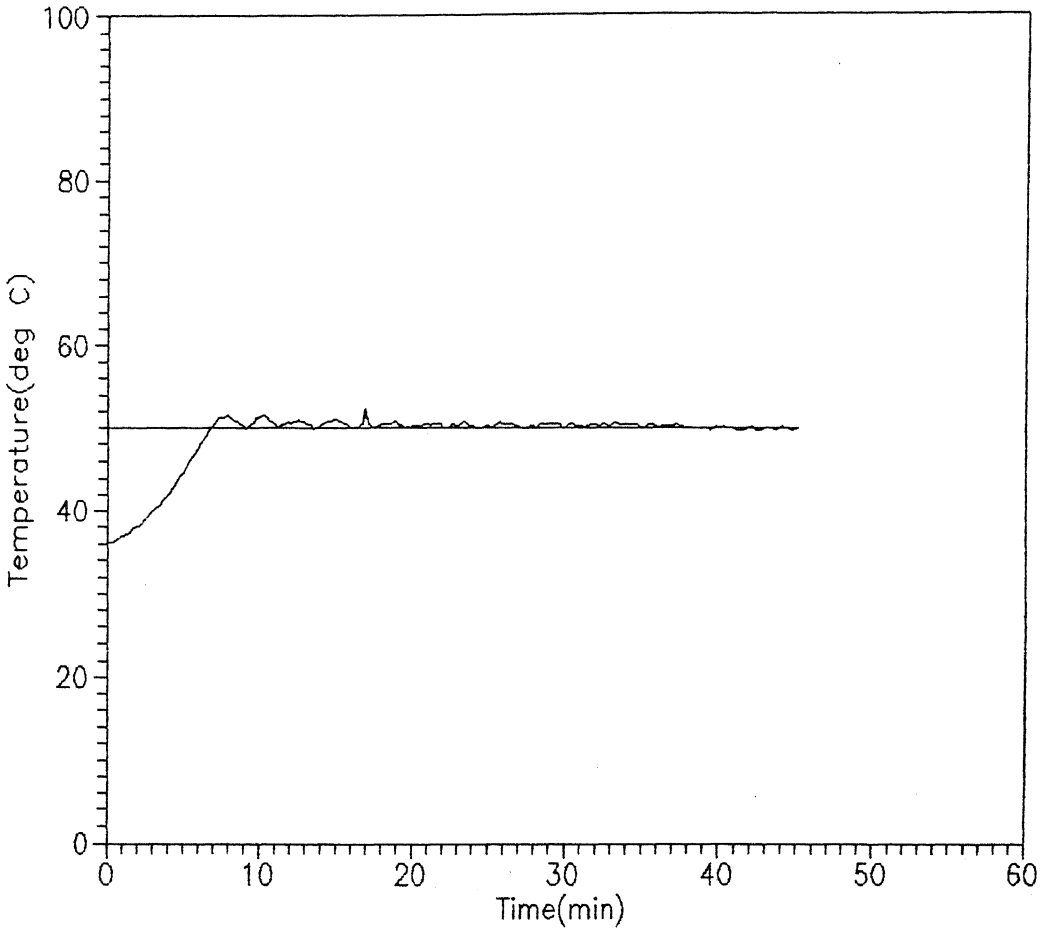

(a)

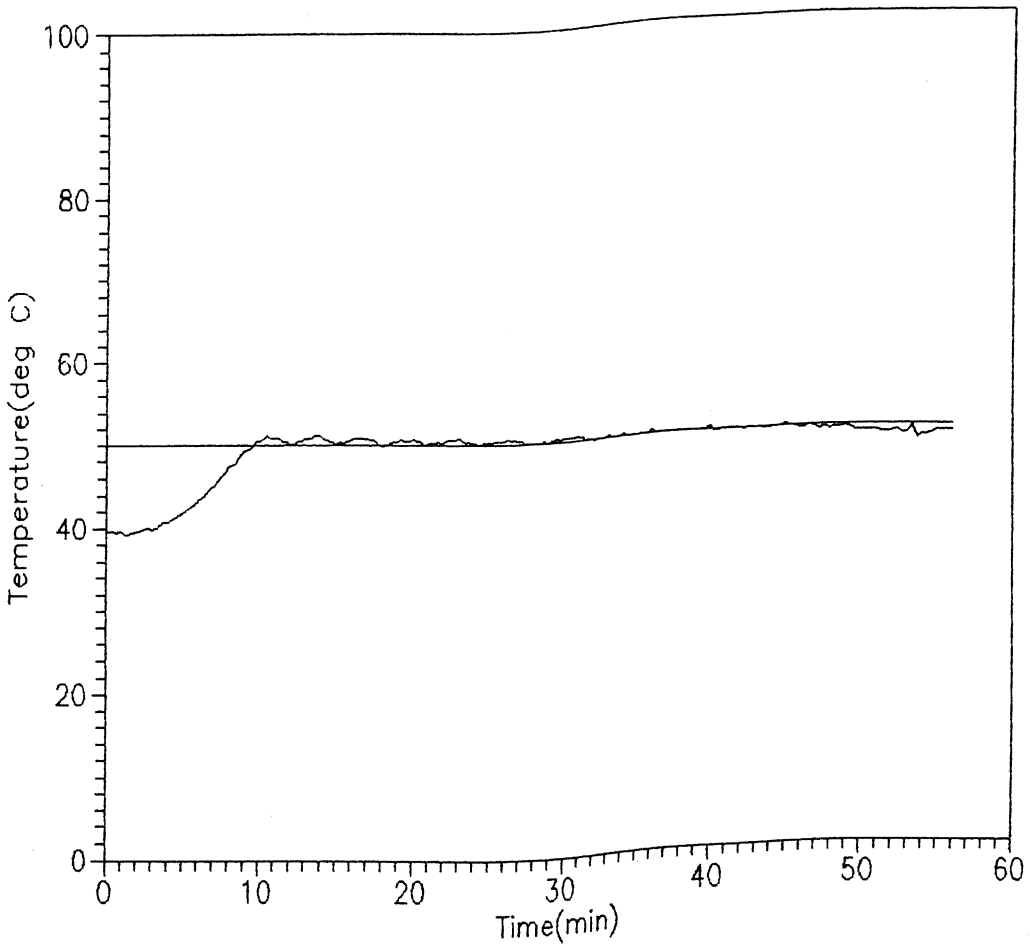

Fig.13 Performance of the tuned controller (using tuned values of Table 4) with (a) water (b) PVA solution in the reactor. T_{sp}=50°

Table - 4 Cohen-Coon and Tuned controller parameters

Parameter	Cohen-Coon values	Tuned values
K_c^h	0.0708	0.07
τ_I^h	23.435	900.0
K_c^c	-45.7	-70.0
τ_I^c	1.864	90.0
K_c^{cas}	—	1.0
τ_I^{cas}	—	1.8

Another faster PI controller operates in cascade in the flow-loop to minimize the effect of pressure fluctuations in the water line (Fig.14). This controller operates with a sample time of 5 s (smaller sampling times worsened the control). This controller manipulates the stem position of the valve till the desired and observed flow rates match. The controller parameters were tuned on-line, and the values of K_c^{cas} and τ_I^{cas} are given in Table 4.

3.3 DIGITAL CONTROLLER

. All the controller algorithms were implemented using the velocity form of the control law because the position form of the algorithm requires initial values of the controller output which are not known in practice. Also in this form, one does not compute the absolute value of the control variable at any given instant but only the increment to the control signal over the previous value (30). This method protects the controller from integral "wind-up" or saturation. The algorithm for a PI controller is discussed below.

3.3.1 PROPORTIONAL-INTEGRAL CONTROLLER

. In the continuous time domain the algorithm for a PI controller is given by,

$$m(t) = K_c\, e(t) + \frac{K_c}{\tau_I} \int_o^t e(t)dt \tag{10}$$

where m is the manipulated variable (furnace power / cooling water flow). Discretising Eq.10 at the i^{th} and $(i-1)^{th}$ sampling instants, and taking the difference of the two, one obtains

$$\Delta m_i = K_c(e_i - e_{i-1}) + \frac{K_c}{\tau_I}\, e_i T \tag{11}$$

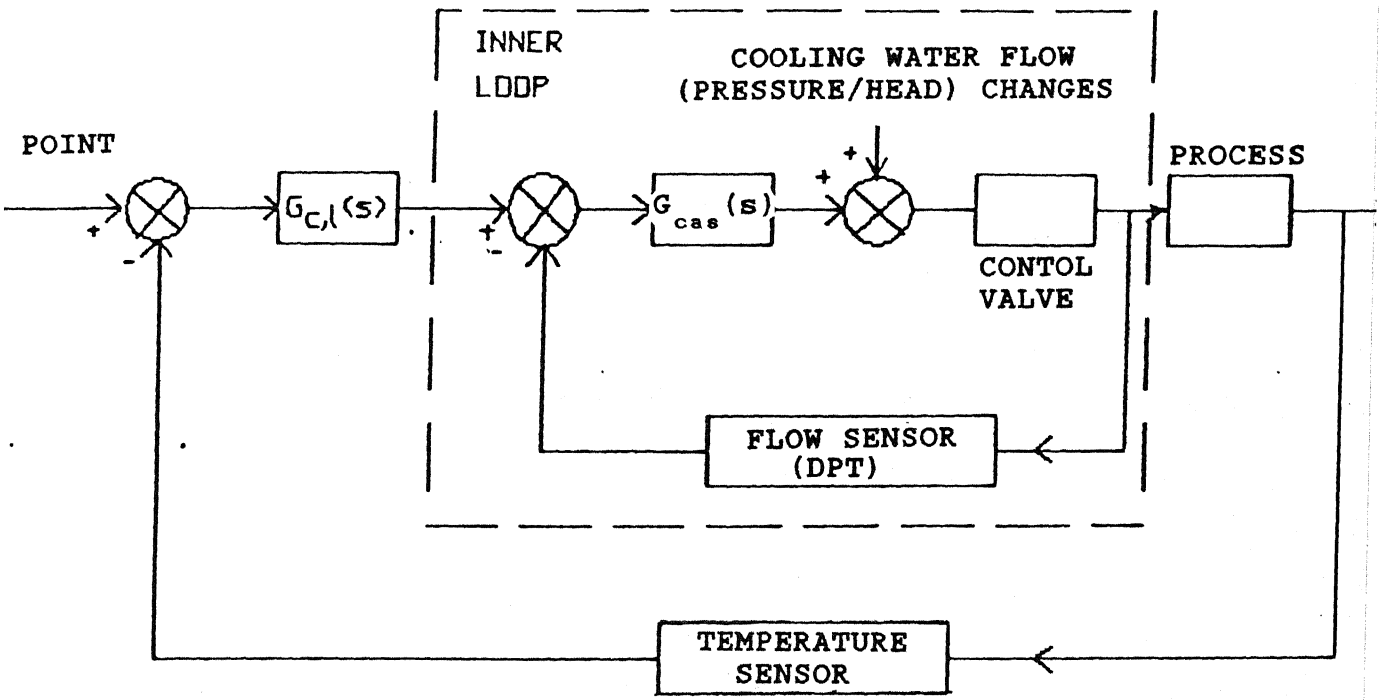

Fig.14 Block diagram for flow cascade control

where T is the sampling time. Eq.11 represents the PI controller in its velocity form.

3.4 COHEN-COON CONTROLLER DESIGN

. The first estimates of the controller parameters were obtained using the Cohen-Coon relations (30) . These parameters were subsequently tuned on-line. The controller parameters were further fine-tuned for rapid heating (to attain the desired set point faster) and cooling dynamics, using viscous solutions of PVA (Jams Chemicals, Bombay, India) in water (concentrations chosen somewhat arbitrarily, to simulate approximately, the conditions of the reaction mass in the gel effect region) by giving step changes in temperature until smooth dynamics were obtained. For the cooling cycle, the calculated parameters required only very slight adjustments. The Cohen-Coon settings and on-line tuned parameters are given in Table 4. Further tuning of the controller parameters was done from time to time to account for changes in the ambient temperature and inlet temperature of cooling water with changes in season.

3.5 SOFTWARE DEVELOPED

. In this study the real-time software was developed in Turbo Pascal. The interfacing was done by a TURBO PASCAL driver using DT 2805 interfacing card and DT 707T screw terminal panel [PCLAB manual, Data Translation Inc., Marlborough, MA, U.S.A, (29)]. The program was developed in a modular form with many procedures meant for specific purposes. The program can be used for both dynamics and control. The flow control procedure closely follows the work of Jana (34). The flow chart and listing of the program developed are included in Appendix 2. Some of the important procedures are discussed below.

READ_IN_CONTROL : This procedure reads in the set point, mode of control (P, PI or PID), and the controller parameters for the heating, cooling and the flow cascade loops.

READ_IN_STEP : This procedure reads in the desired values of the control variables, namely, heating time per cycle time, and cooling water flow rate during open loop testing. Once the steady state is reached with the given conditions, a step change in one or both of the manipulated variables can be given.

DISPLAY_CONTROL : This procedure displays the temperature, control action (heating time and/or cooling water flow rate) at each instant.

DISPLAY_STEP : This procedure gives the position of the manipulated variables and the temperature at each instant when the step test is being carried out.

FLOW_CONTROL : Once the cooling water flow rate is specified by the primary temperature controller, this procedure takes up the job of obtaining the desired flow rate with the aid of the cascade PI controller.

ORIFICEMETER : This routine reads in the voltage drop from the channel connected to the DPT and calculates the flow rate from the calibration information stored in the form of a polynomial.

ORFW_CTRL_ACTION : This procedure manipulates cascade controller's output with PI action in order to obtain the desired flow rate.

VALVE_MANIPULATION : This routine calculates the stem position required for a given flow rate and operates the stepper motor accordingly.

S_GFILTER: This procedure smoothens the flow measurement data using seven measurements taken at intervals of 2 s. The Savitzky-Golay formula (35) is used.

ON : This sets the bit 1 of port 0 high (1) to switch on the furnace through the solid state relay.

OFF : This sets the bit to low (0) to switch off the furnace.

The general purpose routines which have been developed are described below.

DECO.INC : This "include" file has routines to read the system time interacting with DOS and a procedure to draw boxes with the given corners.

STEP.INC : This program runs the stepper motor in a given direction for the specified number of pulses. This program issues the next set of pulses after analyzing the previously existing digital value. This program is currently designed for running the stepper motor in 0, 1, 2 and 3 bits of one of the ports. By suitably changing the mask and the set of digital value, any set of bits can be used.

The program can be interrupted at any time. The next action can be chosen from the given set of options. There is provision to change the set points and parameters in between. Information about interfacing routines like MeasureThermocouple, OutputDigitalValue, MeasureVolts, etc., are available in the PCLAB manual [Data Translation Inc., Marlborough, MA, U.S.A, (29)].

CHAPTER 4

POLYMERIZATION PROCEDURE AND CHARACTERIZATION TECHNIQUES

In this chapter the techniques of monomer and initiator purification and the procedure for batch polymerization in a Parr reactor are described. The analytical procedures used for determining the monomer conversion and the molecular weight of the polymer produced are also discussed.

4.1 PURIFICATION OF CHEMICALS

4.1.1 MONOMER

LR grade methyl methacrylate (MMA) (Burgoyne, Burbidges & Co., Bombay, India) was purified prior to use (6,36,37). The monomer was washed three times with equal volumes of a 5% NaOH (GPR, BDH, Bombay, India) solution in water to remove the phenolic stabilizers [hydroquinone(HQ) or methyl ether of HQ] present in it. The mixture was allowed to settle in a separating funnel forming two layers, the bottom inorganic layer was discarded leaving the monomer. The MMA was then washed at least three times with equal volumes of distilled water to remove traces of NaOH. Settling times of at least two hours after each NaOH and water wash were allowed. The residual water was removed from the monomer by passing it through beds (placed in series) of molecular sieves (type 30-541, 4-5°A, Linde Division, Union Carbide, USA) and silica gel blue (LR, coarse, mesh 3-8, NICE, Kochi, Kerala, India). Fresh batches of regenerated silica gel and molecular sieves (by washing and drying in an oven at 70°C for 5 hrs) were used for every 250 ml of monomer. The regenerated drying agents (silica gel regains its original blue color after

drying) were stored in air tight containers.

The monomer obtained after the above steps was distilled under vacuum (P=50 mm Hg) at about 30°C (room temperature). Ice cold water was circulated in the condenser (Fig.15). The distilled monomer was stored in a refrigerator over fused $CaCl_2$ (Loba Chemie Pvt. Ltd., Bombay, India) in a desiccator. The final yield of the pure monomer was about 60% of the original sample.

4.1.2 INITIATOR

The initiator, azobis isobutyronitrile (AIBN) (LR, Ranbaxy Labs. Ltd., S.A.S Nagar, Punjab, India) was recrystallized from methanol (LR, S.D.Fine Chemicals, India) (6). A saturated solution of AIBN was prepared (at room temperature) in a test tube by mixing an excess of AIBN with about 30 ml of methanol. The solution was filtered (No:1 ordinary filter paper) into another test tube. The filtrate was then cooled in a refrigerator to crystallize the AIBN. The crystals were recovered by filtration. The crystals were dried in a vacuum oven at room temperature (heating causes thermal decomposition).

4.2 BATCH POLYMERIZATION

A 500 ml solution of required initiator concentration in monomer was prepared in a one liter round bottom flask. The solution was thoroughly mixed to ensure complete dissolution of AIBN.

The solution was transferred to the Parr reactor. The reactor was carefully closed with the head and sealed with the half-rings and the steel retaining ring. All the valves were

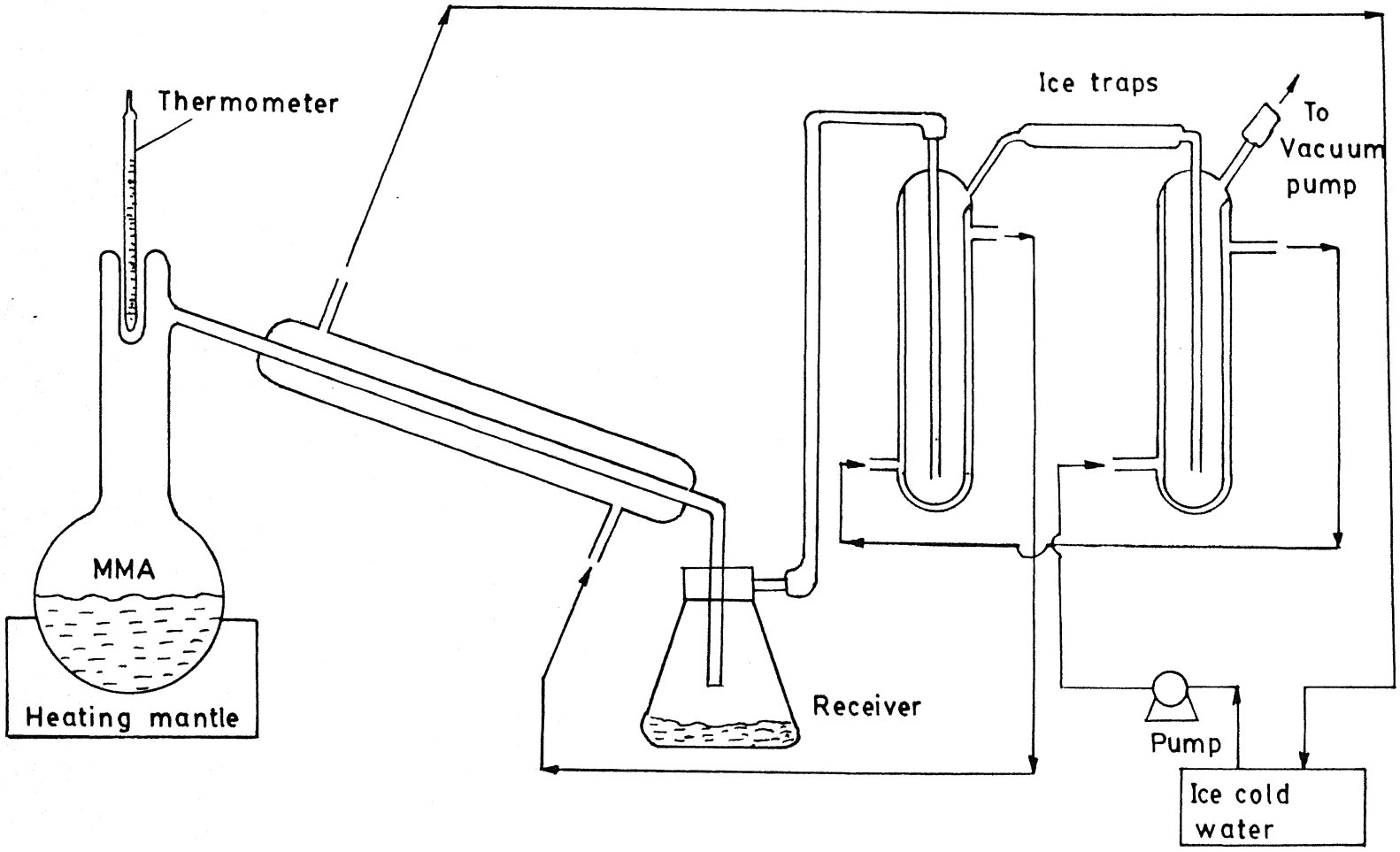

Fig.15 Vaccum distillation set-up

closed. The reactor contents were degassed by applying vacuum (P= 5 mm Hg) through the gas release valve for about 30 min. The vacuum pump (model 150D, Leo Engineering, Kalletumkara, Kerala, India) was connected to the reactor through ice-traps to remove any condensables in the gas. After degassing, the reaction mass was pressurized with argon (IOL-AR-2, Indian Oxygen Ltd., New Delhi, India) charged through the gas-charge valve. After about 20 seconds of the commencement of this operation the valve connected to the pressure gauge line was opened. Once the desired pressure of about 900 kPa was achieved, the gas-charge valve was closed. Argon was re-charged during a run if the pressure fell below 850 kPa.

All the peripherals connections (temperature sensors, etc.) to the reactor-PC set-up (Fig.2) were checked and activated. The controller parameters and desired set point were supplied as inputs to the control program. Samples were withdrawn at required intervals of time through the valve V_3 (see Fig.1a). The sampling times were decided by the expected dynamics of the system. Samples of about 3 ml were collected in 50 ml sample bottles containing weighed amounts of solvent (10 ml of benzene, Extra pure, S.D Fine Chemicals Ltd., Boisar, India) and trace amounts of inhibitor (MEHQ). The sample bottles were kept ice-cooled in order to freeze the reaction as soon as the sample was collected. Before drawing the sample, about 2 ml of the sample coming out of the port was discarded, this being the estimated hold-up of material in the sample line. This procedure ensured that the samples drawn were really representative of the reaction mixture. The copper tube connected to the sample collecting port was cleaned with commercial grade acetone and dried after each sample before reuse. Sample bottles were reweighed to calculate the mass of the samples drawn. The occurrence of the gel effect can be inferred from the sudden change in the consistency of the material flowing out. During this period, samples were collected as often as possible. It was found that the argon pressure of about 10 atm above the liquid reaction mass was unable to push out the liquid through the sample port shortly after the onset of the gel effect due to the very high viscosity.

The reaction was stopped after the lapse of the required time or as soon as the stirrer stopped due to the high viscosity of the reaction mixture. After the reaction was complete, the reactor pressure was released slowly by opening the gas release valve and the reactor was then opened for cleaning up immediately. Most of the material inside was removed mechanically. The residual polymer was dissolved using dichloromethane (LR, NICE, Kochi,Kerala, India). In some cases (specially bulk polymerization at 70°C) it was quite difficult to open up the reactor after the reaction was complete. The contents had to be heated to higher temperatures (130-140°C) and kept at that point for a sufficiently long time (30 min) to melt the polymer near the walls of the reactor. This enabled pulling out the reactor head with the cooling coils, stirrer and thermowell along with most of the polymer, in which these had become embedded. A considerable amount of polymer was first removed mechanically, and then the remaining polymer was dissolved with solvent (CR) acetone followed by (LR) dichloromethane.

4.3 ANALYSIS OF MONOMER CONVERSION

The monomer conversion was estimated gravimetrically (6). The polymer was precipitated from the solution in the sample tube by adding about 100 ml of methanol (non-solvent). The precipitated polymer was filtered through a dried and preweighed filter paper (Whatman 41, Whatman International limited, Maidstone, UK). A few drops of the filtrate were tested with about 10 ml of methanol to ensure that complete precipitation had taken place. The polymer was dried at 50°C under vacuum (P=5 mm Hg) for about 24 hr (tested to be sufficiently long to ensure complete drying). The mass of the precipitated polymer was found by weighing the filter paper again. The polymer samples were stored in a desiccator till molecular weight analysis was done.

4.4 DILUTE SOLUTION VISCOMETRY

The average molecular weights, M_v, of polymer samples were determined by dilute solution viscometry (38-40). About 0.25 g of the dried polymer was dissolved in 30 ml of filtered extra pure benzene. The solution was kept in a stoppered standard flask for more than 24 hr (in a refrigerator) to ensure complete dissolution. The solution was carefully examined for complete dissolution before use. Keen observation was required as the polymer particles are transparent, making their presence difficult to detect. This solution was filtered through a sintered-glass filter (G4, Por 4, Vensil Glass Works, Bangalore, India) to remove minute suspended particles. Benzene was filtered for further solution preparation, for dilution and rinsing of the viscometer in a separate filter. The glass filters were cleaned with chromic acid and distilled water, and dried in an oven.

15 ml of the polymer solution was pipetted into the viscometer (Ubbelohde viscometer No: 501 01, Schott-Gerate, Hofheim, West Germany) (Fig.16). The viscometer was carefully mounted on a stand built in-home and placed in a constant temperature bath (maintained at 30°C, using an Indotherm and a PT100 sensor, IT401 D, PI controller, Indotherm Instruments Ltd., New Bombay, India). Efflux time measurements were carried out as described below. Suction is applied to tube 1 (Fig.16) by closing tube 2 with a rubber stopper to fill the working capillary (7), time bulb and upper reservoir (9). Then suction is discontinued and tube 2 is opened again. This causes the liquid column to separate at the lower end of the working capillary (7). The efflux times are measured for descent from marks M_1 to M_2. These flow time measurements were repeated at least four times, with a reproduceability within 0.5 s. The original solution was diluted by pipetting 5 ml of benzene into the viscometer. To help complete mixing of the solution with the added solvent, air was bubbled through the mixture in the viscometer using the pipette filler. The next efflux time measurement was taken after about 40 min. This was to ensure

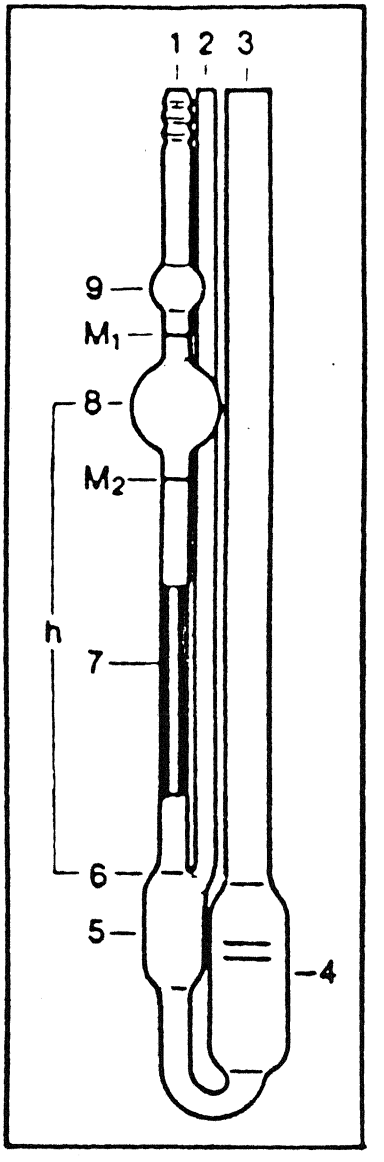

Fig.16 Ubbelohde viscometer

attainment of homogeneity of the sample as well as temperature equilibration.

As further dilution could not be made inside the viscometer (capacity of only 20 ml), the solution was taken out. 10 ml of this solution and 5 ml of filtered benzene were pipetted back into the viscometer. This was mixed as before and placed in the constant temperature bath and efflux time measurements were carried out. Flow times were measured for one more dilution by adding 5 ml of benzene. In this manner four efflux times were taken for any polymer sample. After thoroughly cleaning the viscometer, efflux time for the pure solvent was also measured.

Appendix 3 gives the details of the calculations performed to obtain the intrinsic-viscosity average molecular weight from the efflux time measurements and concentration. The listing of the Fortran program used for double extrapolation and one specimen plot is also given in Appendix 3.

CHAPTER 5

RESULTS AND DISCUSSION

The main thrust of this work was to provide an experimental verification of the kinetic model developed by Ray et al. (23) for polymerization of MMA under step changes in temperature. Such operations are often encountered in industrial reactors.

Before conducting the actual experimental runs, we attempted to find out if temperature gradients existed within the Parr reactor during operation. A relatively concentrated solution of polyvinyl alcohol in water, having a consistency which was about the same (by visual inspection) as the polymerization reaction mass in the gel-effect region, was taken in the open reactor and heated with stirring. The thermocouple in the thermowell was moved around and the temperature was recorded at several different positions. These are given in Table 5. It is observed that the temperature is relatively uniform within the reactor, with a mean of 50.56°C and a standard deviation of 0.39, for a set point of 50°C.

A series of experiments on bulk polymerization of MMA with different temperature histories [near-isothermal (NI), step decrease (SD) and step increase (SI)] at a fixed initiator (AIBN) loading, of 25.8 mol/m^3, have been conducted. Two important process output variables, namely, monomer conversion, x, and average molecular weight, M_v, as determined from intrinsic viscosity, have been measured at different sampling times during the course of polymerization. Table 6 lists the controller parameters in all the runs conducted, while the detailed results of the monomer conversion and molecular weights are given in Appendix 1. It may be added that the controller gain was changed on-line to obtain faster heating (or cooling) during step changes in the temperature.

The first two experimental runs were conducted under *near isothermal* conditions at

Table - 5

Radial temperature distribution using PVA solution
Set point T_{sp}= 50°C

Distance (radial) from wall (cm)	Location of stirrer (cm)	Height from top of reactor (cm)	
		8 (cm)	4 (cm)
		Temperature (°C)	Temperature (°C)
0 (wall)	at center	51.01	51.04
2	at center	50.81	50.73
4	at center	50.63	50.48
6	at one side	50.76	49.96
8	at center	49.99	50.09
10	at center	50.08	50.36
other (wall)	at center	50.98	50.99

Table - 7
Controller parameters used for each run

Sno.	Run No.	K_c^h	τ_I^h	K_c^c	τ_I^c	Comments
1	NI50a	0.07	900	-70	90	–
2	NI50b	0.07	900	-70	90	–
3	NI70	0.08 0.07	900	-70	90	K_c^h changed at t=8 min
4	SD1a	0.08	900	-70	90	–
5	SD1b	0.07 0.08	900	-70	90	K_c^h changed at t=30 min
6	SD2	0.07 0.08 0.07	900	-70 -60	90	K_c^h, K_c^c changed at t=30 min changed at t=80 min
7	SI	0.07 0.08	900	-70	90	K_c^h changed at t=120 min

$K_c^{cas} = 1$
$\tau_I^{cas} = 1.8$
for all runs

50°C and 70°C (Run Nos. NI50 and NI70, respectively). The conditions are refered to as *near isothermal* due to the fact that the reactor system takes about 6 to 8 min to attain the desired polymerization temperature (Figs.17a and 18a). Vaporization of the monomer is prevented by a applying pressure of about 1400 kPa absolute, using an inert gas such as argon. The argon pressure also helps in driving out samples of the reaction mass through a port.

The monomer conversion (x) for the two NI50 runs (NI50 a and b) are shown in Fig.17b. The average molecular weight (M_v) based on intrinsic viscosity measurements are shown as a function of conversion for the NI50 b run in Fig. 17c. The duplicate runs were made to establish reproducibility of the results. Since the rise time (time taken to reach 50°C from room temperature) for the NI50 runs is very small, the conversion *vs.* time results are comparable to those obtained by Balke and Hamielec (6) on ampoule reactors (in which mixing and heat and mass transfer effects are negligible) under isothermal conditions. The excellent agreement between our conversion data (x *vs.* t) with those of Balke and Hamielec (6) is observed from Fig.17b.

The measured temperature history (Fig.17a) for the NI50 runs has been curve-fitted by:

$$T(°C) = 37.56 - 0.65\,t + 0.2756\,t^2 \qquad \text{for } 0 < t \leqslant 8.3 \text{ min}$$

$$T(°C) = 50.0 \qquad \text{for } t > 8.3 \text{ min} \qquad (12)$$

where t is the time in minutes. These equations are used in the model of Ray et al. (23) to obtain theoretical predictions. Two sets of parameter values have been provided by Ray et al. (23). The *individually optimized parameters* (IOPs) have been obtained by curve fitting *each* of the isothermal experimental runs of Balke and Hamielec (6), and are available for every set of values of $[I]_o$ and T studied by them. These lead to excellent fits between model results and experimental data (6). On the other hand, *best fit correlations* (BFCs) have

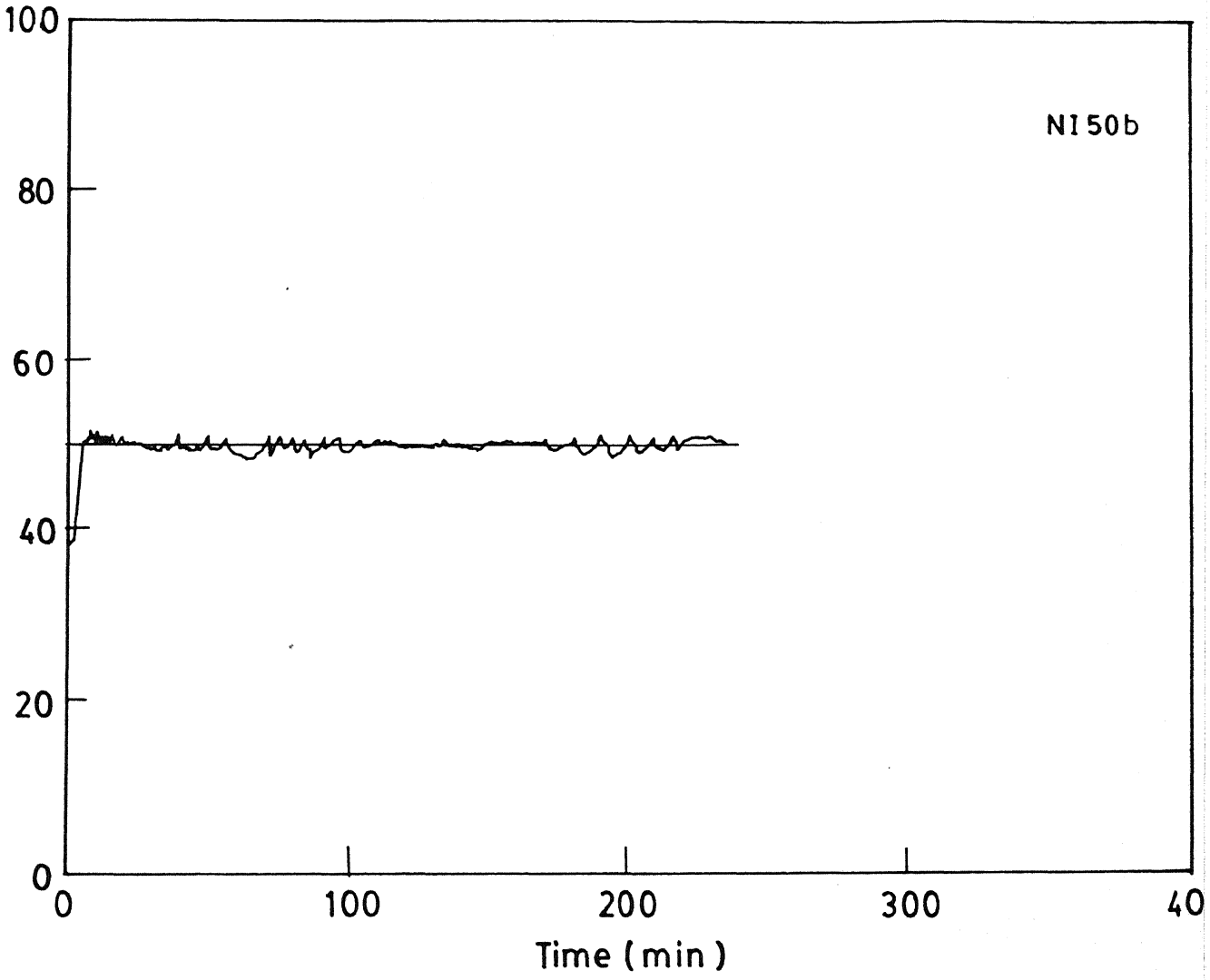

(a)

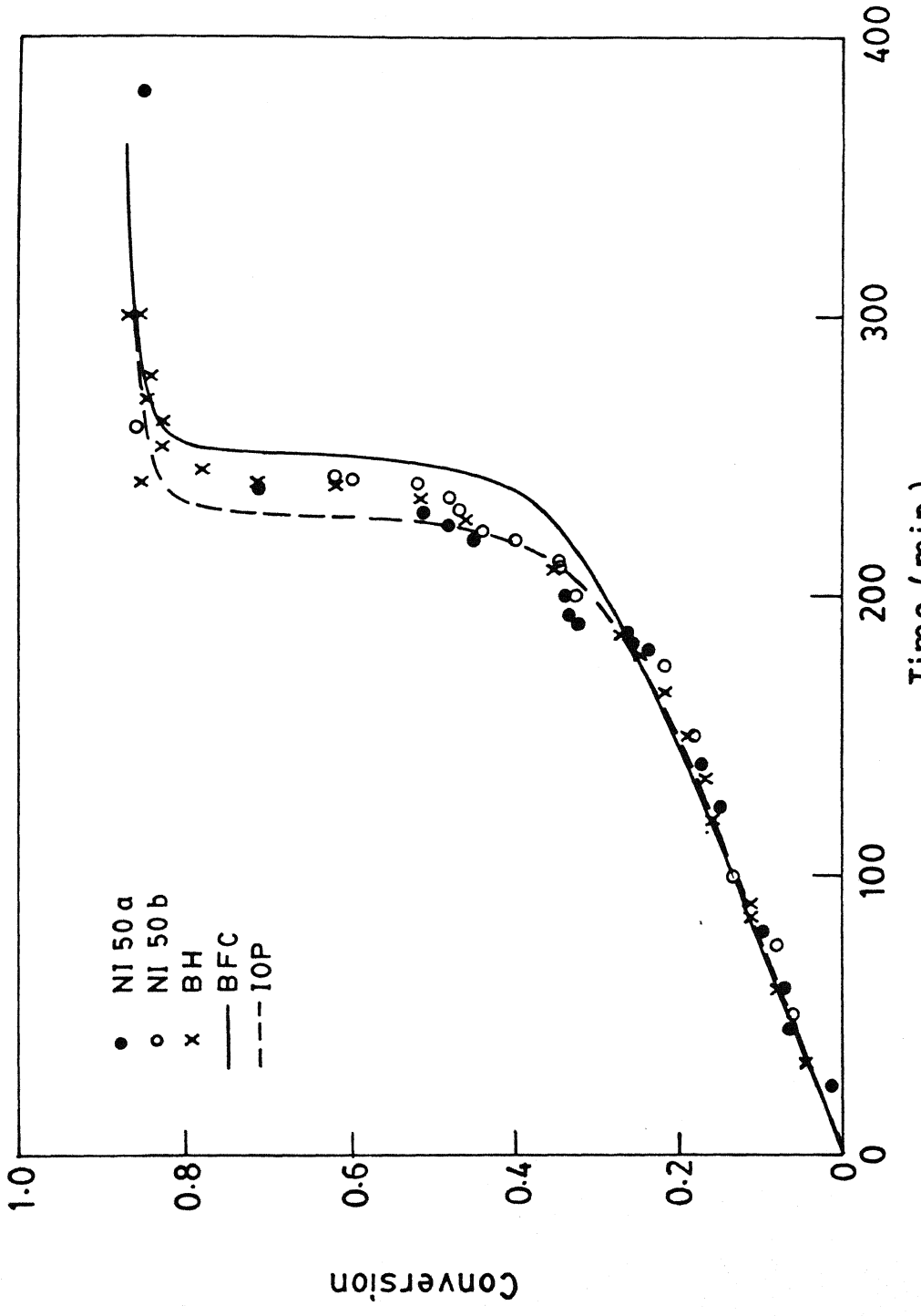
Conversion
1.0
0.8
0.6
0.4
0.2
0
0
100
200
300
400
Time (min)
NI 50 a
NI 50 b
BH
BFC
IOP

(b)

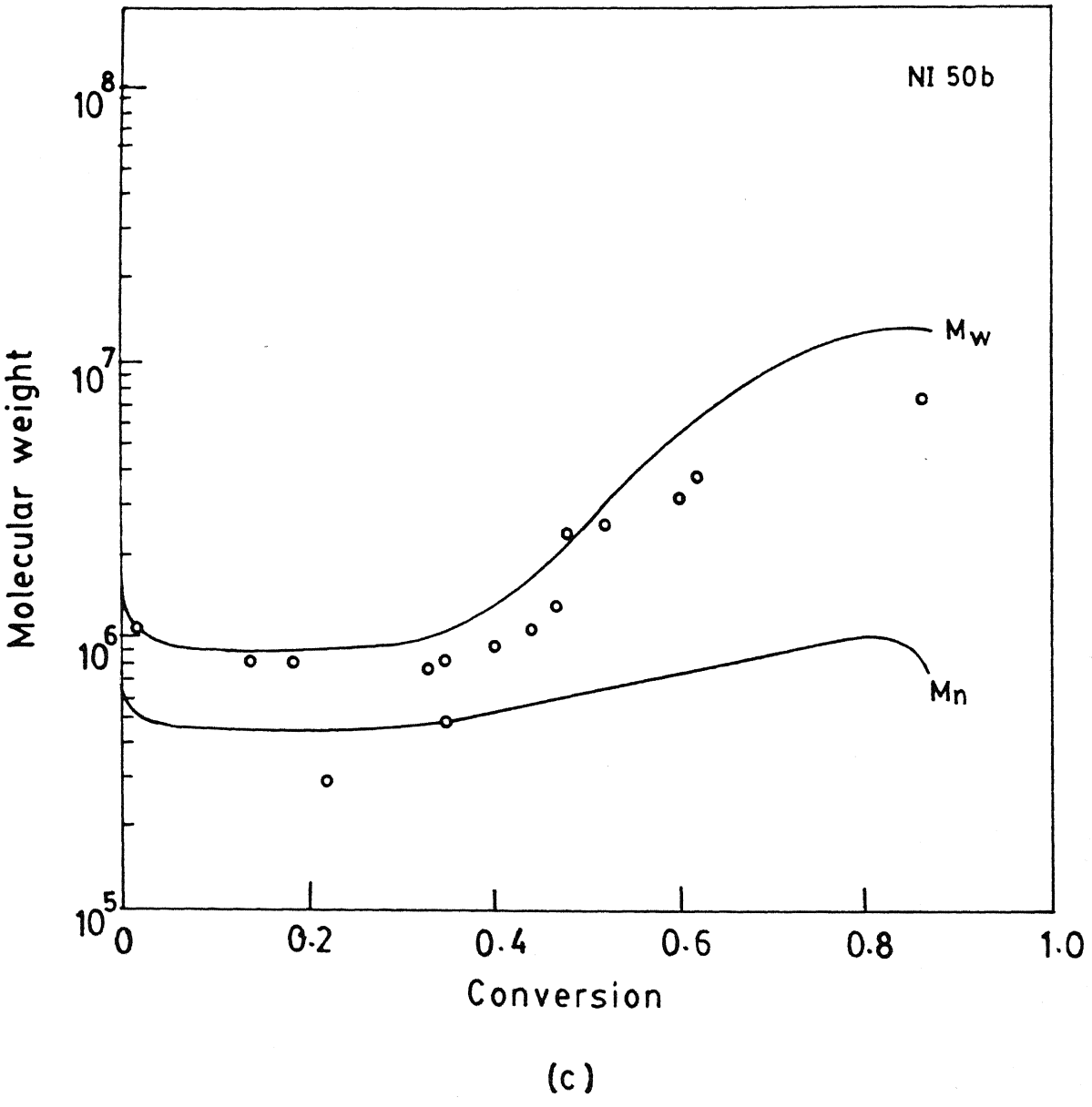

Fig.17 Experimental results on the near isothermal (NI50) run
(a) temperature history for the NI50 a and b runs
(b) conversion history for the NI50 a and b runs
(c) molecular weight *vs.* x for the NI50b run
Theoretical predictions using the measured temperature history (Fig.17a) and the BFCs in the model of Ray et al. (23) shown by solid curves. Isothermal results (BH) (6) also shown for comparision Dotted curve in Fig.17b shows model results using the individually optimized paremeters (IOPs). $[I]_o$=25.8 mol/m^3, f_s^o=0.

also been developed which relate the model parameters to the temperature in a functional form. These are more general since they can be used for values of $[I]_o$ and T which differ from those studied by Balke and Hamielec. These give curve fits which are not as good as those obtained using the IOPs, but are reasonably good. The IOPs and BFCs developed using isothermal data (6) are used *without change* for predicting nonisothermal results in our study.

Equation 12. is used with BFCs to predict (solid curves in Fig.17 b and c) the monomer conversion and the number and weight average molecular weights (M_n and M_w) as a function of time. The dashed curve in Fig.17b gives the model (23) predictions for the near-isothermal run using the IOPs corresponding to T=50°C and $[I]_o$=25.8 mol/m^3. Good agreement is observed between our experimental data on monomer conversion and either of these predictions from the model (it may be noted that strictly speaking, we should not use the IOPs for cases where temperature is varying with time, as in the NI50 runs). The experimental results on M_v are found (Fig. 17c) to lie close to the predicted values of M_w using the BFCs, as expected.

In the case of the NI70 run, the rise time (time taken to reach 70°C from room temperature) is much larger, and has an important effect on the conversion history. Our results are found to deviate from those of Balke and Hamielec (6). Fig.18b shows this deviation. The temperature history for this run is shown in Fig.18a and has been curve-fitted by the following equations:

$$\begin{aligned} T(^\circ C) &= 24.76 - 0.749\ t + 0.5412\ t^2 \quad \text{for } 0 < t \leqslant 10 \text{ min} \\ T(^\circ C) &= 70.0 \qquad\qquad \text{for } t > 10 \text{ min} \end{aligned} \tag{13}$$

Model (23) results for conversion using both the sets of parameter values (IOP and BFC) with this temperature history have been generated and are shown in Fig.18b. Fig.18c

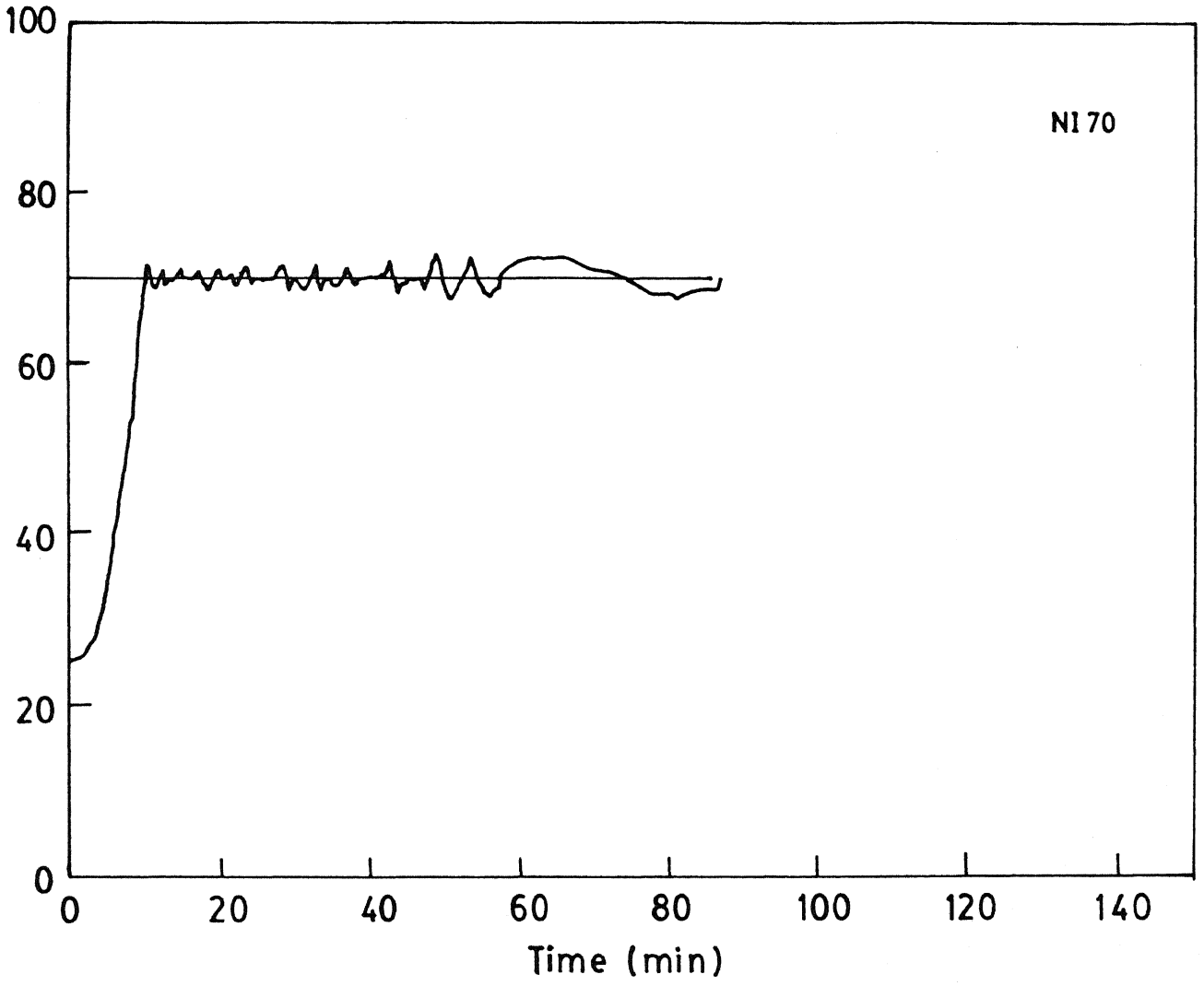

(a)

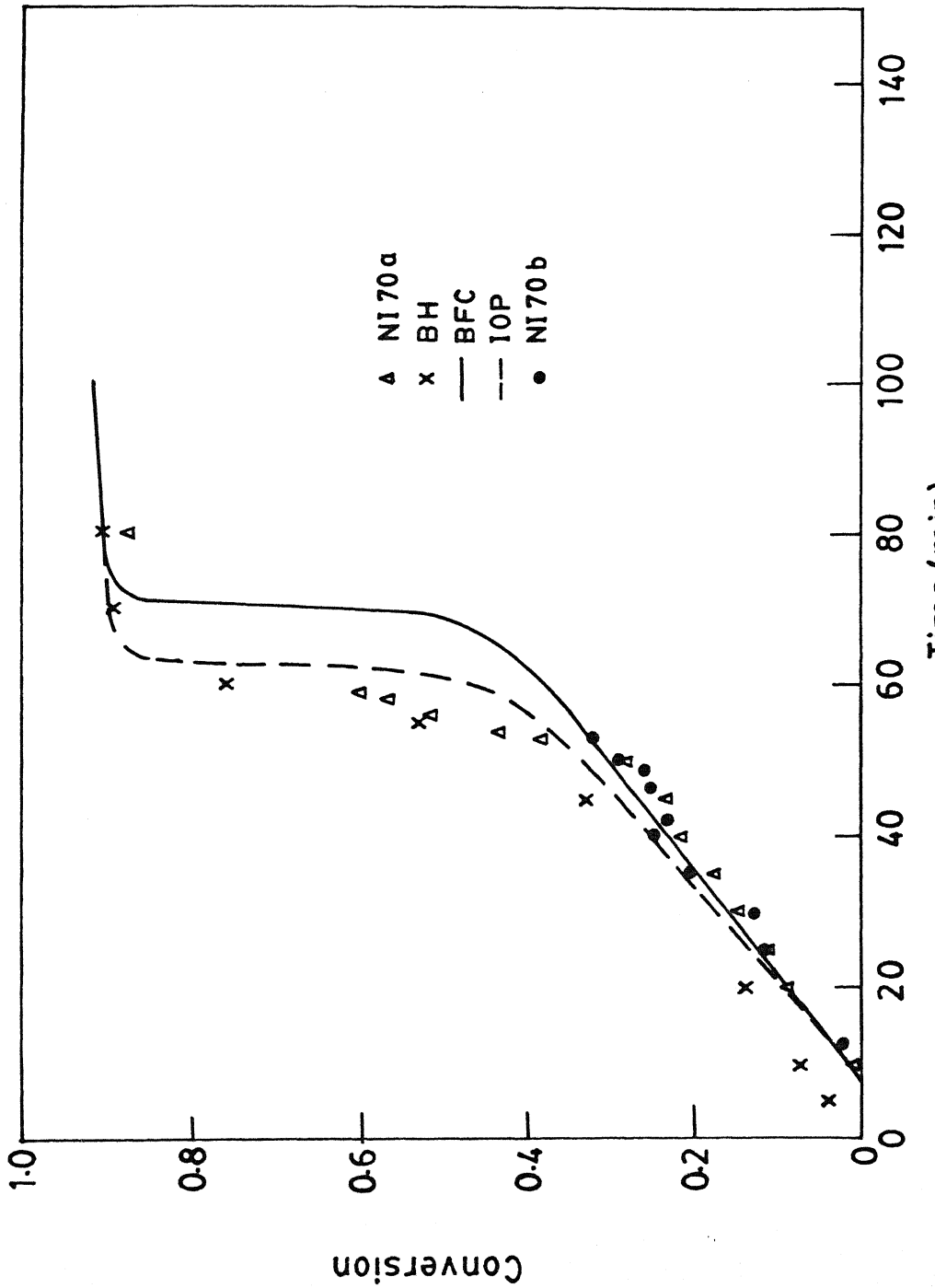
Conversion
1.0
0.8
0.6
0.4
0.2
0
0
20
40
60
80
100
120
140
Time (min)
NI 70a
BH
BFC
10P
NI 70b

(b)

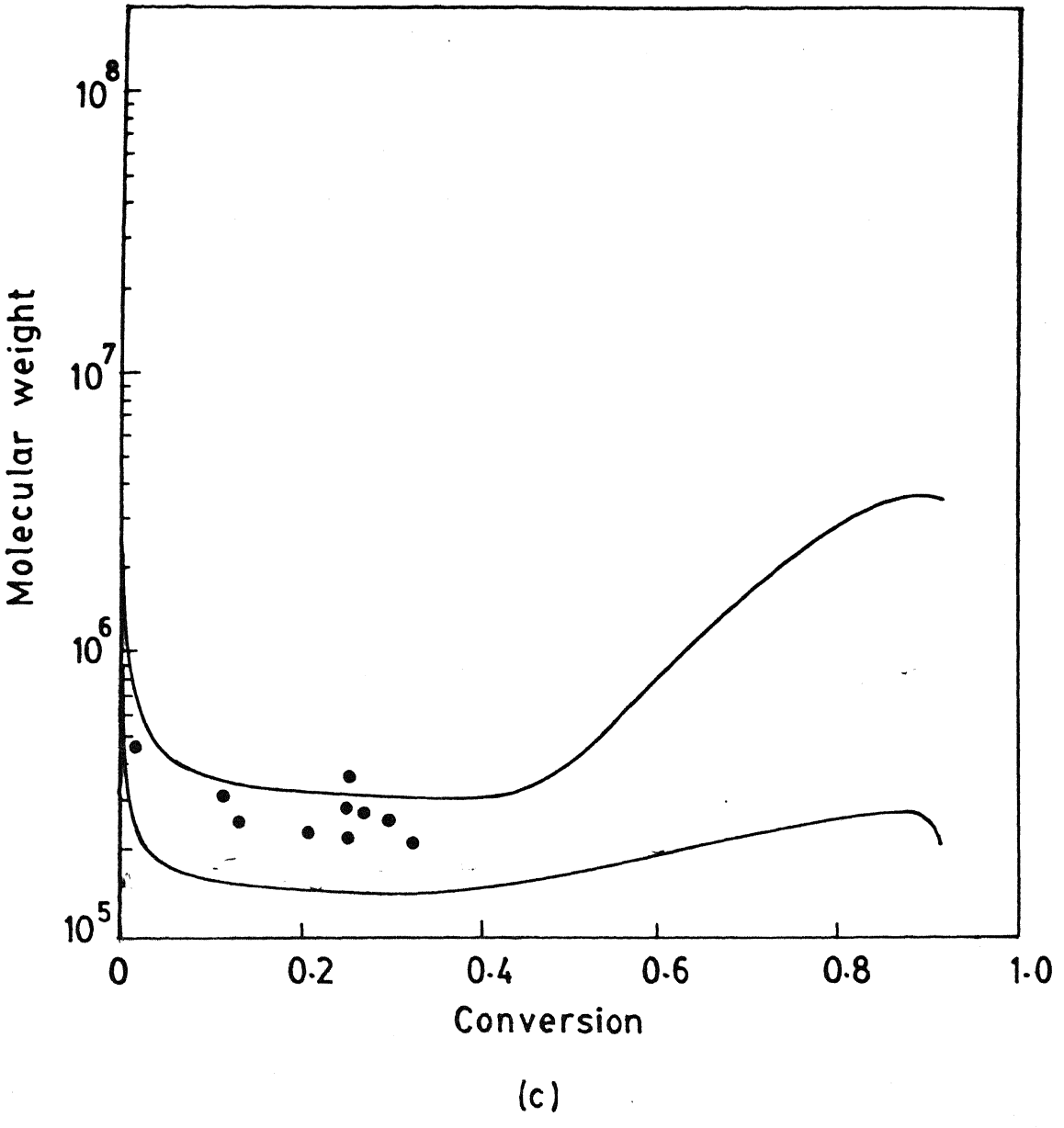

Fig.18 Experimental results on the near isothermal (NI70) run. Other details same as in Fig.17.

shows the experimental results and model predictions (using BFCs) for the molecular weights. The experimental values of M_v are observed to close to the predicted values of M_w. Unfortunately, M_v data in the gel effect region could not be taken (this run is planned to be repeated) The x *vs.* t plot agrees reasonably well with model predictions.

The next phase of the work was to obtain experimental data with step changes in temperature [step increase (SI) and step decrease (SD)] at different times and compare them with predictions from the model. Polymerization of MMA with the initiator (AIBN) loading of $[I]_o$=25.8 mol/m^3 was carried out at 70°C (similar to NI70) for some time. After the system attained a steady temperature of 70°C, a step decrease of the temperature (SD1) at t=25 min (point a, Fig.19a) to 50°C was effected using set point changes in the digital controller. The experimental results on conversion and M_v along with the temperature history are shown in Figs.19a-c. Two runs (SD1a and SD1b) were made for this case to ensure reproducibility of the results with temperature transients. The temperature curve-fit equations are given by

$$\begin{aligned}
T(°C) &= 24.7556 - 2.69\ t + 1.28\ t^2 - 0.0629\ t^3 \qquad \text{for } 0 < \text{t} < 10.2 \text{ min} \\
T(°C) &= 70.0 \qquad \text{for } 10.2 < \text{t} < 25 \text{ min} \\
T(°C) &= 246 - 7\ t \qquad \text{for } 25 < \text{t} < 28 \text{ min} \\
T(°C) &= 50.0 \qquad \text{for t} > 28 \text{ min}
\end{aligned} \tag{14}$$

The model results are also shown in Figs.19 b and c using the BFCs (23). It can be observed that the reaction slows down (due to lower rates at lower temperatures) significantly, and the gel effect is postponed compared to the NI50 run. A reasonably good agreement is observed between our experimental data and the model predictions.

In order to study the effect of a step decrease in the temperature at a later time, another polymerization run (SD2) was conducted under the same conditions as earlier but with the step decrease effected at t=45 min (point *b*, Fig.20a). The curve-fit equations for the temperature history are given by

$$
\begin{aligned}
T(^{\circ}C) &= 18.069 - 0.9787\ t + 0.934\ t^2 - 0.0438\ t^3 \qquad \text{for } 0 < t \leqslant 9.8 \text{ min} \\
T(^{\circ}C) &= 70.0 \qquad \text{for } 9.8 < t \leqslant 45 \text{ min} \\
T(^{\circ}C) &= 246.713 - 4.297t \qquad \text{for } 45 < t \leqslant 46.01 \text{ min} \\
T(^{\circ}C) &= 50.0 \qquad \text{for } t > 46.01 \text{ min}
\end{aligned} \tag{15}
$$

It can be seen that a delayed step decrease leads to a preponement of the gel effect as compared to the NI50 run (Fig. 20b). Again, a reasonably good agreement of our experimental results against model predictions using the BFCs (without any re-tuning of the parameters of the model) is observed in Figs.20 b and c.

The effect of a step increase (SI) in temperature was also studied. Near isothermal polymerization was conducted at 50°C for some time and then, at a predecided time (t=120 min, point *c*, Fig.21a) the temperature was increased to $70^{\circ}C$ by using a step change in the set point. Since the heating dynamics of the reactor system is a bit slow, the process took about 7 min to reach the desired set point. The experimental temperature history for this case was curve-fitted by

$$
\begin{aligned}
T(^{\circ}C) &= 22.188 - 2.62392\ t + 1.2611\ t^2 - 0.046637\ t^3 \qquad \text{for } 0 < t \leqslant 7.13 \text{ min} \\
T(^{\circ}C) &= 50.0 \qquad \text{for } 7.13 < t \leqslant 120 \text{ min} \\
T(^{\circ}C) &= 6786.5 - 111.538\ t + 0.4616\ t^2 \qquad \text{for } 120 < t \leqslant 124.8 \text{ min} \\
T(^{\circ}C) &= 70.0 \qquad \text{for } t > 124.8 \text{ min}
\end{aligned} \tag{16}
$$

Model predictions using the best fit correlations and experimental x and M_v data are shown in Figs.21 b and c respectively. Once again, reasonable accord between these is

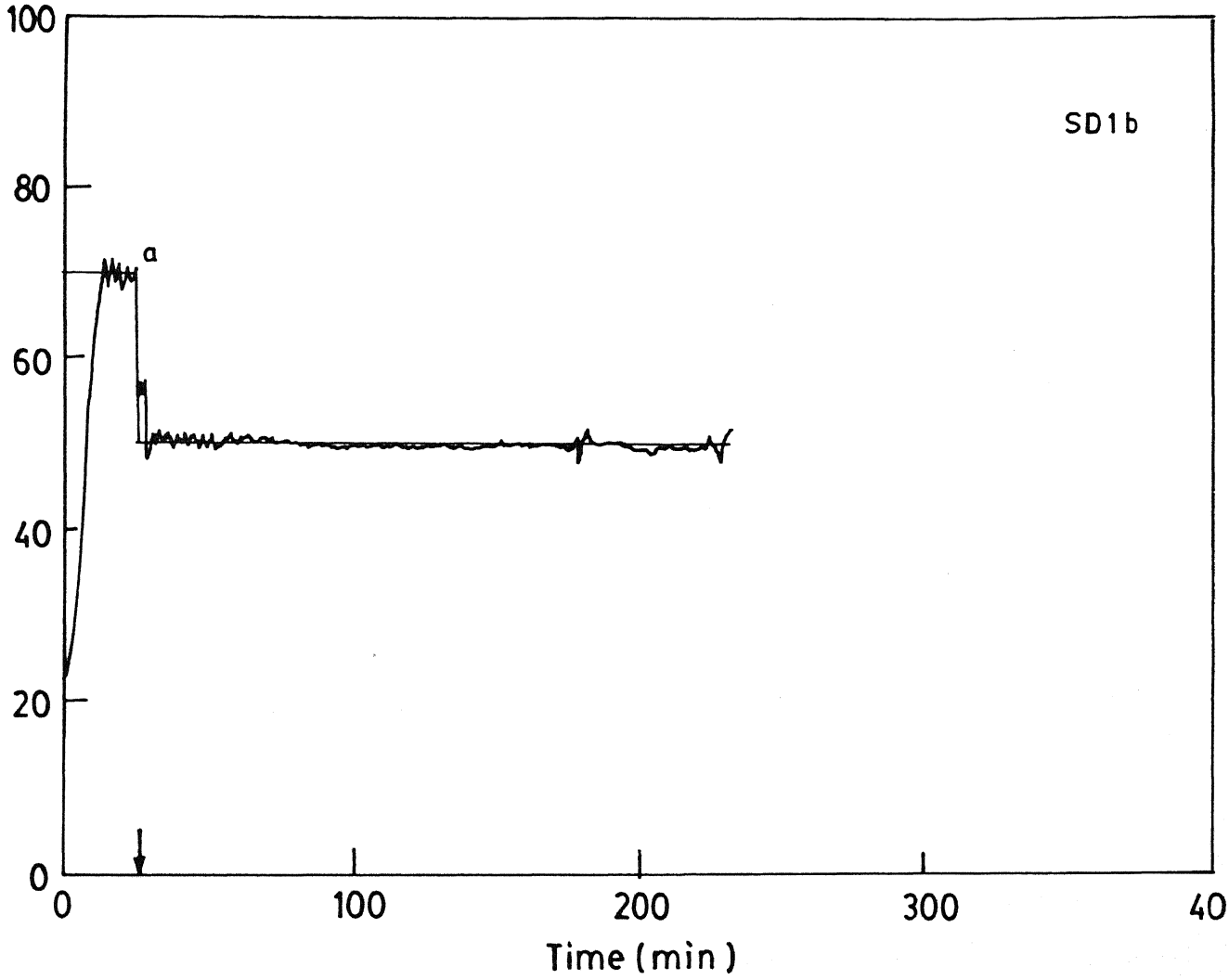

(a)

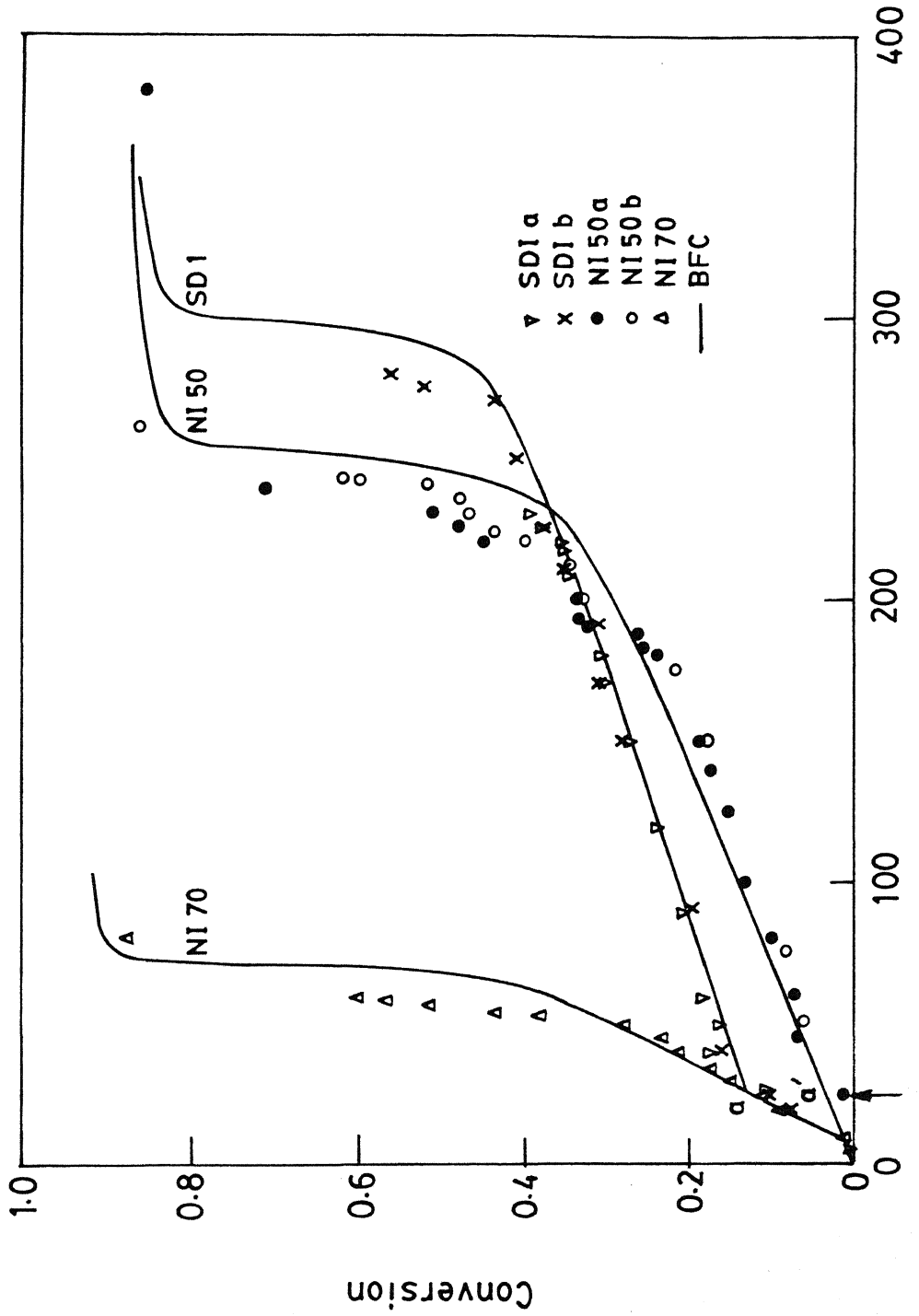
1.0
0.8
0.6
0.4
0.2
0
Conversion
0
100
200
300
400
Time (min)
SDI 1
NI 50
NI 70
SDI a
SDI b
NI 50a
NI 50b
NI 70
BFC
a'
a
b

(b)

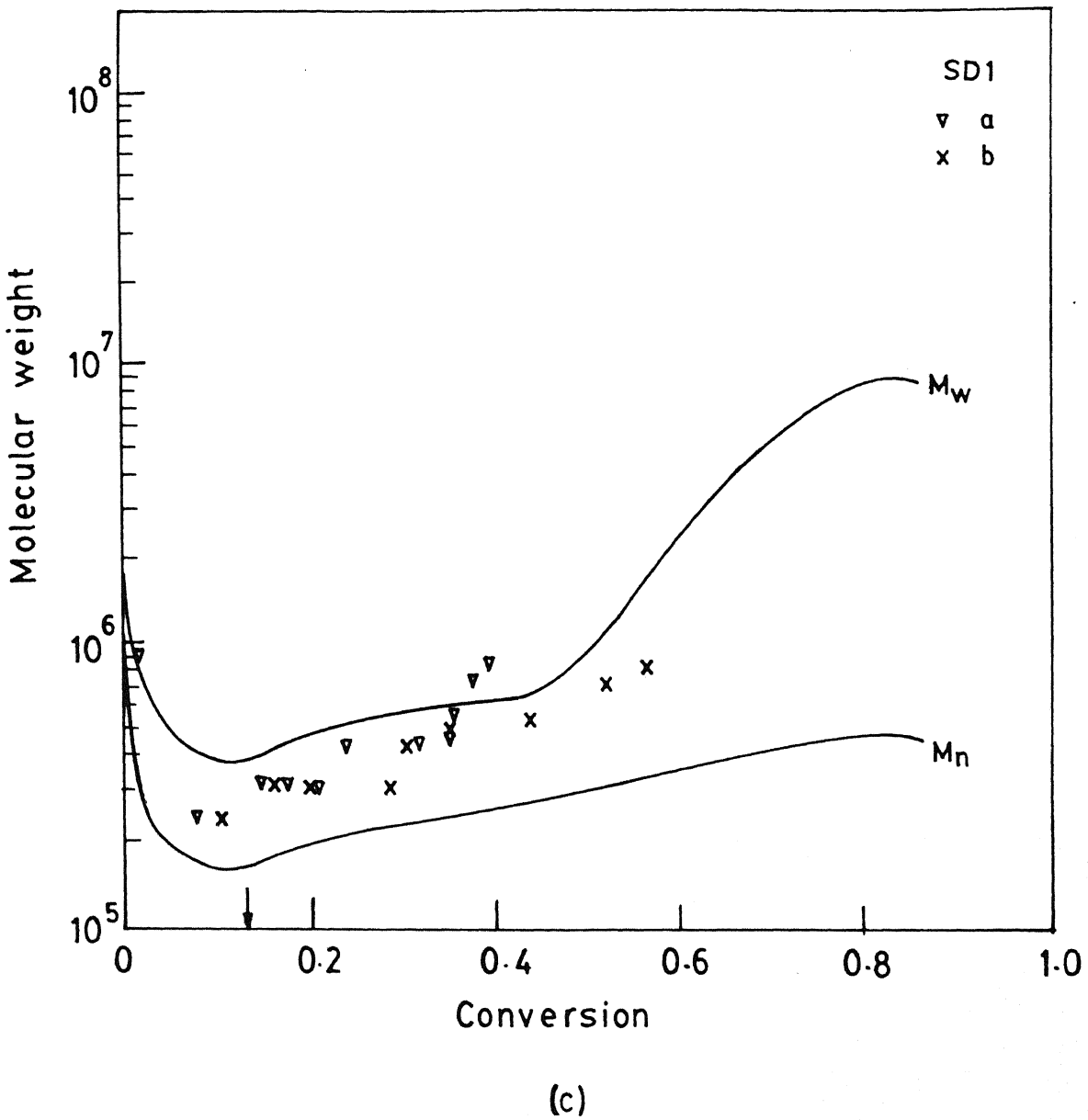

Fig.19 Experimental results on the step decrease (SD1 a and b) runs. Theoretical predictions using the measured temperature history (Fig.19a) and the BFCs in the model of Ray et al. (23) shown by solid curves. $[I]_o$=25.8 mol/m^3, f_s^o=0.

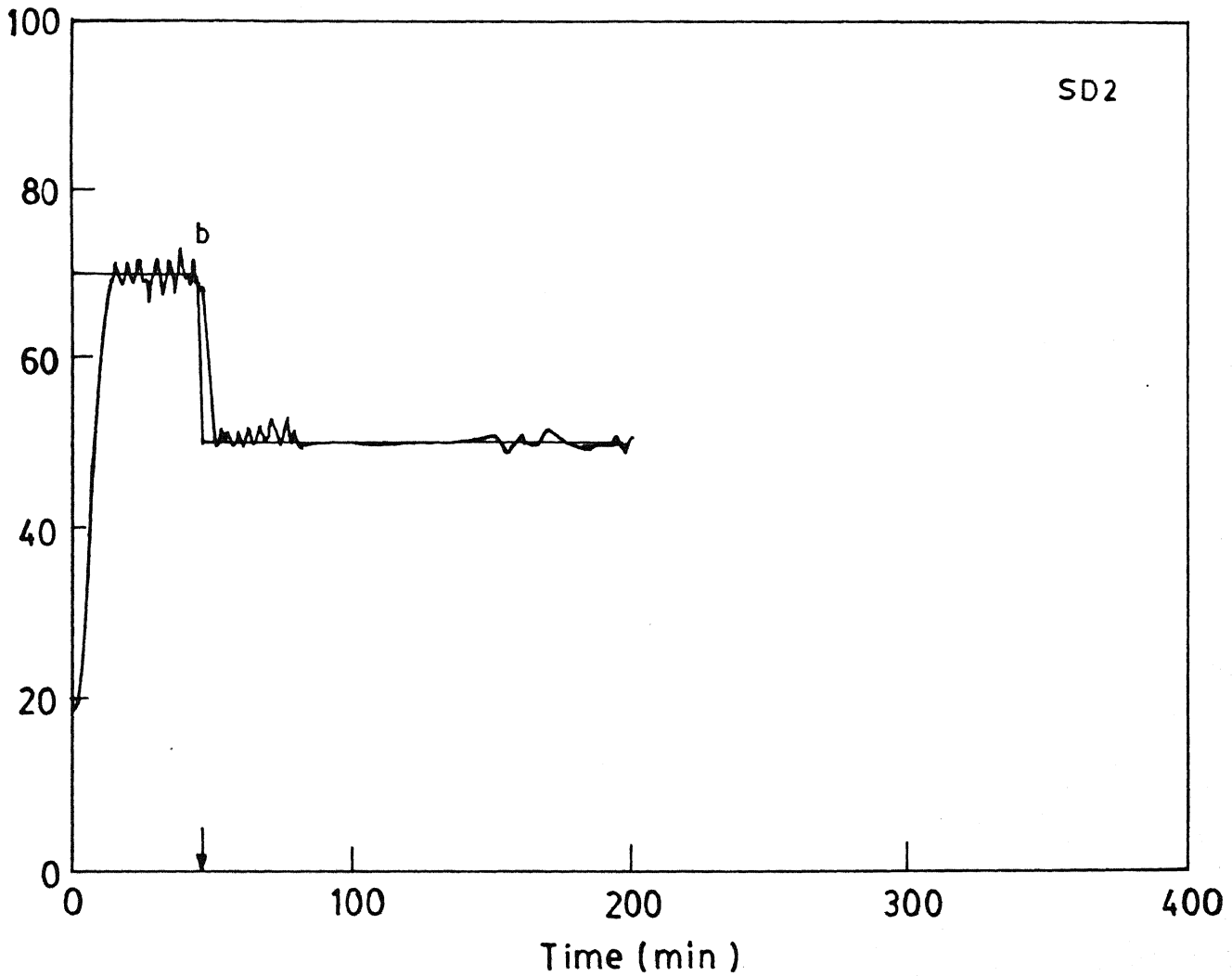

(a)

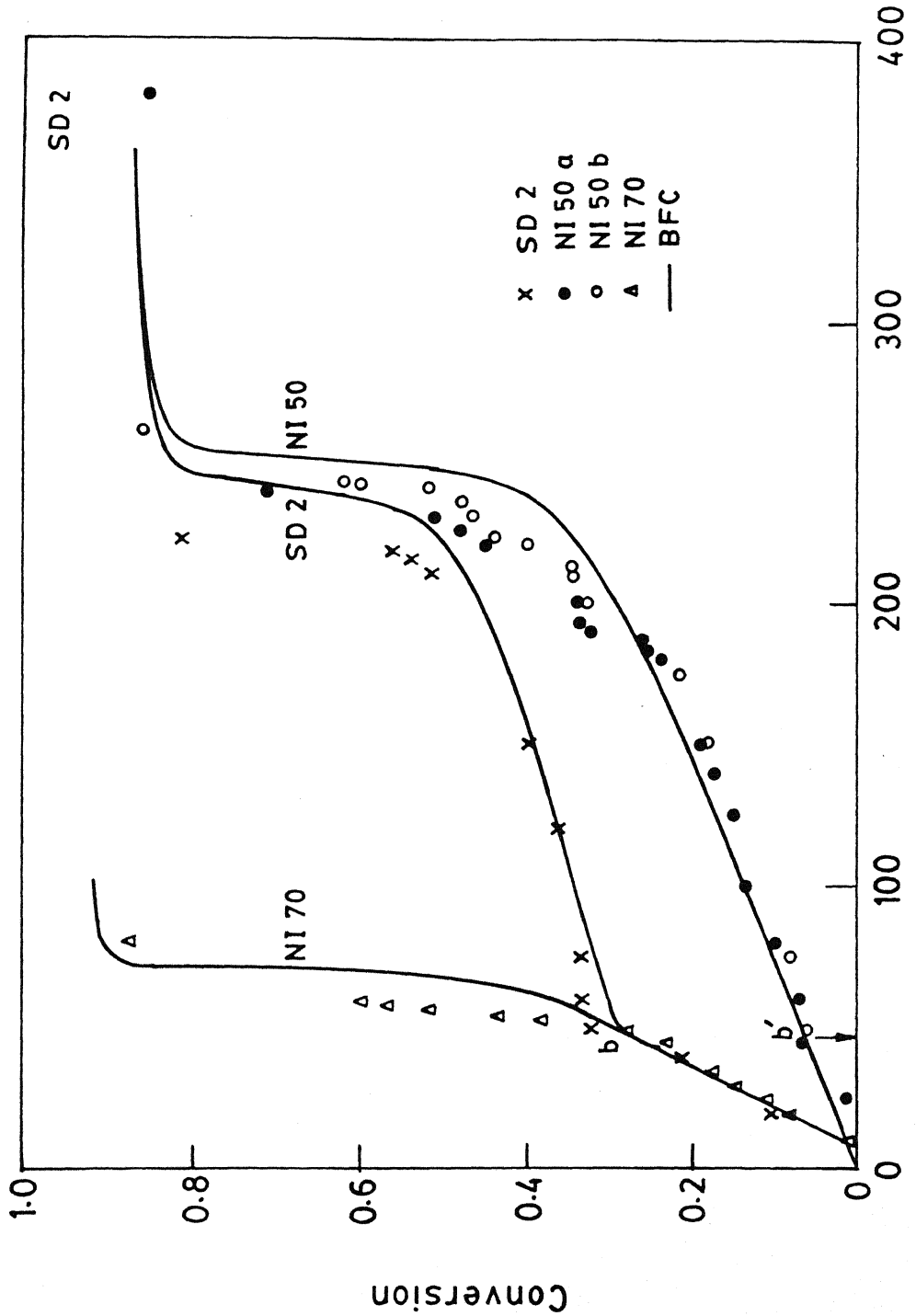
SD 2
NI 50
SD 2
NI 70
x SD 2
● NI 50 a
o NI 50 b
▲ NI 70
— BFC
b
b'
Conversion
1.0
0.8
0.6
0.4
0.2
0
100
200
300
400
Time (min)

(b)

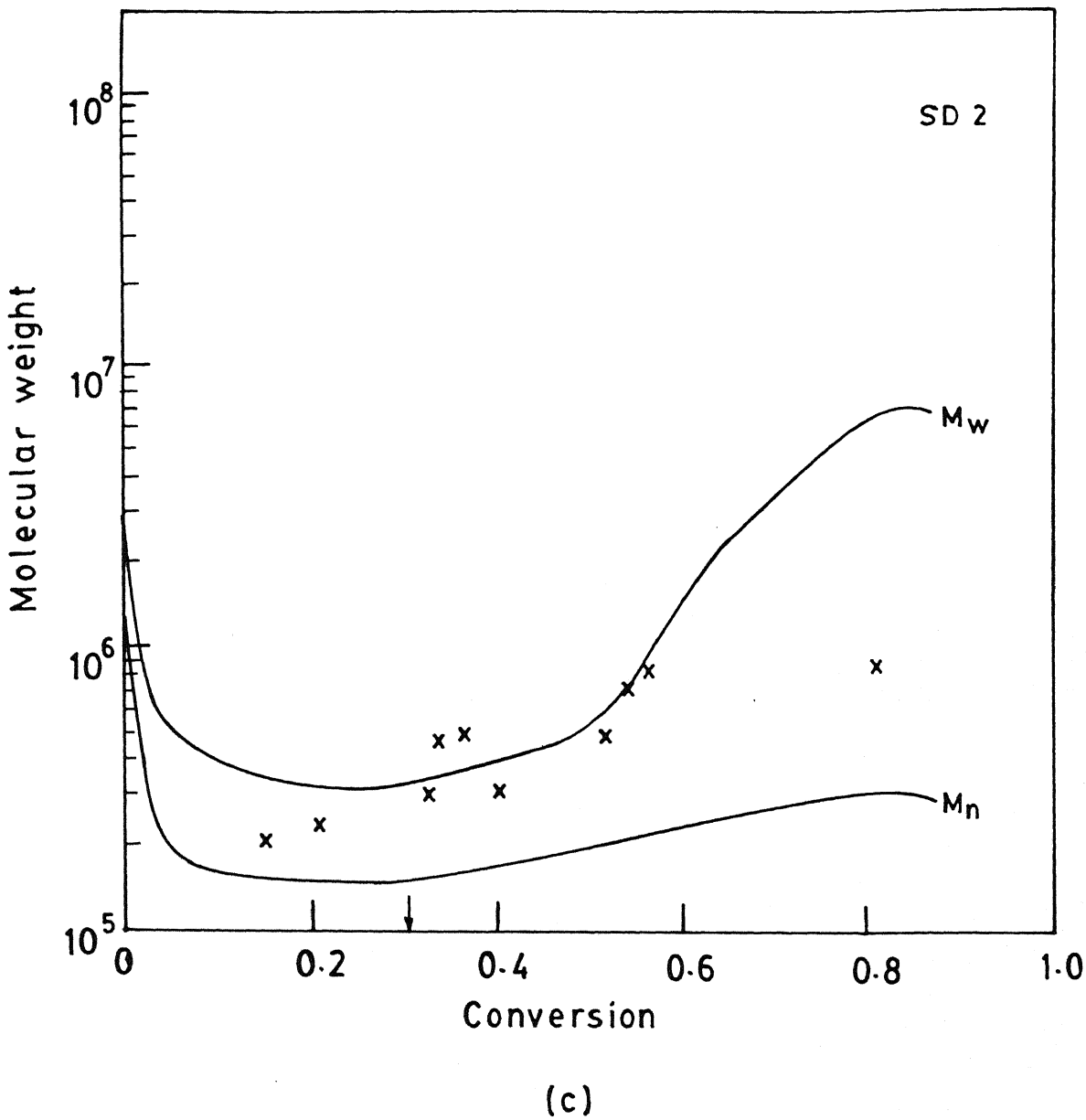

Fig.20 Experimental results on the step decrease (SD2) run. Details same as in Fig.19.

observed.

Figs.19b and 20b demonstrate experimentally the interesting result first predicted theoretically by Ray et al. (23) that the gel effect can either get preponed or postponed when the temperature undergoes a step decrease, as compared to the case when the temperature is maintained constant (at the final value). The exact nature of the x *vs.* t plot depends on the viscosity (strictly speaking, the microviscosity) of the reaction mass at the time the step change is effected. Thus, if the polymer concentration and molecular weight at point a in Fig.19b are such that the viscosity of the reaction mixture is lower than at point a' on the NI50 curve, the gel effect will be postponed. Similarly, if the viscosity at point b (Fig.20b) is larger than at point b' on the NI50 curve, the gel ffect will be preponed.

Our experimental results shown in Figs. 17-21 show an excellent accord with predictions from the theoretical model of Ray et al. (23). It must be emphasized that the parameters (BFCs) in the theory were obtained using *isothermal* experimental data (6) taken on ampoule reactors, and were not re-tuned while predicting the present results using experimental *nonisothermal* histories. This validates the model of Ray et al. (23) at least for nonisothermal reactor operations. Work is continuing to validate the theory for semibatch reactor operation, in which initiator/monomer are added to the reaction mass during polymerization.

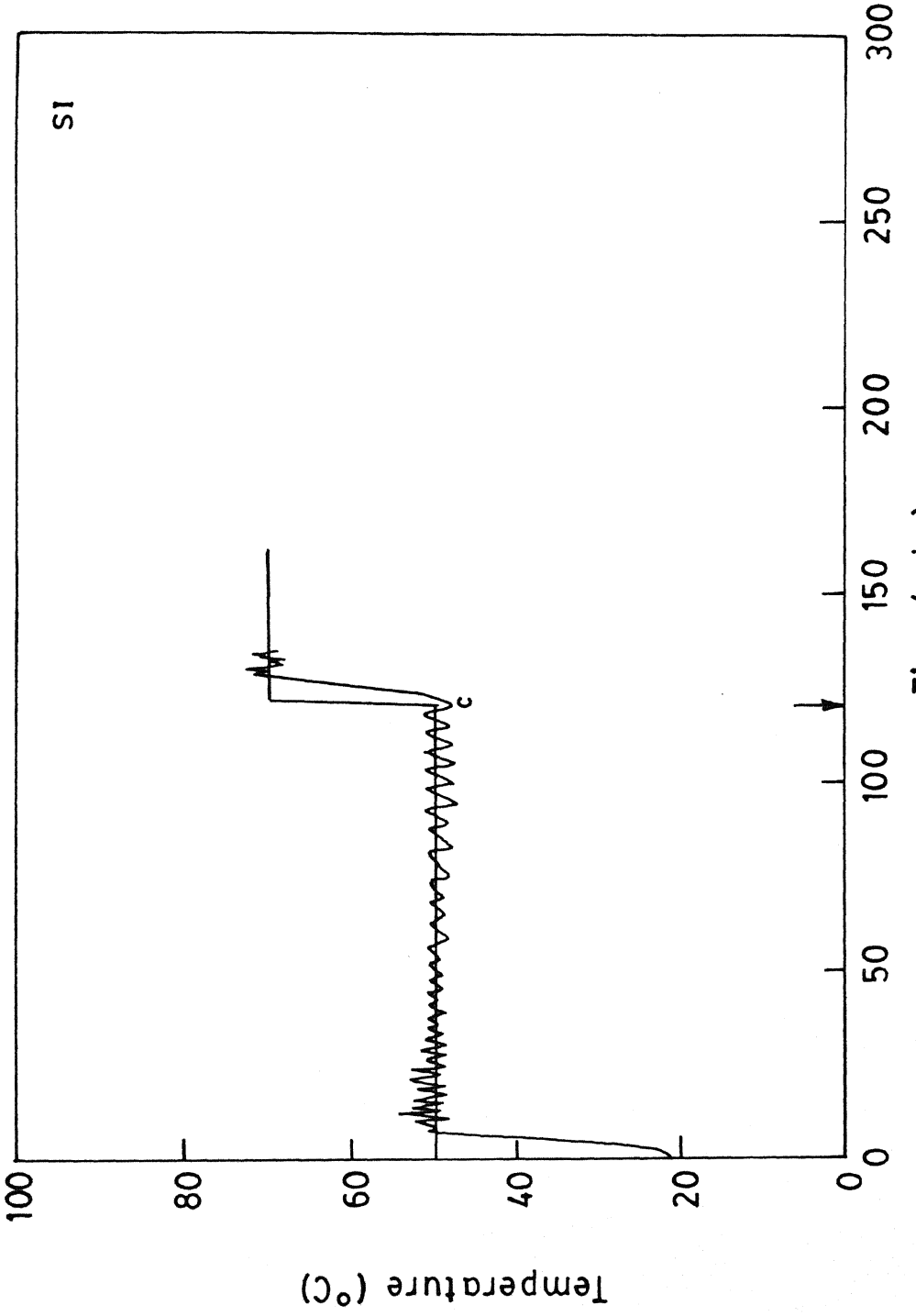
S1
c
Temperature (°C)
Time (min)
0
20
40
60
80
100
0
50
100
150
200
250
300

(a)

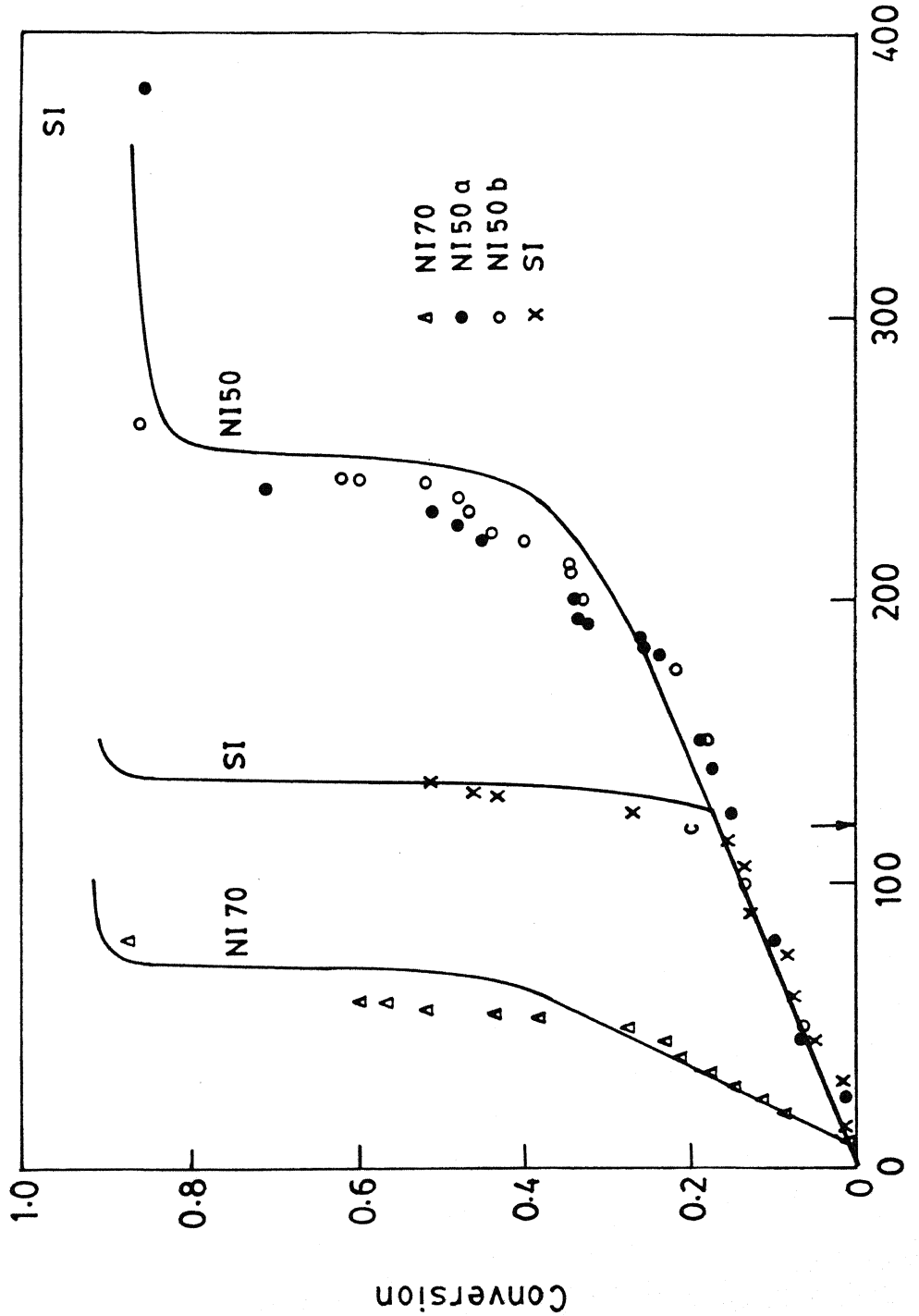
Conversion
1.0
0.8
0.6
0.4
0.2
0
0
100
200
300
400
Time (min)
NI 70
NI 50 a
NI 50 b
SI
NI 70
SI
NI 50
SI
c

(b)

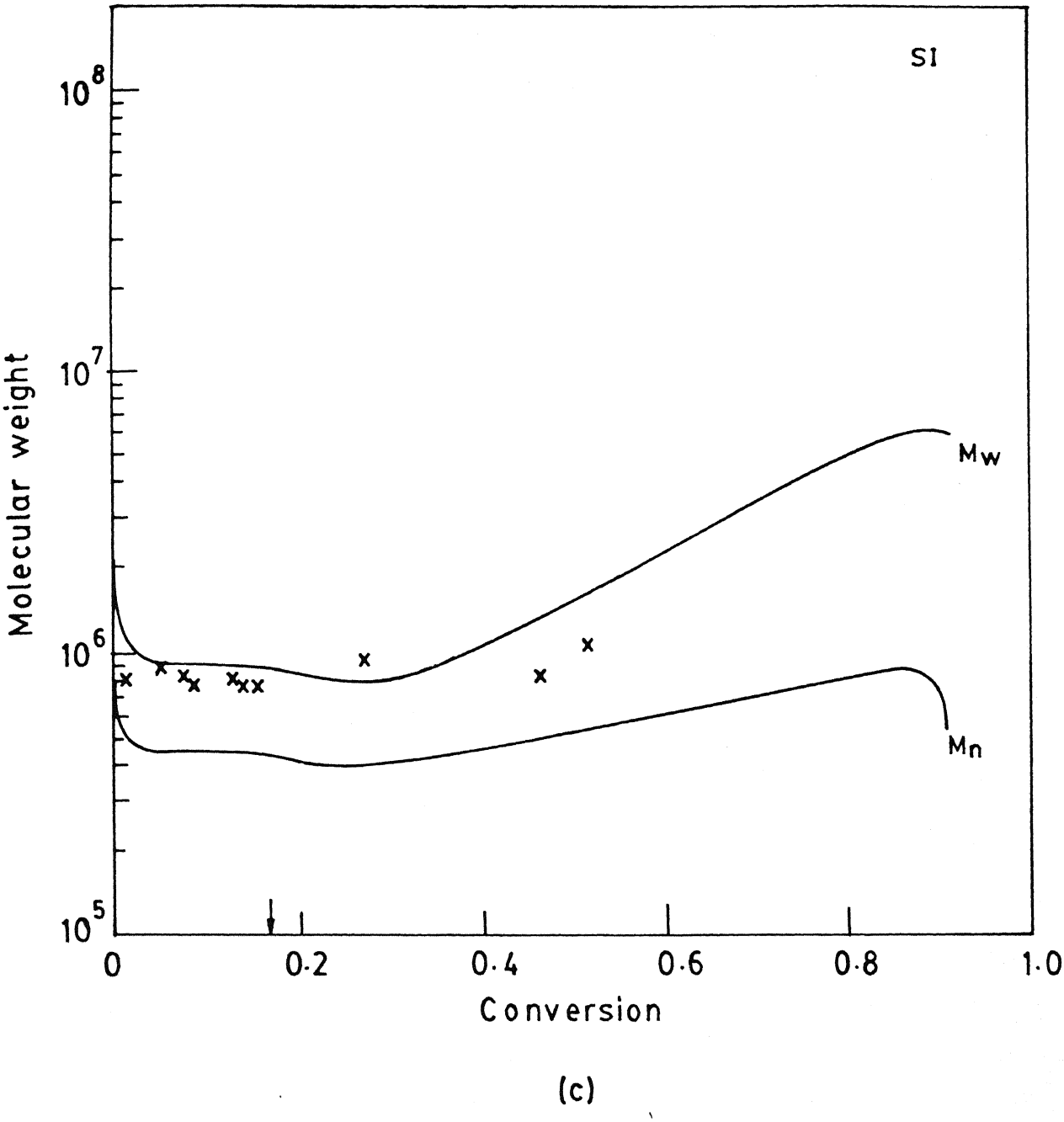

Fig.21 Experimental results on the step increase (SI) run. Details same as in Fig.19.

CHAPTER 6

CONCLUSIONS AND SUGGESTIONS FOR FUTURE WORK

. An experimental set-up to study the effect of temperature changes on bulk polymerization of MMA in a batch reactor has been assembled. A series of experiments under different temperature histories, at a fixed initiator loading, have been conducted. The experimental results (conversion and average molecular weights) obtained show an excellent accord with predictions from the theoretical model of Ray et al. (23). This validates the model of Ray et al. (23) for nonisothermal reactor operations. It must be emphasized that the parameters in the model of Ray et al. were obtained using *isothermal* experimental data of Balke and Hamielec (6), and were not re-tuned for use in the present *nonisothermal* study. These experimental results can be used to obtain better estimates of the model parameters. The present set-up can be used, with modifications, to operate the reactor under semi-batch conditions, in which initiator/monomer are added to the reaction mass during polymerization, and the results tested against the model of Ray et al. to validate the theory for semibatch reactor operations.

ACKNOWLEDGEMENT

This work was supported, in part, through financial support recieved from the Council of Scientific and Industrial Research, New Delhi, India through research scheme No. 22(0232)/93/EMR-II.

REFERENCES

1. Norrish, R.G.W. and Smith, R.R., *Nature*, 1942, **150**, 336.

2. Trommsdorff, E., Kohle, H. and Lagally, P., *Makromol. Chem.*, 1948, **1**, 169.

3. Friis, N. and Hamielec, A.E., *Am. Chem. Soc., Div. Polym. Chem., Polym. Prepr.*, 1975, **16**, 192.

4. Ross, R.T. and Laurence, R.L., *AIChE Symp. Ser.*, 1976, **72** (No. 160), 74.

5. Cardenas, J.N. and O'Driscoll, K.F., *J. Polym. Sci., Polym. Chem. Edn.*, 1976, **14**, 883.

6. Balke, S.T. and Hamielec, A.E., *J Appl. Polym. Sci.*, 1973, **17**, 905.

7. O'Driscoll, K. F., *Pure Appl. Chem.* 1981, **53**, 617.

8. Hamielec, A. H., *Chem. Eng. Commun.* 1983, **24**, 1.

9. Chiu, W.Y., Carratt, G.M and Soong, D.S., *Macromolecules*, 1983, **16**, 348.

10. Carratt, G.M., Shervin, C.R. and Soong, D.S., *Polym. Eng. Sci.*, 1984, **24**, 442.

11. Baillagou, P.E. and Soong, D.S., *Polym. Eng. Sci.*, 1985, **25**, 212.

12. Baillagou, P.E. and Soong, D.S., *Polym. Eng. Sci.*, 1985, **25**, 232.

13. Louie, B.M. and Soong, D.S., *J. Appl. Polym. Sci.*, 1985, **30**, 3707.

14. Louie, B.M. and Soong, D.S., *J. Appl. Polym. Sci.*, 1985, **30**, 3825.

15. Kapoor, B., Gupta, S.K. and Varma, A., *Polym. Eng. Sci.*, 1989, **29**, 1246.

16. Vaid, N.R. and Gupta, S.K., *Polym. Eng. Sci.*, 1991, **31**, 1708.

17. Ravi Kumar, V. and Gupta, S.K., *Polymer*, 1991, **32**, 3233.

18. Agarwal, B. and Gupta, S.K., *J. Polym. Eng.*, in press.

19. Achilias, D. and Kiparissides, C., *J. Appl. Poly. Sci.*, 1988, **35**, 1303.

20. Achilias, D. and Kiparissides, C., *Macromolecules*, 1992,

21. Vrentas, J.S. and Duda, J.L., *AIChEJ*, 1979, **25**, 1.

22. Soh, S.K. and Sundberg, D.C., *J Polym. Sci., Polym. Chem. Edn.*, 1982, **20**, 1315.

23. Ray, A.B., Saraf, D.N. and Gupta, S.K., *Polymer*, to be submitted.

24. Elicabe, G.E. and Meira, G.R., *Polym. Eng. Sci.*, 1988, **28**, 121.

25. Amrehn, H., *Automatica*, 1977, **13**, 533.

26. Congalidis, J.P., Richards, J.R. and Ray, W.H., *AIChEJ*, 1989, **35**, 891.

27. Hidalgo, P.M. and Brosilow, C.B., *Comp. and Chem. Eng.*, 1990, **14**, 481.

28. Soroush, M. and Kravaris, C., *AIChEJ*, 1992, **38**, 1429.

29. PCLAB Manual, Data Translation Inc., Marlborough, USA, 1987.

30. Stephenopoulos, G., "Chemical Process Control : An Introduction to Theory and Practice", Prentice Hall, Englewood Cliffs, NJ, 1984.

31. Cuthbert, T.R., "Circuit Design Using Personal Computers", John Wiley, New York, 1983.

32. Maiti, S.N., PhD Thesis, Dept. of Chemical Eng., I.I.T. Kanpur, 1993.

33. Sivakumar, S., M.Tech Thesis, Dept. of Chemical Eng., I.I.T. Kanpur, 1993.

34. Jana, S.K., M.Tech Thesis, Dept. of Chemical Eng., I.I.T. Kanpur, 1989.

35. Savitzky, A. and Golay, M.J.E., *Ana. Chem.*, 1984, **36**, 1627.

36. Ito, K., *J. Polym. Sci., Polym Chem. Edn.*, 1975, **13**, 401.

37. Suddaby, K.G., O'Driscoll, K.F. and Rudin, A., *J. Polym. Sci., Part A: Polym. Chem. Edn.*, 1992, **30**, 643.

38. Braun, D., Cherdron, H. and Kern, W., "Techniques of Polymer Synthesis Characterization", Interscience, New York, 1972.

39. McCaffery, E.M., "Laboratory Preparation For Macromolecular Chemistry", McGraw Hill, New York, 1970.

40. van Wazar, J.R., Lyons, J.W., Kim, K.Y. and Colwell, R.E., "Viscosity and Flow Measurements", Interscience, New York, 1963.

41. Brandrup, J. and Immergut, F.H., (Eds.), "Polymer Handbook", Second Edition, John Wiley, New York, 1975.

APPENDIX 1

Table - A-1-1
Conversion results for NI50a run

Mass of monomer at $t = 0$ in reactor = 364.26 g
Mass of initiator at $t = 0$ in reactor = 1.067 g
Solvent fraction, $f_s^o = 0.0$; $[I]_o = 25.8$ mol/m^3

No.	Sampling time (min)	mass of empty sample bottle w_1 (g)	w_1+mass of benzene + inhibitor w_2 (g)	w_2+mass of polymer sample w_3(g)	mass of polymer sample w_4(g)	mass of polymer precipitated w_5(g)	monomer conversion*
1	25.00	42.1818	50.8478	51.0720	0.2242	0.0029	0.0131
2	45.00	63.1956	71.8840	73.3340	1.4500	0.0989	0.0682
3	60.00	63.8669	72.5351	76.6868	4.1517	0.2960	0.0713
4	80.00	54.4975	63.1141	71.5454	8.4313	0.8364	0.0992
5	100.00	51.8205	60.4698	63.6862	3.2164	0.4310	0.1340
6	125.00	49.8981	55.5580	61.6065	6.0485	0.9133	0.1510
7	140.00	55.0350	63.6920	65.1961	1.5041	0.2602	0.1730
8	150.00	50.5054	59.1649	59.5500	0.3851	0.0728	0.1890
9	180.00	42.2414	50.9066	51.1360	0.2294	0.0548	0.2390
10	186.00	61.7470	70.4100	73.6900	3.2800	0.8561	0.2610
11	190.00	62.2074	70.8570	75.9600	5.1030	1.6483	0.3230
12	193.00	61.6740	70.3488	74.6400	4.2912	1.4333	0.3340
13	200.00	58.7476	67.4358	76.6340	9.1982	3.1090	0.3380
14	220.00	64.6650	73.3320	78.5892	5.2572	2.3710	0.4510
15	225.00	64.9650	73.6532	79.6530	5.9998	2.8919	0.4820
16	230.00	61.9486	70.6368	78.5380	7.9012	4.0533	0.5130
17	238.00	62.4820	71.1744	78.2360	7.0616	5.0279	0.7120
18	260.00	61.5632	70.2514	75.2130	4.9616	4.2322	0.8530

conversion $x = \frac{w_5}{w_4}$

Table - A-1-2
Conversion results for NI50b run

Mass of monomer at $t = 0$ in reactor = 541.72 g
Mass of initiator at $t = 0$ in reactor = 2.394 g
Solvent fraction, $f_s^o = 0.0$; $[I]_o = 25.8$ mol/m^3

No.	Sampling time (min)	mass of empty sample bottle w_1 (g)	w_1+mass of benzene + inhibitor w_2 (g)	w_2+mass of polymer sample w_3(g)	mass of polymer sample w_4(g)	mass of polymer precipitated w_5(g)	monomer conversion*
1	25.00	42.2474	50.8801	58.9550	8.0749	0.1130	0.0140
2	50.00	56.9174	65.5693	67.5825	2.0132	0.1278	0.0635
3	75.00	51.8283	60.4727	65.0394	4.5667	0.3745	0.0820
4	100.00	48.6316	57.2556	60.9876	3.7320	0.5038	0.1350
5	150.00	61.6728	70.3271	71.8861	1.5590	0.2853	0.1830
6	175.00	39.6350	48.2803	52.3484	4.0681	0.8868	0.2180
7	200.00	48.9352	57.5823	59.1000	1.5177	0.4978	0.3280
8	210.00	58.8449	67.4713	67.7429	0.3209	0.1107	0.3450
9	212.00	64.1432	72.7765	73.8853	1.1088	0.3845	0.3468
10	220.00	51.0863	59.0520	60.6854	1.6334	0.6534	0.4000
11	223.00	49.2256	57.8671	58.2238	0.3567	0.1569	0.4400
12	230.00	62.2216	70.8113	70.9363	0.1250	0.0585	0.4680
13	235.00	49.3197	57.9417	58.9563	1.0146	0.4870	0.4800
14	240.00	51.1434	59.7930	60.1611	0.3681	0.1914	0.5200
15	242.00	65.4352	74.7545	81.6118	6.8573	5.8973	0.8600

conversion $x = \frac{w_5}{w_4}$

Table - A-1-3
Conversion results for NI70 run

Mass of monomer at $t = 0$ in reactor = 373.6 g
Mass of initiator at $t = 0$ in reactor = 1.6924 g
Solvent fraction, $f_s^o = 0.0$;$[I]_o = 25.8$ mol/m^3

No.	Sampling time (min)	mass of empty sample bottle w_1 (g)	w_1+mass of benzene + inhibitor w_2 (g)	w_2+mass of polymer sample w_3(g)	mass of polymer sample w_4(g)	mass of polymer precipitated w_5(g)	monomer conversion*
1	10.00	41.4161	50.1764	68.2180	18.0416	0.1967	0.0109
2	20.00	41.5387	50.2505	55.3020	5.0515	0.4551	0.0901
3	25.00	56.7561	65.4333	73.5700	8.1367	0.9064	0.1114
4	30.00	49.2877	57.9870	64.5700	6.5830	0.9749	0.1481
5	35.00	49.2972	56.9795	64.1130	7.1335	1.2491	0.1751
6	40.00	49.2976	57.9609	64.5460	6.5851	1.4171	0.2152
7	45.00	62.5471	71.2286	75.5664	4.3378	1.0090	0.2326
8	50.00	58.8406	67.5330	69.4391	1.9061	0.5305	0.2783
9	53.00	62.5241	71.2989	74.1855	2.8866	1.1087	0.3841
10	54.00	50.5061	59.1823	61.8772	2.6949	1.1752	0.4361
11	56.00	49.2356	57.9206	59.8110	1.8904	0.9760	0.5163
12	58.00	59.3727	68.0559	69.0857	1.0298	0.5851	0.5682
13	60.00	49.8990	58.5703	59.8832	1.3129	0.7894	0.6013
14	80.00	56.3214	65.0122	66.8011	1.7889	1.5664	0.8756

conversion $x = \frac{w_5}{w_4}$

Table - A-1-4
Conversion results for SD1a run

Mass of monomer at $t = 0$ in reactor = 373.6 g
Mass of initiator at $t = 0$ in reactor = 1.6512 g
Solvent fraction, $f_s^o = 0.0$;$[I]_o = 25.8$ mol/m^3

No.	Sampling time (min)	mass of empty sample bottle w_1 (g)	w_1+mass of benzene + inhibitor w_2 (g)	w_2+mass of polymer sample w_3(g)	mass of polymer sample w_4(g)	mass of polymer precipitated w_5(g)	monomer conversion*
1	5.00	42.1818	50.8881	52.7634	1.8753	0.0034	0.0018
2	10.00	63.8669	72.5730	74.5840	2.0110	0.0402	0.0200
3	20.00	63.1956	71.9019	74.7360	2.8341	0.2281	0.0805
4	30.00	54.4975	63.2038	65.3850	2.1812	0.3300	0.1513
5	40.00	51.8205	60.5268	61.6380	1.1112	0.1948	0.1753
6	50.00	49.8981	58.6044	61.3230	2.7186	0.4385	0.1613
7	60.00	55.0350	63.7413	64.9876	1.2463	0.2297	0.1843
8	90.00	42.2414	50.9477	54.8360	3.8883	0.7971	0.2050
9	120.00	50.5050	59.2113	63.8320	4.6207	1.1062	0.2394
10	150.00	49.3483	58.0546	59.9830	1.9284	0.5288	0.2742
11	170.00	62.2074	70.9137	74.9137	4.0000	1.2212	0.3053
12	180.00	61.6740	70.3803	72.1380	1.7577	0.5285	0.3007
13	190.00	63.5631	72.2694	74.2830	2.0136	0.6393	0.3175
14	210.00	58.7863	67.4926	69.9530	2.4604	0.8611	0.3500
15	218.00	59.8363	68.5966	70.2340	1.6374	0.5777	0.3528
16	220.00	63.5463	72.3066	73.9870	1.6804	0.5975	0.3556
17	225.00	63.4320	72.1383	75.3840	3.2457	1.2282	0.3784
18	230.00	59.7634	68.4697	70.4830	2.0133	.7959	.3953

conversion $x = \frac{w_5}{w_4}$

Table - A-1-5
Conversion results for SD1b run

Mass of monomer at $t = 0$ in reactor = 513.7 g
Mass of initiator at $t = 0$ in reactor = 2.2704 g
Solvent fraction, $f_s^o = 0.0$;$[I]_o = 25.8$ mol/m^3

No.	Sampling time (min)	mass of empty sample bottle w_1 (g)	w_1+mass of benzene + inhibitor w_2 (g)	w_2+mass of polymer sample w_3(g)	mass of polymer sample w_4(g)	mass of polymer precipitated w_5(g)	monomer conversion*
1	5.00	42.1207	50.8810	52.3840	1.5030	0.0020	0.0013
2	10.00	63.1415	71.9018	74.5320	2.6302	0.0473	0.0180
3	20.00	63.8127	72.5730	75.8360	3.2630	0.2588	0.0793
4	25.00	49.8441	58.6044	63.8430	5.2386	0.5432	0.1037
5	40.00	51.7781	60.5384	62.2386	1.7002	0.2742	0.1613
6	90.00	42.1874	50.9477	54.9860	4.0383	0.7968	0.1973
7	150.00	49.2853	58.0456	63.2840	5.2384	1.4830	0.2831
8	170.00	62.2238	70.9841	73.8620	2.8779	0.8665	0.3011
9	210.00	54.6779	63.4382	68.5320	5.0938	1.7961	0.3526
10	225.00	61.2253	69.9856	71.9560	1.9704	0.7511	0.3812
11	250.00	58.9251	67.6854	70.8320	3.1466	1.3014	0.4136
12	270.00	61.1047	69.8650	72.9350	3.0700	1.3407	0.4367
13	275.00	58.9251	67.6854	70.8342	3.1488	1.6415	0.5213
14	280.00	60.1047	68.8650	71.9216	3.0566	1.7203	0.5628

conversion $x = \frac{w_5}{w_4}$

Table - A-1-6
Conversion results for SD2 run

Mass of monomer at $t = 0$ in reactor = 373.6 g
Mass of initiator at $t = 0$ in reactor = 1.6512 g
Solvent fraction, $f_s^o = 0.0$;$[I]_o = 25.8$ mol/m^3

No.	Sampling time (min)	mass of empty sample bottle w_1 (g)	w_1+mass of benzene + inhibitor w_2 (g)	w_2+mass of polymer sample w_3(g)	mass of polymer sample w_4(g)	mass of polymer precipitated w_5(g)	monomer conversion*
1	10.00	63.2631	72.0234	75.5857	3.5623	0.0363	0.0102
2	20.00	56.9517	65.7120	67.6157	1.9037	0.2005	0.1053
3	30.00	41.5674	50.3277	52.2001	1.8724	0.2831	0.1512
4	40.00	51.2778	60.0381	65.5886	5.5505	1.1634	0.2096
5	50.00	49.4287	58.1890	61.0580	2.8690	0.9313	0.3246
6	60.00	51.1781	59.9384	61.0450	1.1066	0.3714	0.3356
7	75.00	65.2048	73.9651	76.0670	2.1019	0.7085	0.3371
8	120.00	62.4303	71.1906	71.5672	0 .3766	0.1368	0.3632
9	150.00	62.1590	70.9193	71.3410	0.4217	0.1692	0.4013
10	210.00	49.1239	57.8842	59.0101	1.1259	0.5813	0.5163
11	215.00	52.2817	61.0420	64.9915	3.9495	2.1375	0.5412
12	218.00	40.7731	49.5334	53.0078	3.4744	1.9568	0.5632
13	222.00	15.5167	24.2770	28.2581	3.9811	3.2366	0.8130

conversion $x = \frac{w_5}{w_4}$

Table - A-1-7
Conversion results for SI run

Mass of monomer at $t = 0$ in reactor = 467.0 g
Mass of initiator at $t = 0$ in reactor = 2.064 g
Solvent fraction, $f_s^o = 0.0$;$[I]_o = 25.8$ mol/m^3

No.	Sampling time (min)	mass of empty sample bottle w_1 (g)	w_1+mass of benzene + inhibitor w_2 (g)	w_2+mass of polymer sample w_3(g)	mass of polymer sample w_4(g)	mass of polymer precipitated w_5(g)	monomer conversion*
1	15.00	51.0372	59.7975	63.9566	4.1591	0.0524	0.0126
2	30.00	60.8634	69.6237	77.3404	7.7167	0.1173	0.0152
3	45.00	52.4835	61.2438	65.1651	3.9213	0.2012	0.0513
4	60.00	61.2670	70.0273	78.6636	8.6363	0.6598	0.0764
5	75.00	50.9862	59.7465	73.7833	14:0368	1.1819	0.0842
6	90.00	62.4883	71.2486	84.8275	13.5789	1.7381	0.1280
7	105.00	56.2794	65.0397	74.0980	9.0583	1.2464	0.1376
8	115.00	49.2732	58.0335	66.6431	8.6096	1.3362	0.1552
9	125.00	63.4426	72.2029	83.7706	11.5677	3.1383	0.2713
10	130.00	42.2717	51.0320	57.1059	6.0739	2.6276	0.4326
11	132.00	41.3518	50.1121	55.3437	5.2316	2.4243	0.4634
12	135.00	43.3216	52.0512	60.1365	8.0853	4.4193	0.5132

conversion $x = \frac{w_5}{w_4}$

Molecular weight results for NI50b run

No.	Polymer concentration** c_1 (g/dl)	Efflux times (s) c_1	c_2	c_3	c_4	M_v	x	time min
1	0.75	341.93	289	235.47	215.7	8.162e+05	0.135	100
2	1.0	390.5	341.63	270	234.6	8.1064e+05	0.183	150
3	1.25	373.74	380.92	240.0	203.65	2.96399e+05	0.218	175
4	0.745	341.0	289.0	235.77	215.7	7.70112e+05	0.328	200
5	0.745	341.93	289.06	235.473	215.7	8.319e+05	0.345	210
6	0.832	410.34	340.76	260.45	200.5	4.927e+05	0.3468	212
7	0.75	548.458	405.001	289.684	242.581	9.38955e+05	0.4	220
8	0.84	698.261	496.742	337.126	273.033	1.067649e+06	0.44	223
9	0.8151	405.65	326.85	282.46	—	12.9e+05	0.468	230
10	1.000	231.61	207.98	184.72	175.97	2.40e+05	0.48	235
11	1.0	400.34	310.23	230.65	200.76	3.14022e+05	0.52	240
12	0.819	491.73	367.93	269.12	228.23	7.30049e+05	0.86	242

efflux time for pure solvent (benzene), $t_o = 143.6s$

Molecular weight results for NI70 run

No.	Polymer concentration** c_1 (g/dl)	Efflux times (s) c_1	c_2	c_3	c_4	M_v	x	time min
1	0.3045	189.185	177.655	164.145	159.11	4.62385e+5	0.0183	12.56
2	0.878	256.66	222.73	193.565	179.05	3.13932e+5	0.11498	25
3	1.3215	297.64	251.165	210.5	191.385	2.54268e+5	0.1315	30
4	0.9923	244.39	216.68	191.225	173.595	2.32986e+5	0.2049	35
5	0.922	230.04	211.49	281.75	171.255	2.21975e+5	0.2475	40
6	0.8376	236.305	209.485	186.22	173.475	2.85087e+5	0.2481	42
7	0.7563	234.335	209.715	185.785	176.395	3.65839e+5	0.2522	46.5
8	0.8033	228.265	203.745	182.265	171.385	2.75924e+5	0.2648	48.5
9	0.208	158.9	154.25	149.455	147.525	2.57805e+5	0.2940	50
10	0.8803	230.1	204.97	180.775	169.475	2.15449e+5	0.3195	53

efflux time for pure solvent (benzene), $t_o = 147.08s$

$c_2 = 15\ c_1/20$

$c_3 = 10\ c_2/15$

$c_4 = 15\ c_3/20$

Molecular weight results for SD1a run

No.	Polymer concentration** c_1 (g/dl)	Efflux times (s) c_1	c_2	c_3	c_4	M_v	x	time min
1	0.745	341.43	289.56	235.44	215.77	8.85762e+05	0.020	10
2	1.0	232.205	207.53	185.21	176.68	2.3967e+05	0.0805	20
3	1.0	400.64	312.23	230.42	201.02	3.14132e+05	0.1513	30
4	1.0	400.34	310.23	230.65	200.76	3.14022e+05	0.1754	40
5	1.0	410.43	318.54	240.83	200.32	3.05443e+05	0.2050	90
6	1.0	413.4	320.5	243.4	210.3	4.30934e+05	0.3175	190
7	1.0	421.56	325.52	246.53	214.34	4.66681e+05	0.3500	210
8	0.832	410.23	341.23	260.34	200.78	4.95676e+05	0.3528	218
9	1.0	468.54	354.43	262.53	224.87	5.44117e+05	0.3556	220
10	0.818	490.83	368.23	269.12	228.23	7.27149e+05	0.3784	225
11	0.745	341.8	288.0	235.4	215.4	8.31302e+05	0.3953	230

efflux time for pure solvent (benzene), $t_o = 143.58s$

Molecular weight results for SD1b run

No.	Polymer concentration** c_1 (g/dl)	Efflux times (s) c_1	c_2	c_3	c_4	M_v	x	time min
1	1.00	232.59	208.00	184.62	176.97	2.3998e+05	0.0793	20
2	1.00	232.61	207.98	185.62	176.97	2.3987e+05	0.1037	25
3	1.0	400.64	312.22	230.39	201.00	3.14e+05	0.1613	40
4	1.0	410.39	318.53	240.79	200.30	3.056e+05	0.1973	90
5	1.0	410.43	318.54	240.83	200.32	3.05443e+05	0.2831	150
6	1.0	413.4	320.5	243.38	210.29	4.308e+05	0.3011	170
7	0.830	410.23	341.23	260.30	200.72	4.95e+05	0.3526	210
8	1.0	468.54	354.43	262.53	224.77	5.45e+05	0.4367	270
9	0.819	491.53	367.91	270.02	229.13	7.31e+05	0.5213	275
10	0.744	342.0	289.0	235.4	215.7	8.32e+05	0.5626	280

efflux time for pure solvent (benzene), $t_o = 141.63s$

Molecular weight results for SD2 run

No.	Polymer concentration** c_1 (g/dl)	Efflux times (s) c_1	c_2	c_3	c_4	M_v	x	time min
1	1.0043	230.20	207.9	184.30	173.56	2.0745e+05	0.1512	30
2	1.005	232.61	207.98	185.62	176.97	2.3887e+05	0.2096	40
3	1.0	410.43	318.54	240.83	200.32	3.05443e+05	0.3246	50
4	1.0	421.56	325.52	246.53	214.34	4.66681e+05	0.371	75
5	0.832	410.23	341.23	260.34	200.78	4.95e+05	0.3632	120
6	1.0	400.34	310.23	230.65	200.76	3.139e+05	0.4013	150
7	0.819	491.73	367.93	269.12	228.23	7.29e+05	0.5412	215
8	0.745	341.93	289.06	235.473	215.7	8.319e+05	0.5632	218
9	0.745	341.43	289.56	235.44	215.77	8.85e+05	0.813	222

efflux time for pure solvent (benzene), $t_o = 140.63s$

Molecular weight results for SI run

No.	Polymer concentration** c_1 (g/dl)	Efflux times (s) c_1	c_2	c_3	c_4	M_v	x	time min
1	1.0	390.49	341.629	269.99	234.6	8.1056e+05	0.0152	30
2	0.745	341.43	289.56	235.44	215.77	8.857e+05	0.0513	45
3	0.745	341.93	289.06	235.473	215.7	8.318e+05	0.0764	60
4	0.745	341.0	289.0	235.77	215.7	7.6996e+05	0.0842	75
5	0.75	341.93	289	235.47	215.7	8.162e+05	0.128	90
6	0.745	341.0	288.99	235.6	214.7	7.727e+05	0.1376	105
7	0.745	341.0	289.0	235.77	215.7	7.70112e+05	0.1552	115
8	0.75	548.45	405.0	289.64	242.58	9.3955e+05	0.2713	125
9	0.744	342.0	289.0	235.4	215.7	8.32e+05	0.4634	132
10	0.84	697.251	496.740	337.123	273.003	1.075e+06	0.5132	135

efflux time for pure solvent (benzene), $t_o = 143.62s$

APPENDIX 2

FLOW CHART FOR THE CONTROL PROGRAM

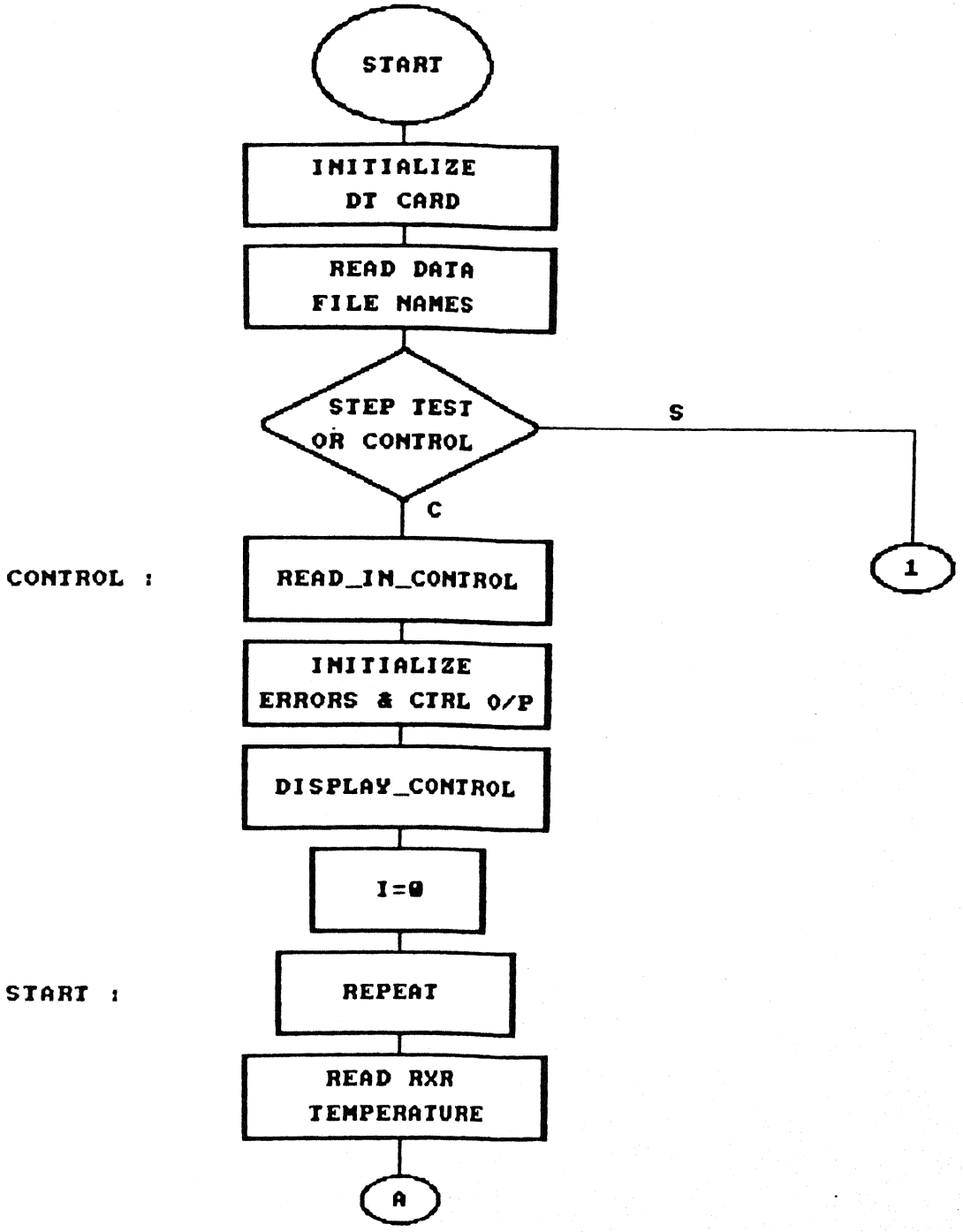

N.B : Procedure names are given in quotations.

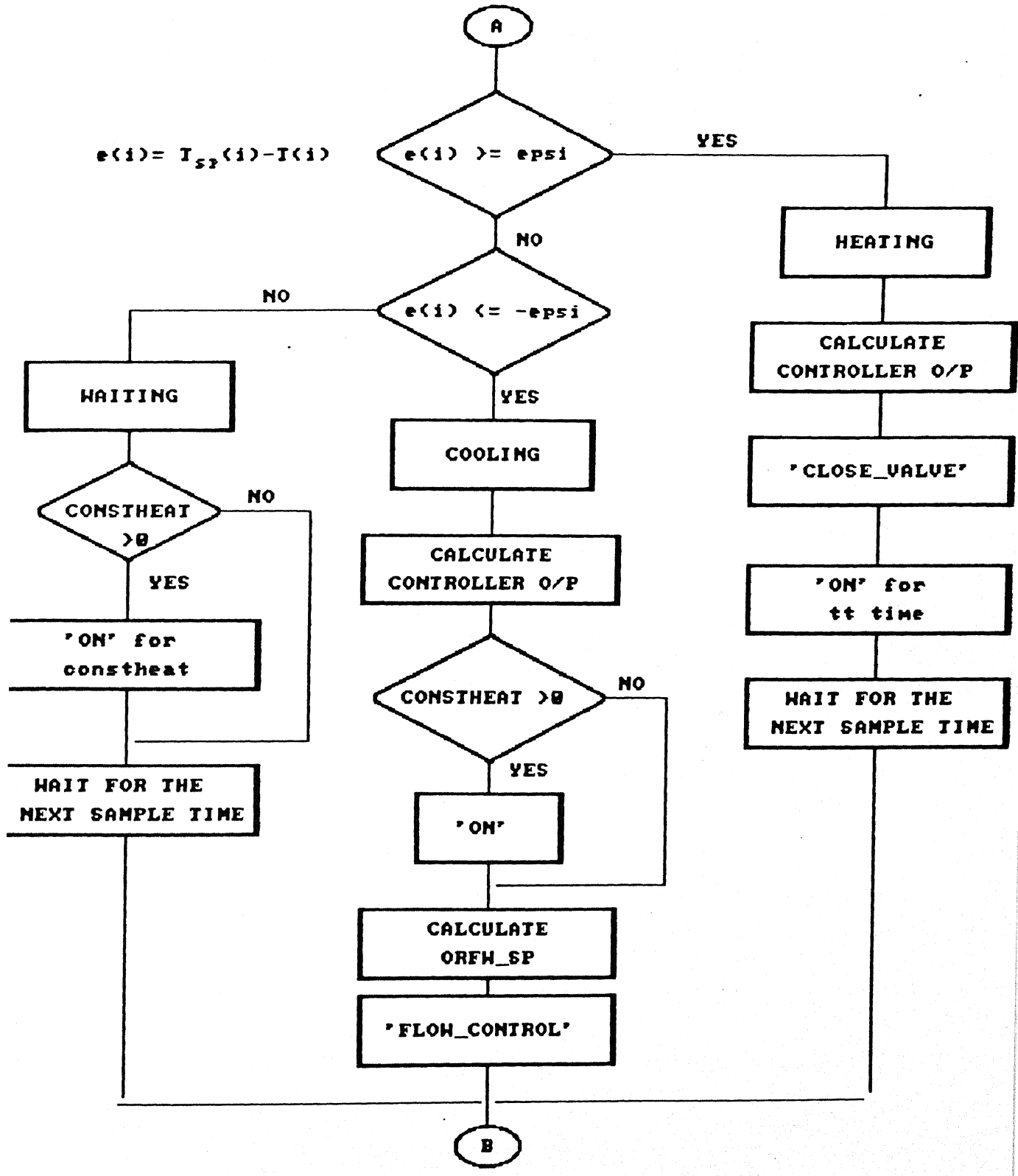
A
e(i)= T_ss(i)-T(i)
e(i) >= epsi
YES
NO
HEATING
CALCULATE CONTROLLER O/P
'CLOSE_VALVE'
'ON' for tt time
WAIT FOR THE NEXT SAMPLE TIME
e(i) <= -epsi
NO
YES
WAITING
CONSTHEAT >0
NO
YES
'ON' for constheat
WAIT FOR THE NEXT SAMPLE TIME
COOLING
CALCULATE CONTROLLER O/P
CONSTHEAT >0
NO
YES
'ON'
CALCULATE ORFW_SP
'FLOW_CONTROL'
B

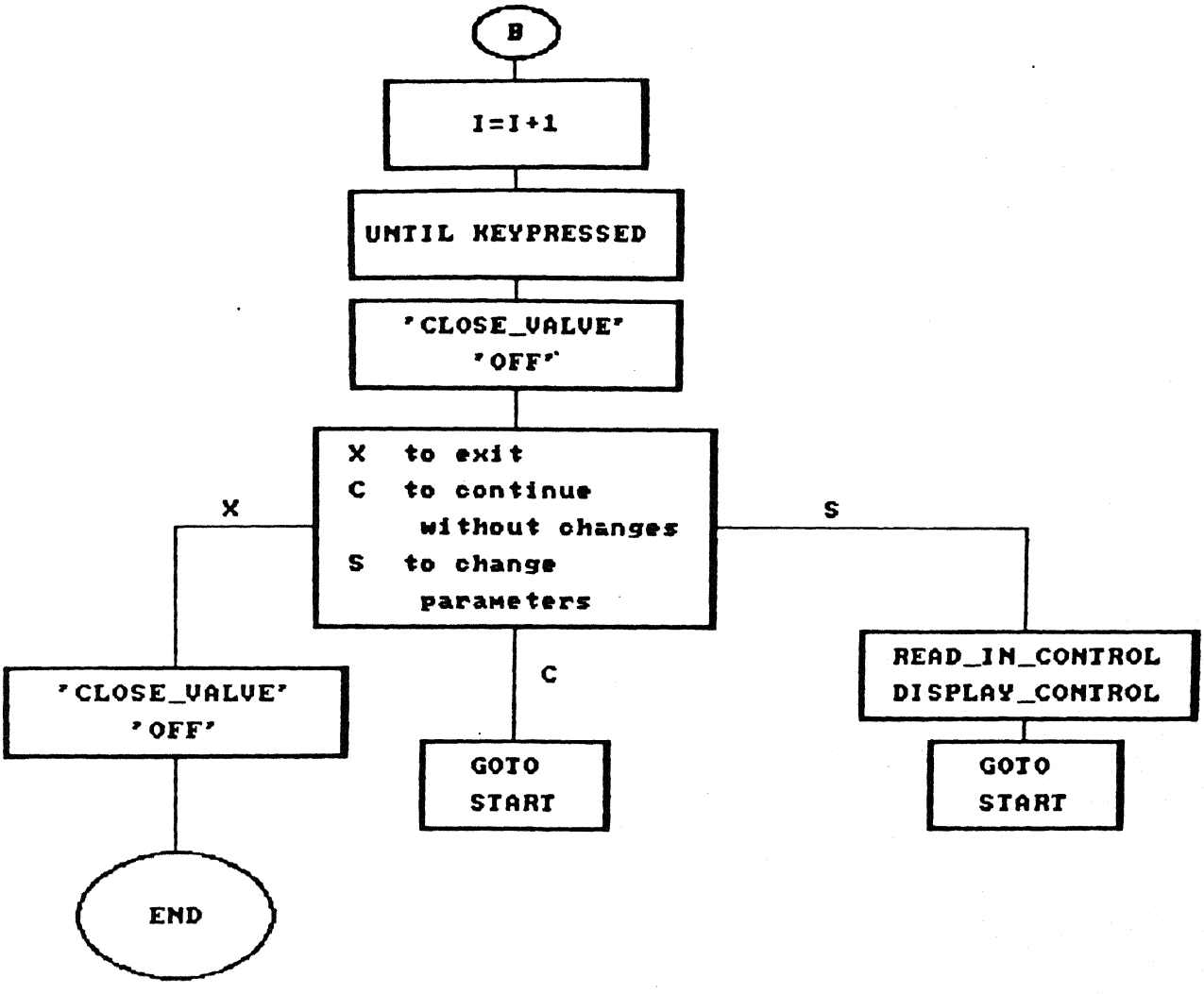
B
I=I+1
UNTIL KEYPRESSED
'CLOSE_VALVE'
'OFF'
X to exit
C to continue
without changes
S to change
parameters
X
C
S
'CLOSE_VALVE'
'OFF'
GOTO
START
READ_IN_CONTROL
DISPLAY_CONTROL
GOTO
START
END

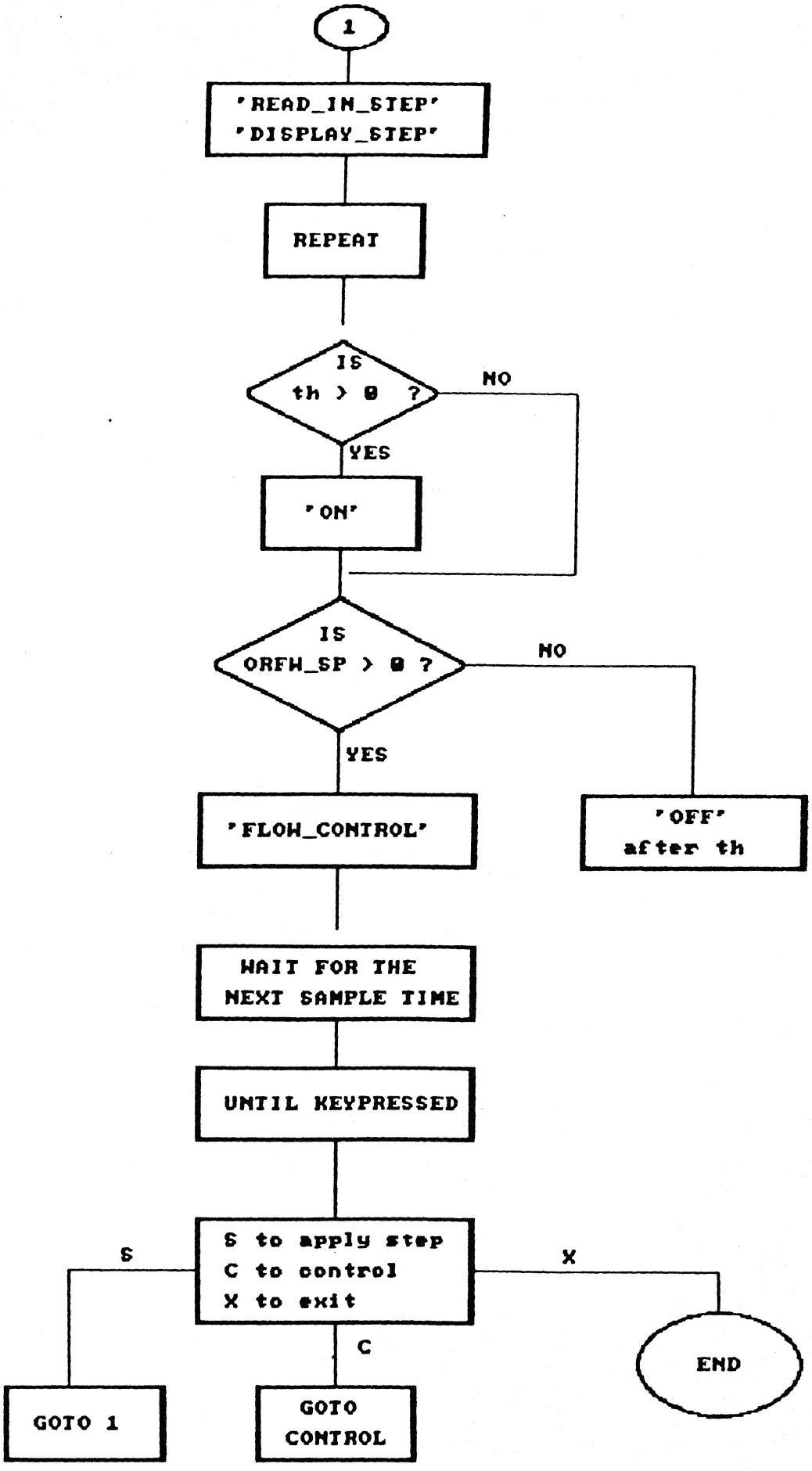
1
'READ_IN_STEP'
'DISPLAY_STEP'
REPEAT
IS
th > 0 ?
NO
YES
'ON'
IS
ORFW_SP > 0 ?
NO
YES
'FLOW_CONTROL'
'OFF'
after th
WAIT FOR THE
NEXT SAMPLE TIME
UNTIL KEYPRESSED
S to apply step
C to control
X to exit
S
X
C
GOTO 1
GOTO
CONTROL
END

PROCEDURE FLOW_CONTROL

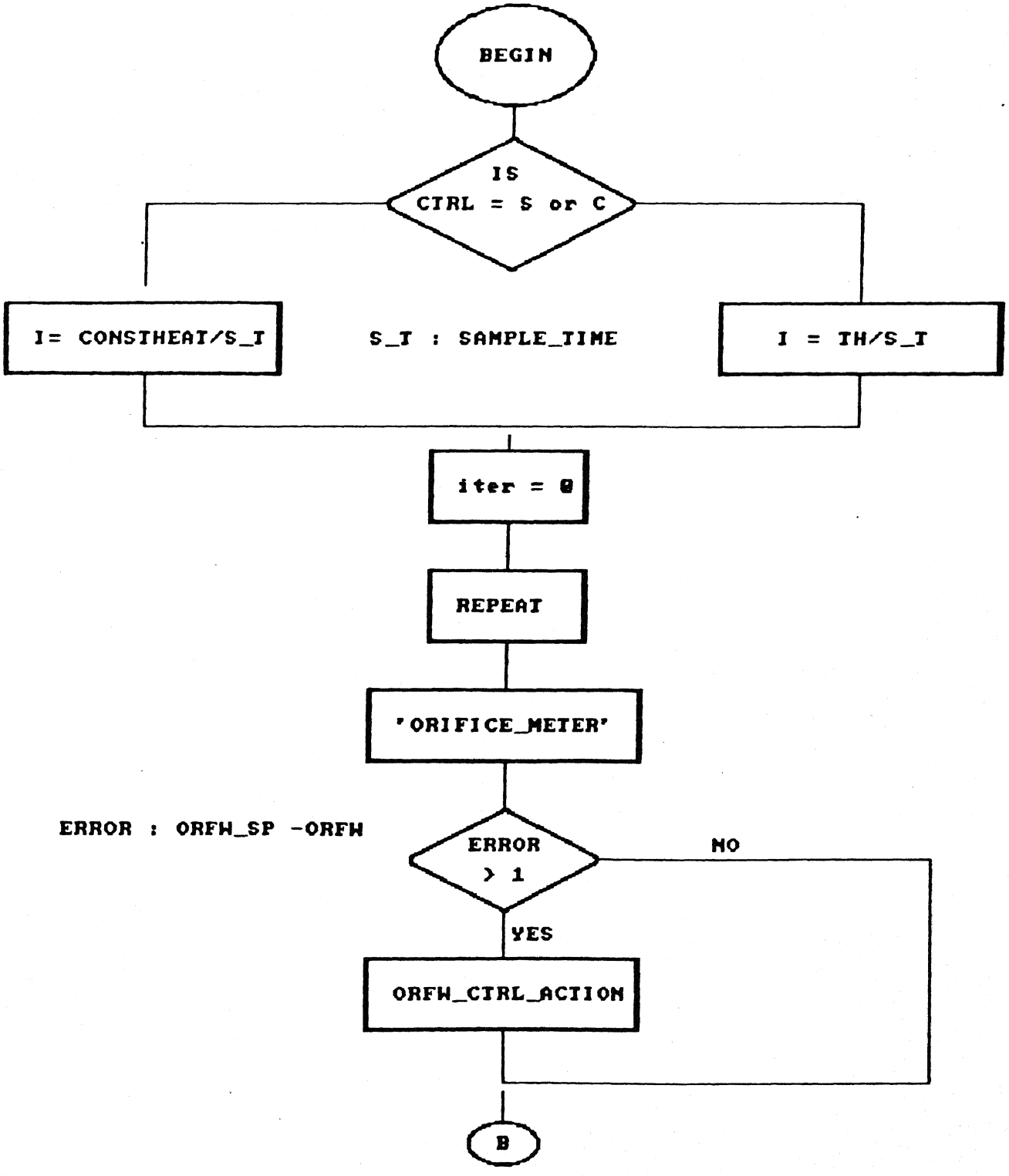

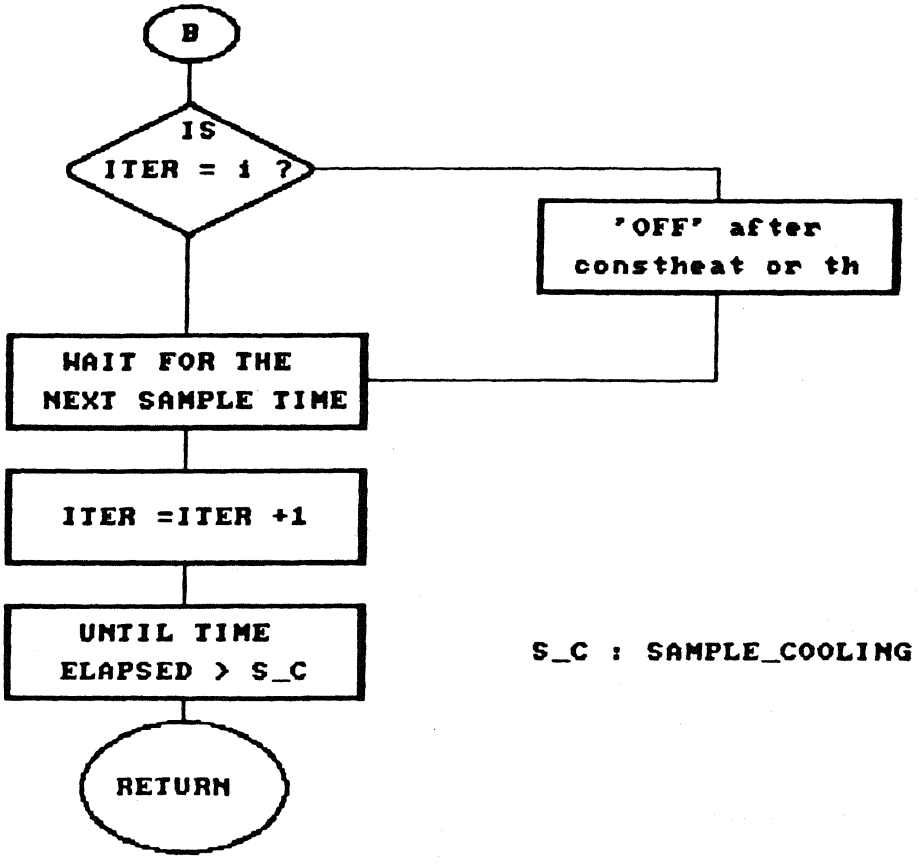
B
IS
ITER = 1 ?
'OFF' after
constheat or th
WAIT FOR THE
NEXT SAMPLE TIME
ITER =ITER +1
UNTIL TIME
ELAPSED > S_C
RETURN
S_C : SAMPLE_COOLING

APPENDIX 3

DETERMINATION OF M_v

Molecular weight M_v is obtained from the efflux times as described below (36-38):

Let C_1 be the concentration of the original solution prepared (all concentrations in g polymer/dl solution). Dilution of 15 ml of this solution with 5 ml of benzene gives $C_2 = 15C_1/20$. 10 ml of this solution is diluted with 5 ml of benzene, to give $C_3 = 10C_2/15$. Dilution of this 15 ml solution with 5 ml of benzene results in $C_4 = 15C_3/20$. Let the corresponding efflux times be t_i, i=1,....,4 (averages of 4 readings which are within about 0.5s). Let t_o be the efflux time for the pure solvent.

The relative viscosity, specific viscosity, reduced viscosity and inherent viscosity for the i^{th} solution are defined as follows:

$$\eta_{r,i} = t_i/t_o \tag{1}$$

$$\eta_{sp,i} = \eta_{ri} - 1 \tag{2}$$

$$\eta_{red,i} = \eta_{sp,i}/C_i \tag{3}$$

$$\eta_{inh,i} = \ln(\eta_{r,i}/C_i) \tag{4}$$

The intrinsic viscosity (which is related to the viscosity average molecular weight) is defined as the reduced viscosity in the limit of vanishing concentration. Mathematically,

$$[\eta] = \lim_{c \to 0} \eta_{red} \tag{5}$$

At low concentrations (below about 0.5 g/dl), plots of reduced viscosity *vs* concentration and of inherent viscosity *vs* concentration are linear, following the established equations:

$$\eta_{red} = [\eta] + k[\eta]^2 c \tag{6}$$

$$\eta_{inh} = [\eta] - k[\eta]^2 c \tag{7}$$

Therefore, it can be observed that both these linear functions have a common intercept at the intrinsic viscosity, $[\eta]$. A double extrapolation routine which fits Equations (A3.6, A3.7) in a least squares sense with a common intercept was used to obtain $[\eta]$. A listing of the program is included at the end of this appendix. A specimen plot of the determination of $[\eta]$ is shown in Fig A3.1.

The M_v is calculated from the Mark-Houwink equation,

$$[\eta] = KM_v^a \tag{8}$$

The values of the constants, K and a, were taken from the Polymer Handbook (39) for the PMMA -Benzene system at 30°C. The last run samples were analyzed at 32°C (in a water bath), as the room temperature had gone above 30°C. Still the same constants were employed. This is not expected to lead to much little error as these constants, K and a, are not sensitive functions of temperature (39). The following values of K and a are used for the calculations:

$$K = 5.2 \times 10^{-5}\ dl/g$$

$$a = 0.76$$

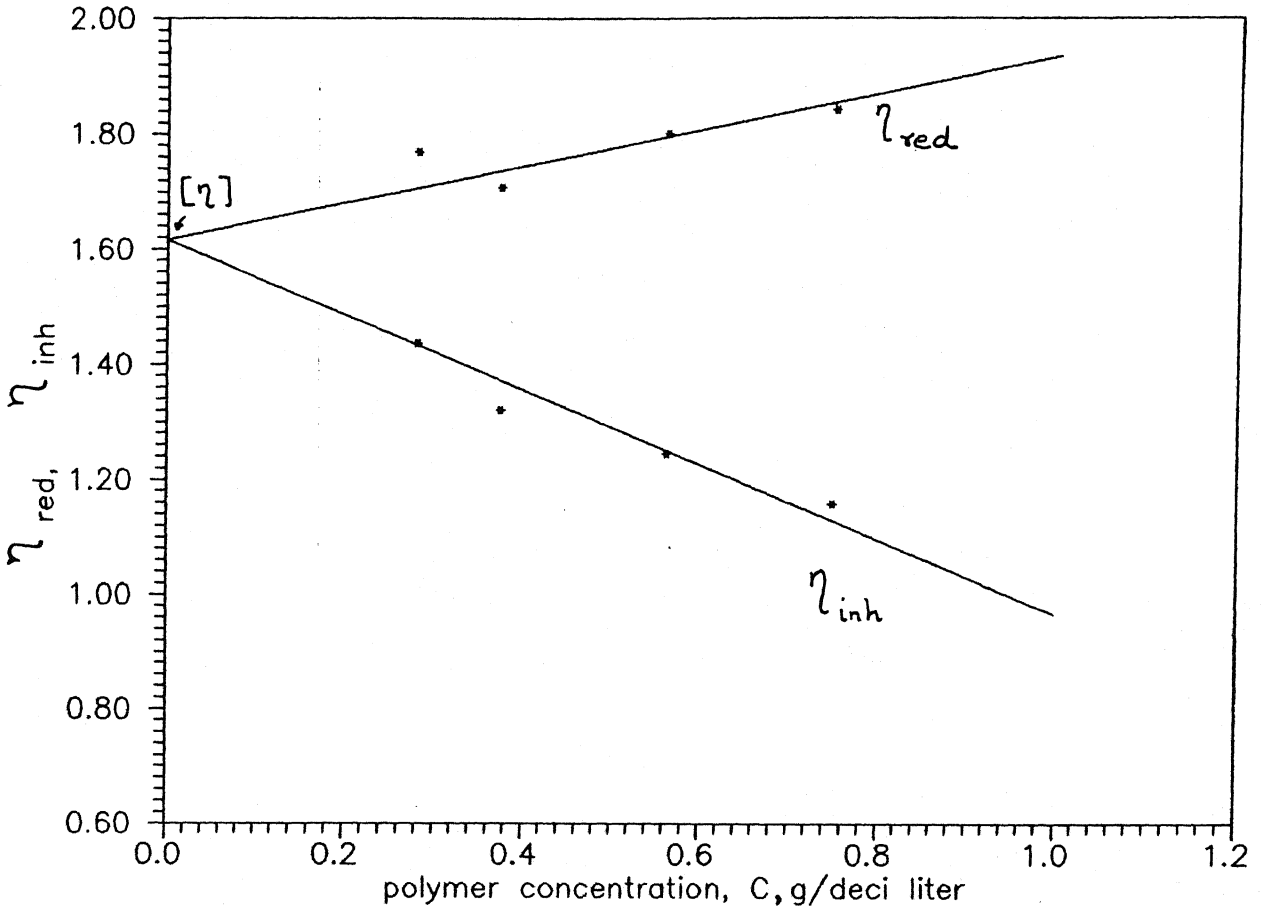

Fig. A3.1 Double extrapolation plot to estimate the intrinsic viscosity (of sample 4, NI50b run). $[\eta]$ = 1.618 dl/g, M_v= 8.162 x 10^5